ELUCIDATING THE POTENTIAL OF BIOCHAR & ITS AMENDMENTS DERIVED FROM *EICHHORNIA CRASSIPES* (WATER HYACINTH) IN ALLEVIATION OF ARSENIC & FLUORIDE FROM SPIKED WATER

THESIS

Submitted in partial fulfilment of the requirements for the
award of the degree of

Master of Technology
in
Environmental Biotechnology

by

AKSHAY GAURAV

University Roll Number : 002030904007
Registration Number : 154528 of 2020 - 2021
Examination Roll Number : M4EBT22007

Under the esteemed guidance of

Dr. Tarit Roychowdhury
School of Environmental Studies (SOES)
Jadavpur University, 188, Raja S. C. Mallick road,
Kolkata – 700032 (India)

JUNE 2022

UNDERTAKING BY THE STUDENT

I, Akshay Gaurav hereby declare that this thesis titled **"Elucidating the potential of biochar & its amendments derived from *Eichhornia crassipes* (water hyacinth) in alleviation of arsenic & fluoride from spiked water"** submitted for the partial fulfilment of the continuous assessment of Master of Technology in Environmental Biotechnology to the School of Environmental Studies (SOES), Jadavpur University, Kolkata – 700032 is record of original work done by me under the guidance of **Dr. Tarit Roychowdhury.**

This thesis is written in my own words, with reference to several published scientific papers which have been adequately cited from the original sources. It is also to be declared that this thesis does not contain any fictional or misreported data or result.

The thesis is not submitted to any other University or Institution for the award of any degree, diploma or fellowship or published any time before.

I understand that any violation of the above will be a cause for disciplinary action against me.

____

Student Name: Akshay Gaurav
Registration number: 154528 of 2020-2021
Examination Roll No.: M4EBT22007

Date: _____ / _____ / __________

Place: School of Environmental studies

Jadavpur University

Kolkata – 700032 (India)

TO WHOM IT MAY CONCERN

It is hereby recommended that this thesis titled **“Elucidating the potential of biochar & its amendments derived from *Eichhornia crassipes* (water hyacinth) in alleviation of arsenic & fluoride from spiked water”** is prepared and submitted for the partial fulfilment of the continuous assessment of **Master of Technology in Environmental Biotechnology** course of Jadavpur university by **Akshay Gaurav**, a student of the said course for the session 2020 – 2022, under my supervision and guidance. It is also declared that no part of this thesis has been presented or published elsewhere.

Director
Prof. Joydeep Mukherjee
School of Environmental Studies
Jadavpur University, Kolkata – 700032

Thesis Supervisor
Dr. Tarit Roychowdhury
School of Environmental Studies
Jadavpur University, Kolkata - 700032

DEAN
Faculty of Interdisciplinary Studies (FISLM)
Jadavpur University, Kolkata - 700032

CERTIFICATE BY THE SUPERVISOR

This is to certify that the thesis entitled, **“Elucidating the potential of biochar & its amendments derived from *Eichhornia crassipes* (water hyacinth) in alleviation of arsenic & fluoride from spiked water”** being submitted by **Akshay Gaurav (Reg. No. 154528 of 2020-2021)** to the School of Environmental Studies, Jadavpur University Kolkata for partial fulfilment of the requirement for the award of degree of Master of Technology in Environmental Biotechnology. This study was carried out by him under my guidance and supervision.

____

Dr. Tarit Roychowdhury
Associate Professor
School of Environmental Studies
Jadavpur University, Kolkata

Date: _____ / _____ / __________

Place: School of Environmental studies
Jadavpur University
Kolkata – 700032 (India)

CERTIFICATE OF APPROVAL

This foregoing thesis is hereby approved as a credible study of an engineering subject carried out and presented in a manner satisfactorily to warranty its acceptance as a prerequisite to the degree for which it has been submitted. It is understood that by this approval the undersigned do not endorse or approve any statement made or opinion expressed or conclusion drawn therein but approve the thesis only for purpose for which it has been submitted.

Final examination for evaluation of Thesis

Signature of the Examiners

ACKNOWLEDGEMENT

The blessings of almighty, the heavenly support of my late parents **Late Ajay Kumar** and **Late Arundhuti Pandit**, and loving support of my sisters **Akanksha Priyanka** & **Aanya Tulip** made it possible for me to undertake the post graduate study.

I am profoundly grateful to my guide **Dr. Tarit Roychowdhury** for support, invaluable guidance and constant encouragement throughout the work. His scientific intuition, balanced approach and critical examination have inspired and enriched my growth as a student and as a researcher, and enabled me in shaping up my ideas and research.

I would like to thank my teachers **Prof. Joydeep Mukherjee**, **Dr. Subarna Bhattacharyya**, and **Dr. Reshmi Das** of School of Environmental Studies, Jadavpur University for their suggestion and support during my dissertation work.

I would also like to thank the research scholars, **Sharmistha Majumder, Antara Das, Ayan De, Madhurima Joardar, Deepanjan Mridha, Swetanjana Ghosh, and Urvashi Lama** for the constant support and help in the experimentation throughout my work.

I sincerely admire the constant support of all my friends who were always by my side and ready to provide every help needed during the study period.

____

Student Name: Akshay Gaurav
Registration number: 154528 of 2020-2021
Examination Roll number: M4EBT22007

Date: _____/ _____ / _______
Place: School of Environmental studies
Jadavpur University
Kolkata – 700032 (India)

CONTENTS

LIST OF FIGURES

LIST OF TABLES

ACRONYMS

AAS	Atomic Absorption Spectrometer
AD	Adsorbent Dose
ADP	Adenosine diphosphate
As (III)	Arsenite
As (V)	Arsenate
ASTM	American Socirty for Testing and Materials
ATP	Adenosine triphosphate
BIS	Bureau of Indian Standard
BS	British Standards
C	Carbon
Ca	Calcium
$CaCO_3$	Calcium Carbonate
CaO	Calcium oxide
Cd	Cadmium
C_e	Equilibrium / Final concentration
CFL	Calcium-Iron modified leaf biochar
CFR	Calcium-Iron modified root biochar
CFS	Calcium-Iron modified stem biochar
CGWB	Central Ground Water Board
C_i	Initial concentration
CL	Calcium modified leaf biochar
CO_2	Carbon dioxide
CR	Calcium modified root biochar
Cr	Chromium
CS	Calcium modified stem biochar
DIN	Deutsches Institut für Normung
DMA (III)	Dimethylarsinous acid
DMA (V)	Dimethylarsenic acid
DTG	Derivative thermogravimetric
EDX	Energy dispersive spectroscopy
EPA	Environmental Protection Agency
F	Fluoride
Fe	Iron
FL	Iron modified leaf biochar

FR	Iron modified root biochar
FS	Iron modified stem biochar
FTIR	Fourier transform infrared spectroscopy
GMB	Ganga-Meghna-Brahmaputra
H	Hydrogen
HCl	Hydrochloric acid
HCO_3	Bicarbonate
Hg	Mercury
IAC	Initial Arsenic Concentration
ICP-AES	Inductively coupled plasma atomic emission spectrometry
ICP-MS	Inductively coupled plasma mass spectrometry
IFC	Initial Fluoride Concentration
ISE	Ion Selective Electrode
ISI	Indian Standard Institution
ISO	International Organization for Standardization
k_1	Pseudo first order rate constant
k_2	Pseudo second order rate constant
KF	Potassium fluoride
K_f	Freundlich constant
K_L	Langmuir isotherm constant
L	Water hyacinth leaf biochar
MMA (III)	Monomethylarsonous acid
MMA (V)	Monomethylarsonic acid
Mn	Manganese
N	Nitrogen
n	Freundlich exponent
Na	Sodium
Na_2CO_3	Sodium carbonate
NaF	Sodium Fluoride
$NaHCO_3$	Sodium bicarbonate
NF	Nano filtration
Ni	Nickel
NRDWP	National Rural Drinking Water Programme
NWP	National Water Policy
O	Oxygen
OH	Hydroxide

q_e	Adsorption capacity at equilibrium
Q_{max}	Maximum adsorption rate
q_t	Amount of metal ions adsorbed at time t
R	Water hyacinth root biochar
R_L	Constant separation factor
RO	Reverse osmosis
S	Water hyacinth stem biochar
S	Sulphur
SEM	Scanning electron microscope
SF	Surface functionality
SH	Sulphohydrl
SOES	School Of Environmental Studies (Jadavpur University)
TGA	Thermogravimetric analysis
TISAB	Total Ionic Strength Adjustment Buffer
UNICEF	United Nations International Children's Emergency Fund
US	United states
USA	United States of America
V	Volume taken
VM	Volatile matter
W	Mass of adsorbent
WH	Water hyacinth
WHO	World Health Organization
XPS	X-ray photoelectron spectroscopy
XRD	X-ray diffraction
XRF	X-ray fluorescence

ABSTRACT

Heavy metal pollution has become a growing problem as industrialization and urbanization have increased. Heavy metal pollution is becoming a major issue on a local, regional, national, and global scale. The United States Environmental Protection Agency has classified these as priority pollutants. Heavy metal toxicity poses a variety of risks to plants, animals, and human health. These are difficult to remove from the environment due to their non-biodegradable nature. The burning of fossil fuels, mining and smelting of metalliferous ores, municipal wastes, fertilizers, pesticides, and sewage are the primary sources of metal pollution.

Heavy metal exposure to human population may cause neurobehavioral disorders, developmental retardation, various types of cancer, kidney damage and auto immunity. Arsenic leads to cardiovascular problems, skin cancer and other skin effects, peripheral neuropathy, and kidney damage. Fluoride is considered dangerous like a double edged sword, as both its excessive intake and low intake causes problems such as dental caries, fluorosis.

Biochar and its amendments prepared from roots, stem & leaves of water hyacinth was prepared under laboratory conditions. Tests were run on water sample induced with R (Root biochar), FR (Iron modified root biochar), CR (Calcium modified root biochar), CFR (Calcium-iron modified root biochar), S (Stem biochar), FS (Iron modified stem biochar), CS (Calcium modified stem biochar), CFS (Calcium-iron modified stem biochar), L (Leaves biochar), FL (Iron modified leaves biochar), CL (Calcium modified leaves biochar), CFL (Calcium-iron modified leaves biochar). From preliminary studies it was established that 20g/L dose & 15 min residence time as efficient for both fluoride and arsenate removal. It was found that FR, FS & FL are highly efficient (> 95%) in volatilizing 100 ppb As (V). Also, FL was observed to have high potential in controlling 10 ppm Fluoride spiked water.

Keywords – Arsenic remediation; Defluoridation; Biochar; *Eichhornia crassipes*; Iron modified biochar; Calcium modified biochar.

CHAPTER

1

INTRODUCTION

Water is the most fundamental and precious component of all aspects of human life, as well as an essential component of the global life support system. Water scarcity, gradual destruction, and increased pollution of water resources, combined with the progressive encroachment of incompatible activities, have resulted in a variety of water crises around the world. The total amount of water available on Earth has been estimated to be 1.37 billion cubic kilometres, enough to cover the planet with a layer 3 km thick (Garrison, 2022). Water covers more than two-thirds of the earth's surface, but 97.5 percent of it is salt water. This results in only 2.5 percent fresh water. To compound the paradox, only a small portion of the total fresh water resource is available for human consumption. Approximately 70% of the world's fresh water is trapped in ice at the poles, with the remainder retained as soil moisture or deposited in deep underground aquifers. In the end, less than 0.5 percent of the world's fresh water is technologically and economically accessible for human use. Distribution of water present on Earth is depicted in **Fig. 1.1.**

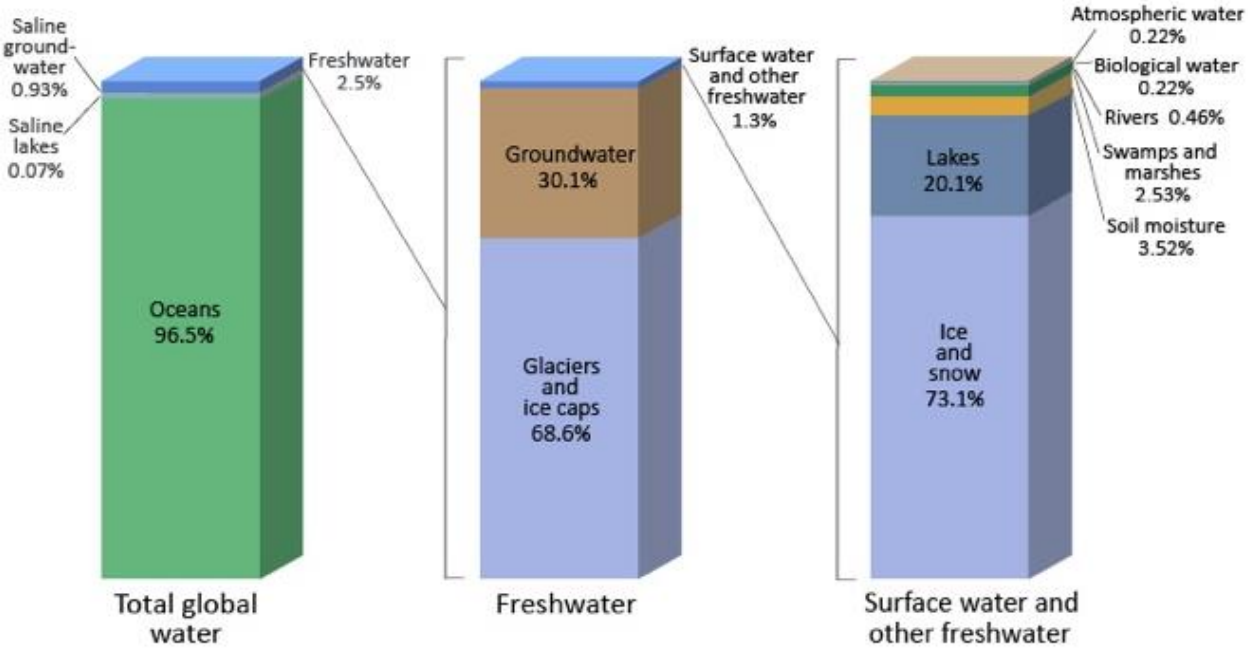

Figure 1.1: Distribution of Earth's water (Source: Gleick, 1993)

India is a key player in the global water crisis. Water is a valuable national asset & a prime natural resource for meeting basic human needs (NWP, 1987). India is rapidly urbanising, and as a result, water demand will rise rapidly. The growing population, urbanisation, and demand for fresh water must be met with caution. Rapid population growth, changing agricultural land use, and changing rural lifestyles have increased the demand for fresh water in rural areas. Many villages in India lack access to water or have no access to water at all (Ramakrishna and Babu, 1999).

India is a land of rivers. It has large rivers that carry a large amount of fresh water. The majority of fresh water flows as surface runoff, with only a small percentage seeping inside to form ground water. This surface water is used to meet a variety of human needs, including agriculture, irrigation, domestic use, industrial purposes, and power generation. However, the majority of locations have poor surface water quality due to pollutants from various sources such as domestic waste discharges, industrial wastes, pesticides, herbicides, chemical manure, and many other human activities.

1.1. Groundwater contamination

Groundwater has recently been identified as the world's primary source of safe and potable water (Zektser and Everett, 2004). It is widely used and regarded as a primary source of drinking water because it is less prone to contamination and pollution than surface water resources (Kumar and Shah, 2004). Groundwater is critical in reducing rural-urban water demand in India. Currently, the country is experiencing 1.4 percent annual population growth with higher economic growth rates (Bloom, 2011), which increases the demand for and use of water. According to recent studies, India extracts about 200 billion cubic metres of groundwater reserve each year, the most on the planet. Groundwater supplies nearly 80 percent of rural domestic needs and 50 percent of urban water needs in India (Aguilar, 2010). Groundwater is currently in crisis, both in terms of quantity and quality. Water levels have dropped rapidly in several parts of the country over the last two decades as groundwater development has increased. The number of irrigation wells drilled has increased rapidly and indiscriminately (Ahmad et al., 2007). The rising population, urbanisation, and industrialization, combined with intense competition in agriculture, industry, and domestic sectors, are pushing the groundwater table ever lower. As a result of the overdraft, the quality of groundwater is suffering greatly. Untreated industrial wastewater discharge and haphazard solid waste disposal pollute groundwater. As a result, the quality of fresh groundwater is deteriorating.

In India, groundwater is a critical resource, providing more than 60 percent of irrigation water and 85 percent of drinking water (World Bank, 2012). According to The Times of India (March 12, 2010), 33 percent of the country's groundwater resources are unfit for consumption, and it is estimated that 60 percent of groundwater resources will be in critical condition within the next twenty years (Kumar and Raj, 2013).

A large number of anthropogenic and geogenic contaminants have emerged as serious threats to groundwater use over the last several decades. In India, the main anthropogenic sources of groundwater pollution are sewage disposal, agriculture, and industry. It is estimated that Indian cities generate 20 million m^3 of sewage per day, with only 10% of this sewage being treated before it reaches groundwater or surface water resources (Chakraborty et al., 2011). Furthermore, the vast majority of domestic waste in India is discarded improperly. These issues are exacerbated by rapid urbanisation. According to recent research conducted on the Ganga plain, roughly 70% of rural populations use tube wells and 40% of them are contaminated with bacteria (Chakraborty et al., 2011).

Nitrate contamination in shallow groundwater is caused by run-off from agricultural fields and the disposal of untreated human and animal waste. Eleven states in the country have excessive nitrate concentrations in groundwater (Mehta, 2006). Pesticide application has increased significantly after the green revolution. Pesticide residues affect groundwater for a longer period of time than surface water and soil (Chaudhary, 2002).

Groundwater pollution caused by industrial effluents is a widespread issue in major Indian cities such as Delhi, Mumbai, Kolkata, Ludhiana, and Kanpur (Bobba et al., 1997). In India, there are approximately 2.6 million small-scale industries (Chakraborty et al., 2011), the majority of which are concentrated in urban agglomerations. Untreated industrial discharges, as well as poisonous industrial effluents, contaminate groundwater in many parts of the country (Rajaram and Das, 2008). Heavy metals such as Chromium (Cr), Nickel (Ni), Cadmium (Cd), and Mercury (Hg) have also been discovered in the groundwater of 43 districts in 14 Indian states (Mehta, 2006). Fluoride, salinity, iron, and arsenic are the major geogenic groundwater contaminants that pose a serious threat to public health in the country at the moment (Chakraborty et al., 2011).

1.2.Arsenic pollution

Arsenic contamination of groundwater is widespread, and arsenic contamination of drinking water is significant in a number of areas. It is now known that at least 140 million people in 50 countries have been drinking water contaminated with arsenic at levels higher than the WHO provisional guideline value of 10 g/L.

In an aqueous system, inorganic As exists in two oxidation states: trivalent As (III) and pentavalent As (V) (Chutia et al., 2009). Pentavalent As is stable in oxygenic conditions and exists as monovalent ($H_2AsO_4^-$) or divalent ($HAsO_4^-$) anions, whereas trivalent As (III) is stable in anoxygenic conditions and exists as uncharged ($H_3AsO_3^0$) or anionic species ($H_3AsO_3^0$). (Grossl et al., 1997).

Arsenic can be introduced into the atmosphere as a result of the erosion and weathering of arsenic-containing geological materials, volcanic activity, forest fires, and other natural processes (Sharma et al., 2014). As is released from rock into water during the biogeochemical process as a result of interaction between water and As-containing rocks (Mukherjee et al., 2014). Through reductive dissolution or desorption, the oxidation process also liberates As from sulphide minerals and iron oxide (Camargo and Alonso, 2006). As groundwater mobilisation can occur naturally through physical and chemical weathering or volcanism and biogeochemical activities (Mondal et al., 2010), it can also be caused by anthropogenic activities such as wood preservatives (Chen and Olsen, 2016), acid mine drainage (Paikaray, 2015), fertilisers or herbicides (Jayasumana et al., 2015). Soils are generally contaminated with arsenic as a result of fertiliser, pesticides, mining and smelting, fossil fuel combustion, waste incineration, and sludge use. Soils are significantly contaminated geologically due to weathering of parent rock and arsenic-containing minerals (Nriagu et al., 2007).

Extensive research has been conducted in recent years on arsenic removal techniques to increase arsenic uptake from the environment. The researchers are investigating these processes in laboratory experiments and in the field. Ion exchange, phytoremediation, adsorption, phytoremediation, chemical precipitation, electrokinetic methods, and electrocoagulation are currently used methods. Although these processes are effective at removing arsenic from soil and water, each has significant drawbacks, particularly in terms of cost and efficiency. Various factors influence the selection of appropriate arsenic treatments, such as restrictions for soil and water treatment technologies, local and national government requirements, a country's development stage, and local strategies for arsenic levels in trendy plants and water systems.

Various advancements are being made in this area all over the world. Furthermore, the rate of soil and water management increase is slowed by using fewer synthetic compounds and vitality, which should reduce costs.

1.3.Fluoride pollution

Fluoride is required for humans to have a healthy and normal physiology. It is required for the formation of enamel and has an anti-osteoporosis effect (Zhao et al., 2017). Fluoride enters the human body primarily through contaminated groundwater or through various foods. Adults can die after consuming 1664 mg/kg fluoride, and children can die after consuming 316 mg/kg fluoride (Barbier et al., 2010). According to some researchers, 200 million people worldwide consume fluoride at levels higher than the World Health Organization's (WHO) recommended level of 1.5 mg/L (Kut et al., 2016).

China and India are among the countries most affected by fluoride, with fluoride concentrations in ground water reaching up to 48 mg/L in these two countries (Jadhav et al., 2015). Fluorosis is the most common groundwater disease in India. Fluorosis affects over 66 million people, including 6 million children under the age of 14 (Ayoob and Gupta, 2006). It was discovered that 20 of 29 Indian states (as of March 31, 2014) had some level of groundwater fluoride contamination (Chakraborty et al., 2011).

The majority of fluoride comes from natural sources, such as fluorspar, rock phosphate, cryolite, apatite, mica, and so on. High F^- concentrations are found in large and widespread geographical belts associated with a) marine sediments in mountainous areas, b) volcanic rocks, and c) granitic and gneissic rocks (Murray, 1986). Groundwater gets contaminated by fluoride dissolved from these rocks (Edmunds and Smedley, 1996). Excess F^- is ingested by humans and cattle, primarily through drinking water, but also through vegetables and cereals grown on contaminated soils.

Acute fluoride exposure can cause abdominal pain, nausea, excessive saliva and vomiting, seizures, and muscle spasms in humans. This will not occur as a result of drinking tap water, but may occur as a result of accidental contamination of drinking water, such as an explosion or industrial accident. Dental fluorosis is a disease that can be caused by high fluoride contamination. It can develop during adolescence when the teeth are still developing or at adulthood, and while it has no effect on tooth health, it can result in discoloured teeth. That is why dentists advise children in small caps not to use fluoride-containing mouthwash. To avoid swallowing tooth paste while brushing their teeth, children must always be supervised by an adult. Furthermore, the presence of fluoride may cause skeletal fluorosis, a bone-related disease, and prolonged exposure can result in joint and bone damage (Maguire and Zohoori, 2013). Because the bones harden or lose elasticity, fractures become more common. Joint mobility can be compromised due to bone and tissue thickening.

The gravity of this problem is so severe that immediate action is required. The sole purpose of removing fluoride is to treat the water so that it is fit for consumption and contains fluoride levels below acceptable limits. Fluoride removal techniques are classified into three types: membrane techniques, adsorption techniques, and coagulation.

1.4.Water hyacinth biochar

Eichhornia crassipes (water hyacinth) is a recalcitrant weed that originated in the Amazon basin. It was introduced as an ornamental plant into India from Brazil in 1896 (Jafari, 2010), and it now has a nearly global distribution. Water hyacinth is a common aquatic weed found in temperate and tropical water bodies around the world, particularly in Bangladesh and Eastern India, where ground water is frequently contaminated with high levels of arsenic. The water hyacinth is considered an aquatic nuisance because it forms a floating layer on ponds and lakes, clogs waterways, and makes navigation difficult. The plant reproduces itself by breaking off tiny root fragments from larger plants, which quickly develop leaf stalks and broad green leaves. Runners grow from the base of petioles as well, resulting in a rapid spread of vegetative reproduction. In the early 1980s, it was discovered that water hyacinth could be used to remove heavy metals from water.

Because of its high reproductive (vegetative and sexual) rate and dispersion (Téllez et al., 2008), water hyacinth is a stubborn weed whose management can cause serious environmental issues. It can pose an ecological threat to bodies of water, lakes, irrigation structures, and so on. The presence of water hyacinth on water surfaces increases evapo-transpiration and acts as a conduit for greenhouse gas emissions from bodies of water. Water hyacinth is primarily managed through physical removal and disposal from bodies of water.

The conversion of water hyacinth to biochar represents a more sustainable strategy for weed management. Biochar derived from water hyacinth biomass will improve soil carbon storage and fertility, transforming the previously recalcitrant weed into a valuable resource. Thus, the current study sought to produce biochar from water hyacinth biomass and to assess its potential in alleviating arsenic as well as fluoride from spiked water.

1.5.Framing & organization of thesis

The skeleton of the report is the chronological sequence of the thesis. Before beginning the thesis, it is necessary to frame the dissertation's systematic arrangement for the readers.

The current study on "***Elucidating the potential of biochar & its amendments derived from Eichhornia crassipes (water hyacinth) in alleviation of arsenic & fluoride from spiked water***" is divided into seven chapters.

The first chapter introduces about the water resource as well as Groundwater resource availability and the mode of contamination in India. Along with that the first chapter also briefs about Arsenic & fluoride pollution. The later part of this chapter discusses about the objectives of study. The second chapter reviews the existing research on groundwater arsenic contamination, its history, biogeochemistry, sources, extent & mechanism of contamination, distribution, toxicity, health impacts, and removal technologies. The third chapter surveys the existing research on groundwater fluoride contamination, its history, biogeochemistry, sources, extent & mechanism of contamination, distribution, toxicity, health impacts, and removal technologies. The fourth chapter reviews the existing adsorption technology. This chapter also discusses about biochar as an adsorbent, water hyacinth biochar, isotherms and kinetics of adsorption. The fifth chapter explains the process and procedures that must be followed in order to achieve the desired results. The findings and concluding remarks are covered in Chapter 6. The summary of the current research work and its future scope is concluded in Chapter 7.

1.6. Objectives of study

a) Preparation of biochar & its amendments

The study aims to prepare biochar using Roots, stem, & leaves of water hyacinth. Amendments of biochar has been prepared by doping biomass with Iron & calcium individually, and Iron & calcium salts combined together. The efficacy of prepared biochar as well as amended biochar was tested against removal of fluoride and arsenic from spiked water sample.

b) Arsenic removal from spiked water

The problem of arsenic contamination of groundwater (a major source of drinking water) is becoming increasingly aggravating. Arsenic removal is the only viable option for removing excess arsenic. Among all other techniques, adsorption is the most straightforward, appealing, user-friendly, efficient, environment friendly, and cost-effective. As a result, the arsenic removal capacity of water hyacinth biochar & its amendments has been studied. The effect of various parameters on the percentage removal of arsenic was studied in this study **(Table 1.1)**, and the sorption nature was also determined using isotherm & kinetic models.

Table 1.1: Objectives for arsenic removal from spiked water

Objective of experiment	**Values of variable parameters**	**Values of fixed parameters for verifying optimum conditions**
To study the effect of adsorbent dose on arsenic removal	**AD:** 5, 10, 20, 30, 50 g/L	**IAC:** 100 µg/L**; Temp.:** 30°C**; Time:** 15 min.**; Solution pH:** 5**; Mixing speed:** 250 rpm
To study the effect of contact time on arsenic removal	**Time:** 5min, 15min, 30min, 45min, 1h, 2h, 4h, 24h	**IAC:** 100 µg/L**; Temp.:** 30°C**; AD:** 20 g/L**; Solution pH:** 5**; Mixing speed:** 250 rpm
To study the effect of pH on arsenic removal	**Solution pH:** 3, 5, 7, 9, 12	**IAC:** 100 µg/L**; Temp.:** 30°C**; AD:** 20 g/L**; Time:** 15 min**; Mixing speed:** 250 rpm
To study the effect of initial arsenic ion concentration on arsenic removal	**IAC:** 100, 500, 1000 µg/L	**Temp.:** 30°C**; AD:** 20 g/L**; Time:** 15 min**; Solution pH:** 5**; Mixing speed:** 250 rpm

Here,

AD – Adsorbent dose

IAC – Initial arsenic concentration

c) Fluoride removal from spiked water

The problem of fluoride contamination of groundwater is becoming increasingly aggravating. Water defluoridation is the only viable option for removing excess fluoride. Among all other techniques, adsorption is the most straightforward, appealing, user-friendly, efficient, environment friendly, and cost-effective. As a result, the fluoride removal capacity of water hyacinth biochar & its amendments has been studied. The effect of various parameters on the percentage removal of fluoride was studied in this study **(Table 1.2),** and the sorption nature was also determined using isotherm & kinetic models.

Table 1.2: Objectives for fluoride removal from spiked water

Objective of experiment	**Values of variable parameters**	**Values of fixed parameters for verifying optimum conditions**
To study the effect of adsorbent dose on fluoride removal	**AD:** 5, 10, 20, 30, 50 g/L	**IFC:** 10 mg/L **; Temp.:** 30°C**; Time:** 15 min.**; Solution pH:** 5**; Mixing speed:** 250 rpm
To study the effect of contact time on fluoride removal	**Time:** 5min, 15min, 30min, 45min, 1h, 2h, 4h, 24h	**IFC:** 10 mg/L **; Temp.:** 30°C**; AD:** 20 g/L**; Solution pH:** 5**; Mixing speed:** 250 rpm
To study the effect of pH on fluoride removal	**Solution pH:** 3, 5, 7, 9, 12	**IFC:** 10 mg/L **; Temp.:** 30°C**; AD:** 20 g/L**; Time:** 15 min**; Mixing speed:** 250 rpm
To study the effect of initial fluoride ion concentration on fluoride removal	**IFC:** 5, 10 mg/L	**Temp.:** 30°C**; AD:** 20 g/L**; Time:** 15 min**; Solution pH:** 5**; Mixing speed:** 250 rpm

Here,

AD – Adsorbent dose

IFC – Initial fluoride concentration

CHAPTER

2

ARSENIC CONTAMINATION: A BRIEF REVIEW

Arsenic contamination is a global concern and it has affected almost every country like western USA, Mexico, Chile, Argentina, Hungary, Romania, Mongolia, Nepal, China, Bangladesh, Taiwan, Vietnam, Thailand, and India. According to the latest report by the Central Ground Water Board (CGWB), 21 states across the country have arsenic levels higher than the specified permissible limit of 10 µg/L (BIS, 2012). The most affected regions in India are around the Ganga-Meghna-Brahmaputra (GMB) basin along with states like Uttar Pradesh, Bihar, Jharkhand, West Bengal, and Assam. According to the report by the National Rural Drinking Water Programme (NRDWP) of the Ministry of Jal Shakti about 9.6 million people in West Bengal, 1.6 million in Assam, 1.2 million people in Bihar, 0.5 million people in Uttar Pradesh, and 0.013 million people in Jharkhand are at immediate risk from arsenic contamination in groundwater. The contamination is not only limited to drinking water but it also has entered our food chains. The usage of groundwater for irrigation along these regions has aggravated the situation as the crops will uptake arsenic and makes it bioavailable.

2.1. History & biogeochemistry

Arsenic is present in numerous mineral formations, notably sulphur-enriched minerals (Boyle and Jonasson, 1973). However, it accompanies many elements in their deposits: copper, silver, gold, zinc, cadmium, mercury, uranium, tin, lead, antimony, bismuth, sulphur, selenium, tellurium, molybdenum, tungsten, iron, nickel, cobalt, and platinum metals. Because arsenic is present in group V (A) of the periodic system, chemically its behaviour is much like elements in the group, specifically phosphorous & antimony. The most common inorganic species of Arsenic at circumneutral pH are the negatively charged arsenates ($H_2AsO_4^-$ and $HAsO_4^{2-}$) and zero charge arsenite ($H_3AsO_3^0$) (Nicholas et al., 2003). It is conveyed that the arsenic gets accrued in oxygen rich sediments by adsorption and/or co-precipitation with hydrous iron and manganese oxides. Burial of such types of sediments in anoxic/suboxic conditions escalates their chance of reduction, releasing Fe (II), Mn (II), and associated Arsenic. Soluble and adsorbed arsenic species undergo biotic transformations. As (V) and As (III) bound to ferric oxides can be mobilized by Iron (III) respiring bacteria by the reductive dissolution of iron-arsenate minerals. Sulphate reducing bacteria can endorse deposition of As (III) as sulphide minerals through their production of sulphide. Both prokaryotic, and eukaryotic microbes can modify arsenic toxicity.

Arsenic (As) is a metalloid in the pnictogen group, Group 15 (VA) & period 4 of the modern periodic table and is mostly found in 3 allotropic forms – yellow, black, and metallic grey. Out of these 3, metallic grey is the most common (Britannica, 2020). Yellow arsenic when exposed to light will quickly turn into black. Black arsenic is a poor conductor of electricity with intermediate properties of yellow and grey arsenic. Arsenic reacts with other elements to form stable compounds:

a) Inorganic arsenic compounds
b) Organic arsenic compounds
c) Arsine Gas

Naturally occurring Arsenic compounds – Arsenite (AsO_3^{3-}), Arsenate (AsO_4^{3-}).

a) Mostly found inorganic trivalent arsenic compounds include Arsenic trioxide (As_2O_3), Sodium Arsenite ($NaAsO_2$), and Arsenic trichloride ($AsCl_3$). Arsenic oxides are colourless, odourless, crystalline, and are hygroscopic, and make acidic solutions when exposed to water.

b) Mostly found inorganic pentavalent compounds are Arsenic Pentoxide (As_2O_5), Arsenic acid (H_3AsO_4), and Arsenate (AsO_4^{3-}).

c) Mostly found organic Arsenic compounds are Arsanilic acid ($C_6H_8AsNO_3$), methylarsonic acid (CH_5AsO_3), dimethylarsinic acid (cacodylic acid) ($C_2H_7AsO_2$), and Arsenobetaine ($C_5H_{11}AsO_2$).

2.2. Sources of arsenic in the environment

Arsenic is the 20th most abundant element on the Earth's crust with an overall concentration of nearly 1.5 ppm (Kapp Jr., 2016). One-third of the atmospheric flux of arsenic is of natural origin – mainly volcanic activity (WHO). The levels of arsenic in the environment are a result of the weathering of more than 200 arsenic rich minerals. On the other hand, anthropogenic sources include mining, smelting of metals, fossil fuel burning, arsenical pesticides, leaching of wood preservatives, and disposal of industrial wastes. Commercially, arsenic is used as an additive for alloys. Gallium arsenide (GaAs) is used in the manufacture of ICs, IR-LEDs, laser diodes, solar cells, and optical windows. Indium Arsenide (InAs) is used in diode lasers and infrared photovoltaic photodiode detectors (Kapp Jr., 2016). The currently used organoarsenic veterinary drug is Nitarsone ($C_6H_6AsNO_5$). The crustal concentration of elemental arsenic is in the range of 1.5 to 2 ppm. The arsenic in soil ranges from 1 to 10 ppm, ocean water averages about 1.6 mg/L, surface freshwaters have concentrations below 10 μg/L, groundwater contains about 1–2 μg/L (Kapp Jr., 2016). The average arsenic concentration in air in remote areas is between 0.02 to 4 ng/m^3, whereas in urban air is in the range of 3 to 200 ng/m^3 (Kapp Jr., 2016). The summary of anthropogenic & geogenic sources of arsenic in the environment is listed in Fig. 2.1.

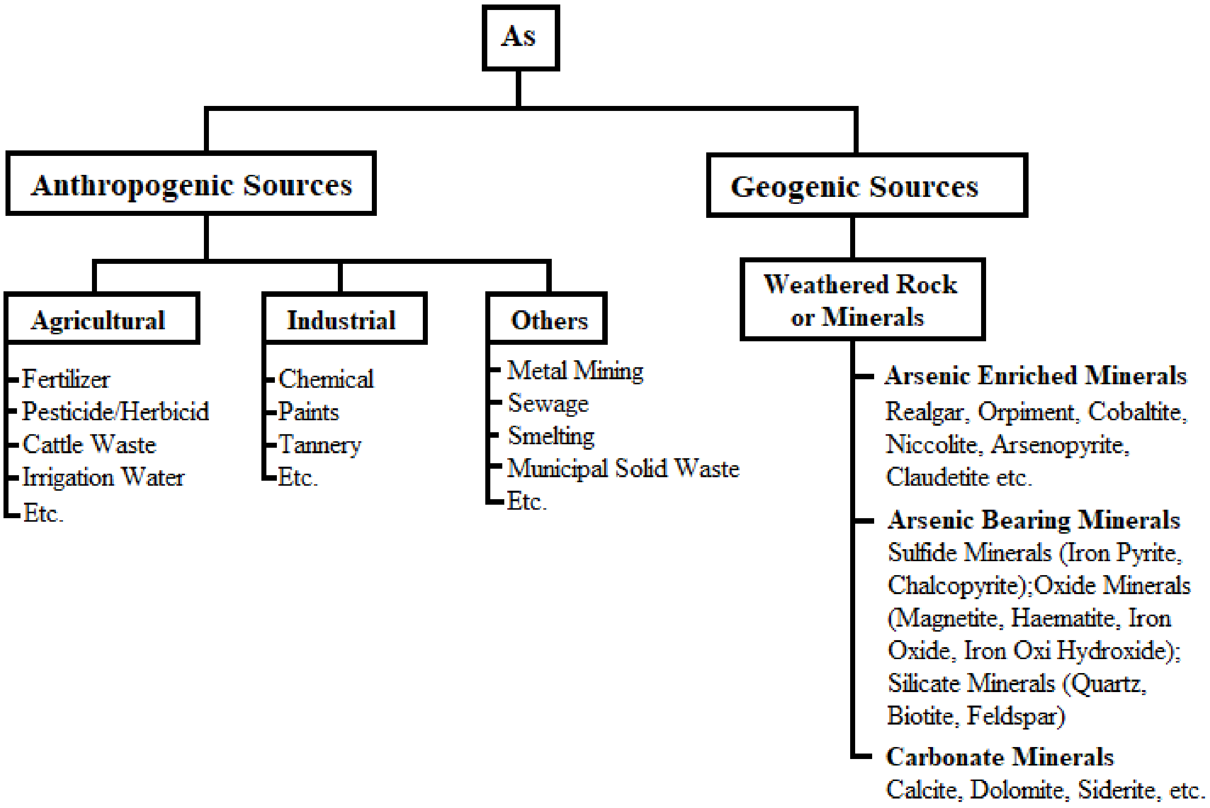

Fig. 2.1: Sources of arsenic

2.3. Extent & mechanism of contamination

A population of 30 million people living in an area of 34,000 km^2 in 6 districts of West Bengal is consuming arsenic-contaminated groundwater above its recommended value in drinking water (Das et al., 1996). Due to heavy withdrawal of groundwater, there is decomposition of iron pyrites. The sources of arsenic in natural water bodies are due to the local geology, hydrology, and geochemical properties of the aquifer (Bhattacharya et al., 1997). Depending on the sensitivity towards changing redox reactions, the retention and mobility of arsenic vary. The location of arseniferous groundwater is mainly in the upper delta plain and in abandoned meander channels (Bhattacharya et al., 1997). Arsenic in the silty clay and sandy layers occurs as coatings in mineral grains. Clayey layers sandwiched with sandy aquifers at depths in the range of 20–80 m is said to be the major source of Arsenic in groundwater. Arsenic is more likely to get co-precipitated or scavenged by Fe (III) and Mn (IV) in the sedimentary environment (Acharyya et al., 2005). About 200 ppm of arsenic are sourced from the Gondwana coal seams in the Rajmahal basins. About 0.8% of arsenic is linked to isolated outcrops of sulphides in Darjeeling and others in the upper reaches of the Ganges river system (Acharyya et al., 2005). Studies of large databases suggest that arsenic decreases with the depth of bore well.

Arsenic is leached to the aquifer mainly because of oxidative dissolution of arsenic rich iron pyrite or due to the reductive dissolution of arsenic rich iron oxi-hydroxide in the sediments (Nickson et al., 2000). The sources of arsenic rich sediments in the district of North 24 Parganas are Rajmahal-Chotanagpur plateau to the west, and Bihar plateau, and the Himalayas. The most common source in almost every country is groundwater. People are exposed to high levels of inorganic arsenic via contaminated drinking water, contaminated food products, irrigation of crops through contaminated water, smoking tobacco, etc. Almost 100 million people are affected by groundwater contamination with Arsenic in India (Bindal and Singh, 2019).

2.4. Global scenario of arsenic distribution in groundwater

Arsenic contamination has affected over 70 countries worldwide (Jha & Tripathi, 2021). Some of the majorly affected countries include western USA, Mexico, Chile, Argentina, Hungary, Romania, Mongolia, Nepal, China, Bangladesh, Taiwan, Vietnam, Thailand, and India. High concentrations of arsenic in ground water have been reported from countries across six continents, including Asia, Europe, North America, South America, Africa, and Oceania (Mukherjee et al., 2006). Majorly affected countries are concentrated in east and south-east asia. The arsenic problem in Europe is most concerning in Hungary (Egyedi and Pataky, 1978); Serbia, and Croatia (Petruseveski and Sharma, 2007); Argentina, (Nicolli et al., 2012; Smedley et al., 2002); Chile, (Ferreccio and Sancha, 2006); Mexico, (Cebrian et al., 1983), and other Latin American countries are aware of the problem of arsenic contamination in water. Aside from that, many other countries, including Ghana, Egypt, and Australia, have significant amounts of arsenic contaminated ground water (Mukherjee et al., 2006). The distribution of arsenic affected countries around the world is shown in **Fig. 2.2.**

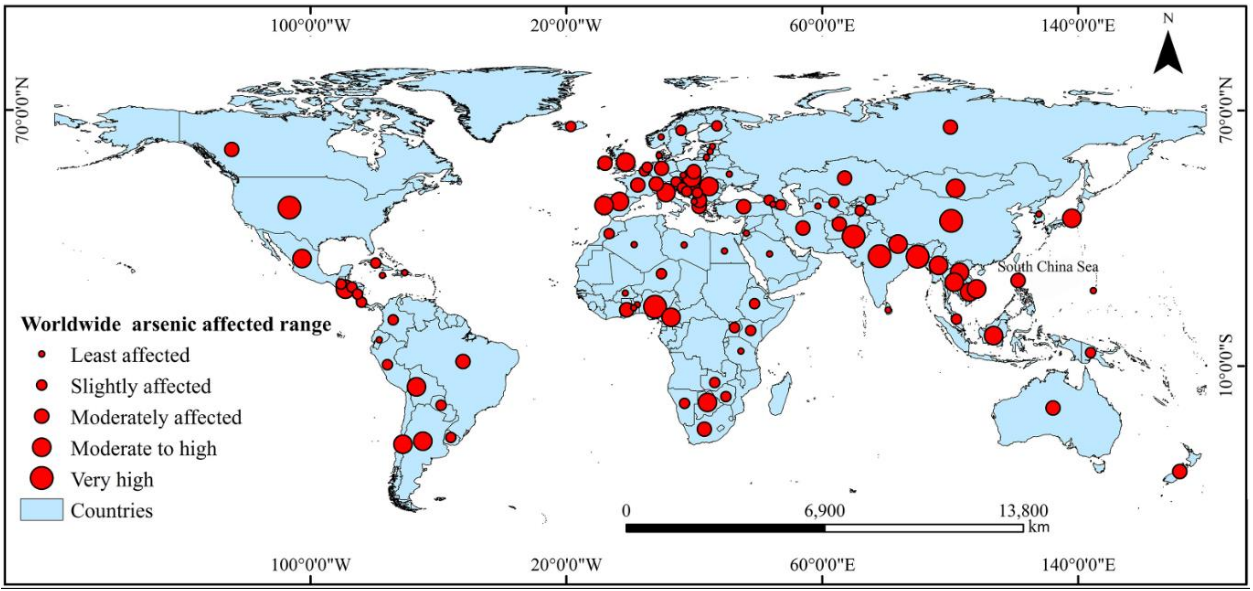

Fig. 2.2: Arsenic affected countries around the world (Source: Shaji et al., 2021)

2.5. Indian scenario of arsenic distribution in groundwater

In 1976, the Indian Union Territory of Chandigarh reported the first groundwater arsenic incident and its health effects (Chakraborti et al., 1999). Groundwater arsenic contamination and reports of arsenicosis patients first appeared in West Bengal in 1982. As time passed, more and more incidents of ground water contamination and the suffering of exposed individuals came to light in Bihar, 2002; Uttar Pradesh, 2003; Jharkhand, 2004; and the Upper Ganga Plain of Uttar Pradesh (Chakraborty, 2009). Geogenic arsenic contamination has been reported in the floodplains of the Ganga Brahmaputra and its tributaries in the states of Uttar Pradesh, Bihar, West Bengal, Manipur, and Assam. Recently, Manipur state reported that among 628 ground water samples tested, 63 percent contained arsenic levels above the World Health Organization (WHO) standard and 40 percent contained arsenic levels above the Bureau of India standard (BIS) (Chakraborty et al., 2008). Arsenic levels in the western and northern parts of Tripura, the Dibang district of Arunachal Pradesh, and the Mokokchung and Mon districts of Nagaland are above the permissible limit (Rahman et al., 2009).

About 70.4 million people have been chronically exposed to drinking arsenic-contaminated hand tube-well water (Chakraborty et al., 2011). The distribution of arsenic affected states in India is shown in **Fig. 2.3.**

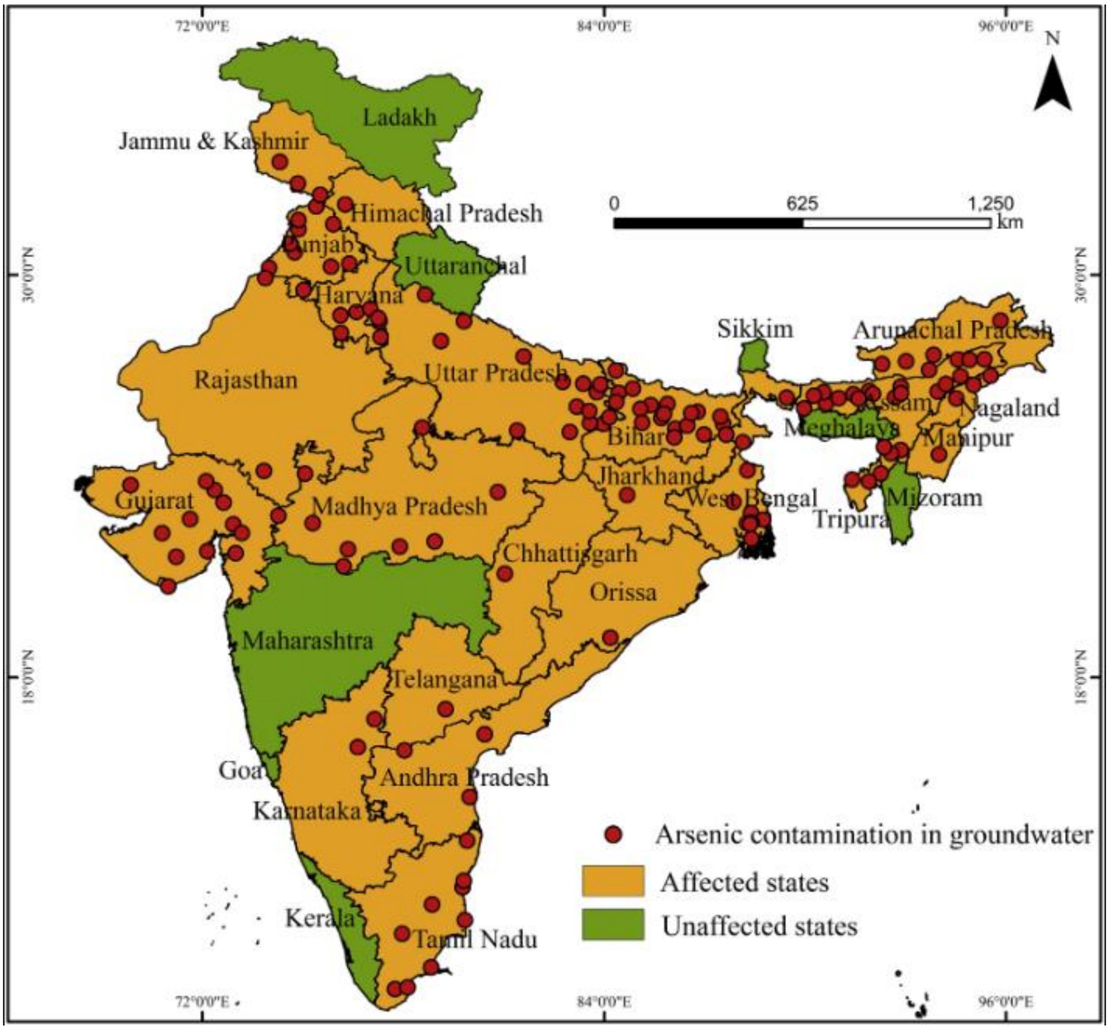

Fig. 2.3: Arsenic affected states of India (Source: Shaji et al., 2021)

2.6. Arsenic distribution in groundwater of West Bengal

In 1983, the first arsenicosis patients were identified in a village in the South 24-Parganas district, with 16 people suffering from arsenical skin manifestations (Roychowdhury, 2010). Groundwater in 22 villages from five West Bengal districts was reported to be arsenic-contaminated above 0.05 mg/L in 1988 (Chakraborty et al., 2009); gradually, its severity and health effects have been reasonably well documented in recent publications (Das et al., 2021;

Joardar et al., 2021; Singh et al., 2007). Nine out of 23 districts in West Bengal have been reported as arsenic contaminated above 0.05 mg/L in shallow aquifers, and 3417 villages from 107 blocks are on the list (Chakraborty et al., 2009). Murshidabad, Malda, Nadia, North 24 Parganas, South 24 Parganas, Burdwan, Howrah, Hooghly, and Kolkata are among the nine districts.

The Ganges, Brahmaputra, and Meghna River deltas is first associated with subsurface arsenic contamination (Acharya et al., 2000). The basin's extensive alluvial plain covers 569,749 km^2 (Chakraborty et al., 2013), and approximately 75 million people are now at risk of arsenic poisoning (Mukherjee and Bhattacharya, 2001). The distribution of arsenic affected states in West Bengal over general geology is shown in **Fig. 2.4** & **Fig. 2.5** shows districts of West Bengal affected by arsenic.

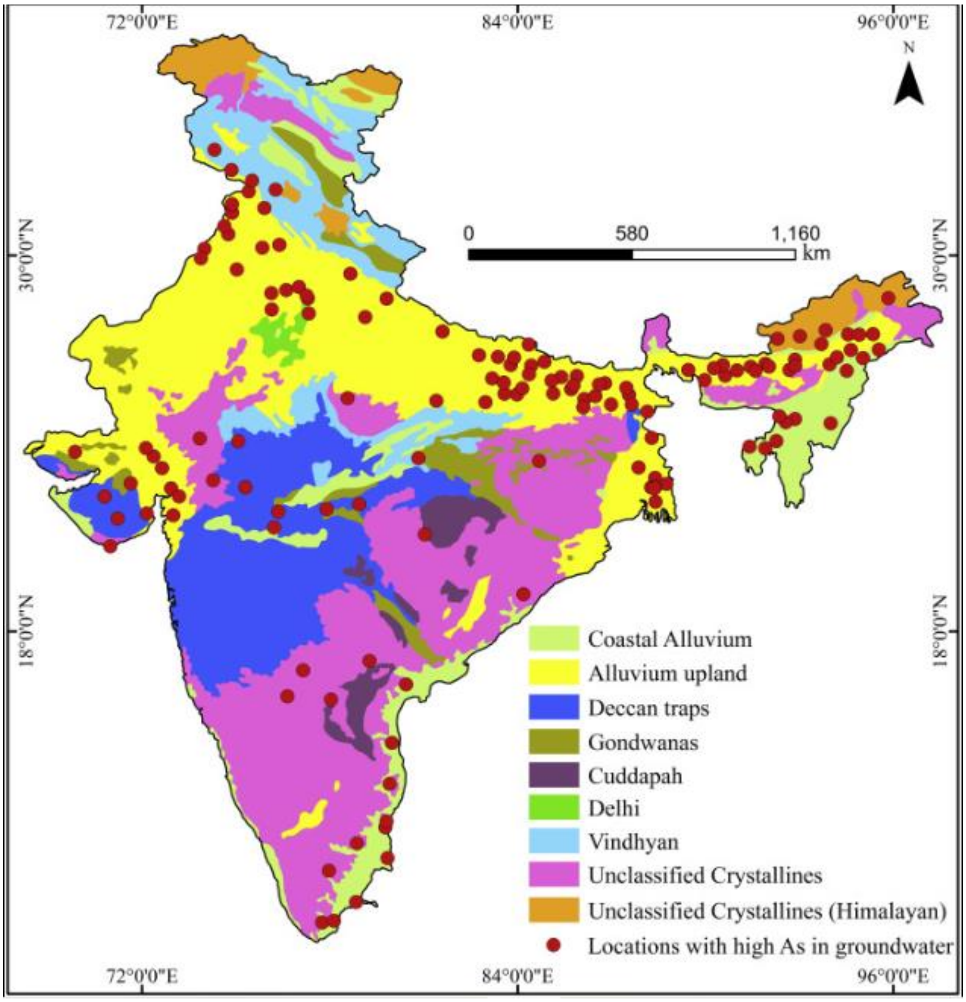

Figure 2.4: Arsenic affected areas superimposed on the general geology of India

(Source: Shaji et al., 2021)

Fig. 2.5: Arsenic affected districts of West Bengal (Source: Mukherjee et al., 2009)

2.7. Toxicity, health impacts & permissible limits

59% of the samples contained arsenic above 50 µg/L when tested on water samples (n = 10,991) collected from 42 arsenic-affected districts of Bangladesh (Chowdhury et al., 2000). About 34% of the groundwater samples (n = 58,166) collected from nine districts of West Bengal exceeded 50 µg/L of arsenic. The earliest symptoms include darkening of the skin (diffuse melanosis) on the palm of the hand or the sole of toes or in the whole body. Spotted pigmentation is common on the chest, back or limbs. Keratosis develops late as a feature of arsenical dermatosis. In severe cases, patients develop complications such as liver enlargement, spleen enlargement, and fluid in the abdomen. The level of unawareness and superstition is such that the villagers claimed these health effects of arsenic an act of God.

Persons who have consumed arsenic-contaminated water can be seen to develop carcinoma affecting the lungs, uterus, bladder, genitourinary tract. Acute promyelocytic leukaemia is being treated by arsenic trioxide (As_2O_3) (Ratnaike, 2003). Mostly absorption occurs from ingestion, very little absorption occurs from skin contact and through inhalation. They have mentioned skin diseases, gastrointestinal problems, cardiovascular system failure, neurological damage, genitourinary system damages as clinical features of chronic poisoning (Ratnaike, 2003). **Fig. 2.6** & **Fig. 2.7** shows health impacts associated with chronic arsenic consumption.

Figure Squamous cell carcinoma on heel. The patient was from the village of Singerdanga (police station Gaighata), North 24-Parganas District.

Figure Hyperkeratosis on sole. The patient died of lung cancer. The patient was from the village of Chandpur (rail line; police station Basirhat), North 24-Parganas District).

Fig. 2.6: Health impacts of arsenic (Source: Chowdhury et al., 2000**)**

By inhibiting several mitochondrial enzymes and by separation of oxidative phosphorylation, the cellular respiration gets impaired and arsenic can exert its toxic effects (Chakraborti et al., 2011). Arsenite species inactivates sulphohydrl (-SH) group of protein and enzymes rendering them inactive and causes cell damage by increasing reactive oxygen species in the cell (Chakraborti et al., 2011). Because arsenite (As^{3+}) is more soluble, it can deactivate essential enzymes of body and is the reason for multi systematic noncancerous effect. There is presence of As^{3+}, As^{5+}, MMA (V), DMA (V) and also MMA (III), and DMA (III). Indirectly inorganic arsenic enhances cancer developing chromosomal alterations, inhibit DNA repair process, oxidative stress, and cell proliferation. Arsenate (AsO_4^{3-}) can substitute phosphate (PO_4^{3-}) because of similarity in their structures. Thus, arsenate substitutes ADP and prevents the formation of ATP that produces energy in the cell (Chakraborti et al., 2011). Several health impacts including dermal effects, cardiovascular effects, respiratory effects, gastrointestinal effects, liver and spleen damage, endocrinological effects, diabetes mellitus, neurological effects, reproduction and developmental effects, cancer effects, and other effects are caused directly or indirectly by arsenic (Chakraborti et al., 2011).

Fig. 2.7: Health impacts of arsenic (Source: Chakraborti et al., 2011)

Arsenic is found in elemental, organic, inorganic, and gaseous forms (Kapp Jr., 2016). Due to its insolubility in body fluids, metallic arsenic is non-toxic. Arsenic reacts with various elements to form stable compounds. If the reaction is with carbon compounds, it is called organic arsenic, otherwise inorganic. The inorganic form of arsenic is the most toxic & carcinogenic. The most commonly found inorganic arsenic compounds are arsenite, As (III) & arsenate, As (V). The order of arsenic toxicity is as below:

As (III) > MMA (III) > DMA (III) > DMA (V) > MMA (V) > As (V)

Here, MMA (III) is Monomethylarsonous acid, DMA (III) is Dimethylarsinous acid, MMA (V) is Monomethylarsonic acid & DMA (V) is Dimethylarsenic acid (Chakraborti et al., 2011).

A summary of sources of arsenic pollution and the associated health hazards have been shown in **Fig. 2.8.**

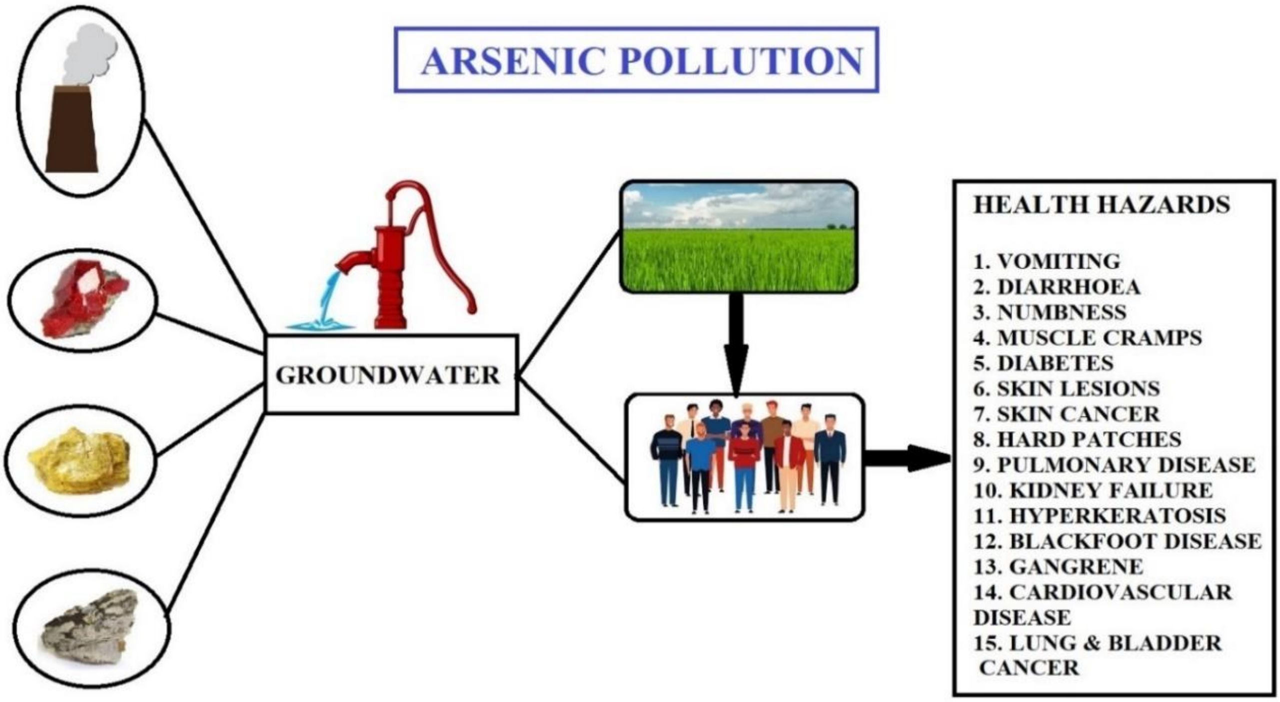

Fig. 2.8: Arsenic pollution and associated health hazard

WHO (2018) has prescribed the guideline and limits arsenic in drinking water to 10 µg/L. This permissible limit varies according to a location's climatic conditions. As a result, each country in the world has different permissible limits based on geography, temperature, and humidity.

2.8. Arsenic Removal technologies

Numerous studies are being conducted to tackle this devastating problem prevailing in East Asia & other parts of the world. Below listed currently used methods are not an exhaustive list:

2.8.1. Adsorption

This method is a suitable and most efficient technique for low-income countries with a lack of skilled manpower. This method is not dependent on chemical addition and can be implemented in an area with an inconsistent electricity supply. There are numerous kinds of adsorbents being used these days like activated alumina (Camcho et al., 2015; Hao et al., 2009), granular activated carbon (Gu et al., 2005), waste carbonaceous materials (Lal et al., 2020), biochar (Agrafioti et al., 2014); Govindaswamy et al., 2011; Zhang et al., 2013; Zhang et al., 2016), polymeric adsorbents (Kumar et al., 2011), nanoparticles (Lata and Samadder, 2016), iron coated sand (Gupta et al., 2013), etc. This method works on the principle of the use of solid with high surface area to eliminate substances from gaseous or liquid solutions. The main advantages of this technique are its low cost, high removal efficiency, flexibility in use, sludge-free and secure operation. However, this technique is suitable for the removal of arsenic from low concentration areas only.

2.8.2. Ion Exchange

This is based on the mechanism of ions sharing with equal numbers of ions from contaminated water. Kartinen and Martin (1995) has explained the process of arsenic removal using Ion exchange method. In vessels for arsenic removal, an ion exchange resin is placed, which is usually loaded with chloride ions at the "exchange sites." Water containing arsenic is passed through the vessels, where the arsenic "exchanges" for chloride ions. The water exiting the vessel contains less arsenic but more chloride than the water entering it. The resin eventually becomes "exhausted," which means that all or most of the "exchange sites" that were previously loaded with chloride ions become loaded with arsenic or other anions. The chloride ions that were previously on the resin were exchanged for arsenic and other anions in the water being treated.

2.8.3. Chemical precipitation – This method works on the principle of precipitate formation which removes ionic metals by reacting with added chemicals. Alum coagulation (Cheng et al., 1994), iron coagulation (Lakshmanan et al., 2010), lime softening (Fields et al., 2000), and iron-manganese (Edwards, 1994) can be used as precipitation method to remove arsenic.

2.8.4. Electrocoagulation – This is an alternative to chemical precipitation where metallic cations are directly produced by the application of a current amid electrodes (Fe) to liquefy soluble anodes in the contaminants (Nidheesh and Singh, 2017). Various electrodes like Iron, aluminium, and titanium are used to immobilize arsenic from water (Kumar et al., 2004).

2.8.5. Electrokinetic technique – This technology is based on the mechanism that guides the transport and movement of pollutants in the soil under an electric field. Example – Electrophoresis (Ahsan et al., 2010), electromigration (Isosaari and Sillanpää, 2010), water electrolysis (Li et al., 2014), and electroosmotic flow (CREED, 1997).

2.8.6. Membrane technology – In this method, a membrane is placed before the contaminants that allow the movement of selective molecules to pass through. This technology requires a driving force which ultimately consumes a lot of electricity. Reverse osmosis (Elcik et al., 2016; Ning, 2002; Schneiter and Middlebrooks, 1983) and eletrodialysis (Mendoza et al., 2014) have been proven to be effective against arsenic removal from water.

2.8.7. Phytoremediation – The process of phytoremediation involves the hyperaccumulator plants accumulating toxic heavy metals from the soil. Several hyperaccumulators such as *Pteris vittata* are being researched for its efficacy against decontamination of heavy metals from the soil and/or water (Tu et al., 2004).

2.8.8. Bioremediation – It utilises the potential of Bacteria (Dey et al., 2016; Sher and Rehman, 2019), Fungi (Čerňanský et al., 2007), and Microalgae (Leong and Chang, 2020) to remediate heavy metals from the soil and/or water.

CHAPTER

3

FLUORIDE CONTAMINATION: A BRIEF REVIEW

Fluorides' beneficial effects on human health have been known for many years. The fluoride ion is a vital dietary component. It is beneficial to human bone and dental development when consumed at specific doses. It is very important in the formation of teeth when consumed at the proper levels (Robinson et al., 2004). Too little fluoride intake during childhood may lead to the development of preventable dental caries later in life. Dental caries is a disease caused by bacteria that live in dental plaque and ferment carbohydrates to produce acids that can demineralize tooth enamel (WHO, 2017). If this demineralization continues, the enamel is penetrated, allowing bacterial invasion and eventual tooth decay & loss in the absence of restorative dental care.

3.1. History & biogeochemistry

Fluorine, in the form of the calcium fluoride mineral fluorite, was first mentioned in writings from the 1500s, where it was used in metallurgy to aid in the working of molten metals (Meiers, 2008). In the 1600s, scientists discovered that adding acid to fluorite etched glass, which led to the discovery of hydrofluoric acid. Fluorine was not isolated until 1886, and in the process, it took several scientists' sight and lives (Meiers, 2008).

Fluorine is regarded as the most reactive element in the halogen family. The ionic form of elemental fluorine is fluoride. Fluoride is regarded as one of the most dangerous and toxic contaminants found in water. It is found in trace amounts in seawater, bone, teeth, and ground water, primarily as the fluoride ion. The majority of fluorides associated with monovalent cations, such as NaF and KF, are water soluble, whereas those associated with divalent cations, such as CaF_2 and PbF_2 are generally insoluble.

Fluoride is the ionic form of fluorine, which, due to its atomic structure, is an extremely reactive element. Fluorine is a yellow-brown poisonous gas that does not exist naturally and must be isolated through experimental methods. Fluorine is found naturally in rock, water, and food products and is used in a variety of products and industries. It has been at the center of controversial weapon manufacture and, for some, a highly controversial public health initiative over the last 200 years.

3.2. Sources of fluoride in the environment

The cradle to grave cycle of fluorine in the atmosphere is been depicted in **Fig. 3.1**. Fluoride in the environment is primarily caused by two sources: geogenic and anthropogenic.

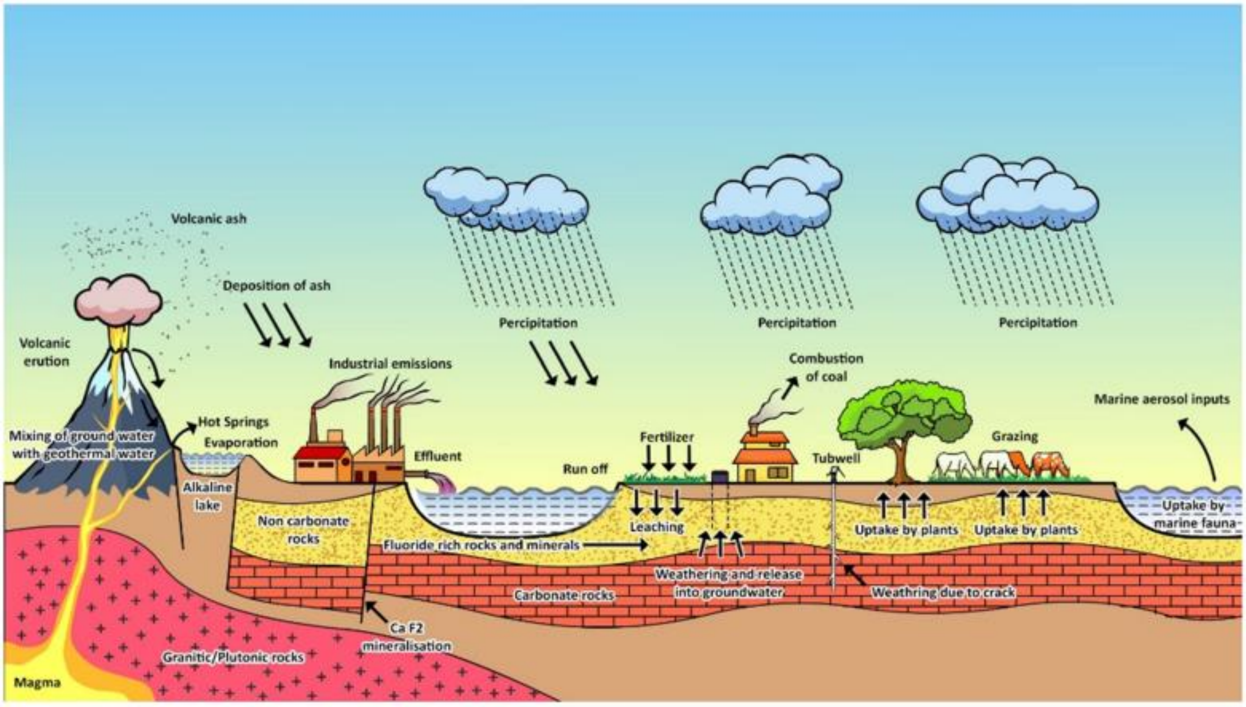

Fig. 3.1: Hydrogeochemical cycle of fluorine (Source: Mukherjee and Singh, 2018)

3.2.1. Geogenic sources

Fluoride presence in groundwater is a naturally occurring phenomenon that is influenced by the region's local and regional geologic setting and hydro-geological conditions. Fluoride is abundant in the earth's crust as a component of rocks and minerals. Fluoride is naturally present in rocks as fluorite (**Fig. 3.2**), fluorspar or calcium fluoride (CaF_2), apatite (**Fig. 3.3**) or rock phosphate [$Ca_3F(PO_4)_3$], cryolite (Na_3AlF_6), and as a replacement of ions in the crystal lattice of mica and many other minerals (Das et al., 1998; Das et al., 1999) and is released into groundwater by slow dissolution of such (Goswami et al., 2011).

Fluoride and OH ions are both negatively charged and have nearly identical ionic sizes. As a result, fluoride ion can easily replace OH ions present in rocks during the chemical reaction, increasing its concentration in rocks and minerals. When carbonate and bicarbonate rich water passes through such rocks, fluoride ion is released as a result of chemical reactions (**Reactions 3.1 and 3.2**) and percolates to the ground water, increasing its concentration (Saxena and Ahmed, 2001).

$$CaF_2 + Na_2CO_3 \rightarrow CaCO_3 + 2F^- + 2Na^+ \quad (3.1)$$

$$CaF_2 + 2NaHCO_3 \rightarrow CaCO_3 + 2Na + 2F^- + H_2O + CO_2 \quad (3.2)$$

Fig. 3.2: Fluorite

Fig. 3.3: Apatite

Fluoride is dissolved from geologic formations by rainwater and repeated irrigation of agricultural lands. As rainwater seep through the soil, it comes into contact with the aquifer's rocks and minerals. Fluoride from country rocks dissolves as a result of acid in the soil. Fluoride dissolved in groundwater may also contribute to the fluoride contamination phenomenon. Because of the drop in water level during the summer, the fluoride content of groundwater rises. The higher fluoride concentration in the summer may also be attributed to higher fluoride dissolution, which may be due to the presence of air in the minerals/rocks cavities, indicating that oxygen in the cavities of the geologic formation catalyzes the fluoride dissolution process. According to the evidence, as groundwater levels gradually drop below the earth's crust, a higher concentration of fluoride is found in the water due to greater fluoride dissolution from rocks and soil.

3.2.2. Anthropogenic sources

Industries are a significant source of groundwater contamination. Pollution is frequently caused by industrial effluents and other byproducts. Fluorosilicone acid and fluorocarbon polymer synthesis, gasoline production and coke manufacture, ceramic, cement, enamel, fibre glass, electronics, pesticides and fertilizers, surface heating operations, metal etching (with hydrofluoric acid), and wood preservatives are among the industries that emit significant amounts of fluoride in process waste streams (Chand, 1999). As a result of the processing of phosphate rock, fluoride discharged from fertilizer manufacturing processes is typically in the form of silicon tetra fluoride.

Fluoride may be present in power plant boiler cleaning wastes due to its presence in the cleaning formulation. Fluorspar and limestone are both basic fluxing materials used in steel production. The primary source of fluoride-containing waste water from this industry is air pollution control scrubber water from steel manufacturing in basic oxygen, open hearth, and electric arc furnaces, as well as in the sintering plant. The fluoride compound Cryolite is used as a catalyst in the primary aluminum processing industry in bauxite ore reduction; the gaseous fluoride produced by this process is discharged directly into the atmosphere, or the fluoride into aqueous waste streams from wet scrubbing of the process fumes (Samal and Naik, 1988). Fluoride levels in wastewater streams range from 107 to 145 mg/L on average for aluminum reduction plants. The number of echinocytes has been found to increase with the duration of fluoride exposure among workers in aluminum smelters (Susheela and Toteja, 2018).

Fluoride concentrations near glass manufacturing processes have been reported to range between 1,000 and 3,000 mg/L (Yadav and Lata, 2003). Depending on the pH of the waste, glass and plating wastes typically contain fluoride in the form of hydrogen fluoride or fluoride ion. A high level of fluoride has been detected in groundwater near the aluminum industry (Susheela et al., 2013). Local clay and coal combustion are the main sources of fluoride in brickworks (Bano et al., 2020; Jha et al., 2008). Fluoride contamination in groundwater has also been reported due to by-products of brick kilns.

To some extent, nonpoint sources of groundwater pollution contribute fluoride to ground water. Modern agricultural practices, which include the use of fertilizers in conjunction with pesticides containing fluoride, also contribute fluoride to groundwater (Naik et al., 2017). The use of phosphate fertilizers may also be one of the factors contributing to high fluoride concentrations in groundwater via irrigation return flow (Jain et al., 2010). Irrigation with fluoride-containing water would tend to concentrate these ions in the soil. Fluoride ions will be absorbed or co-precipitated with calcium ions if they are removed as calcite. If the carbonate concentration is high enough to precipitate calcium as calcite without removing fluoride ions, these ions may migrate to the water front and eventually join the main groundwater body (Handa, 1979). The United States Environmental Protection Agency (EPA Report, 1976) has recommended 1 mg/L fluoride in irrigation water for continuous use but up to 15 mg/L fluoride in fine soils for short term use (< 20 years). Another significant nonpoint source of fluoride contamination is the production of fly ash. More than 150 million tonnes of fly ash are produced globally each year as a result of coal combustion in power plants (Dwivedi and Jain, 2014; Piekos and Paslawska, 1998). At least half of this amount is disposed of in landfills, contributing to environmental pollution from fluoride leaching. Fluoride has been detected in the atmosphere near Agra, India, due to the presence of approximately 16 brickworks in that area (Jain et al., 1999). Groundwater contamination may occur as a result of fluoride traces in the atmosphere during the rainy season. The Geological Survey of India has also released significant data indicating that fluorite, topaz, apatite, rock phosphates, phosphatic nodules, and phosphorites are common in India and contain high fluoride percentages. Fluoride leaches out and contaminates not only groundwater but also soil, contaminating agricultural crops as a result of their high mineral content.

Fluoride has been found in cosmetics and drugs, in addition to foods (Ghosh et al., 2013).

The use of sodium fluoride-containing drugs for osteoporosis, osteosclerosis, and dental caries is very common. Various toothpaste brands contain excessive amounts of fluoride. Fluoride enters the bloodstream directly from the oral cavity via the fine blood vessels of the mouth. Fluoride is a persistent bio accumulator; even small amounts that enter through fluoride toothpaste ensure entry in both children and adults, and the cumulative effects of fluoride are a serious concern.

3.3. Extent & mechanism of contamination

Fluoride concentrations in groundwater are generally determined by the concentration of fluoride-bearing minerals in rock types, as well as their decomposition and dissolution activities via rock-water interactions. An alkaline environment with a high bicarbonate concentration is more conducive to fluoride dissolution in groundwater (Saxena and Ahmed, 2001), implying that the pH of groundwater is more important in determining fluoride concentration. Thus, fluoride in solution is produced by the weathering of primary minerals in rocks and the leaching of fluoride-containing minerals (Saxena and Ahmed, 2003). Mechanism of formation of fluoride in groundwater is shown in **Fig. 3.4.**

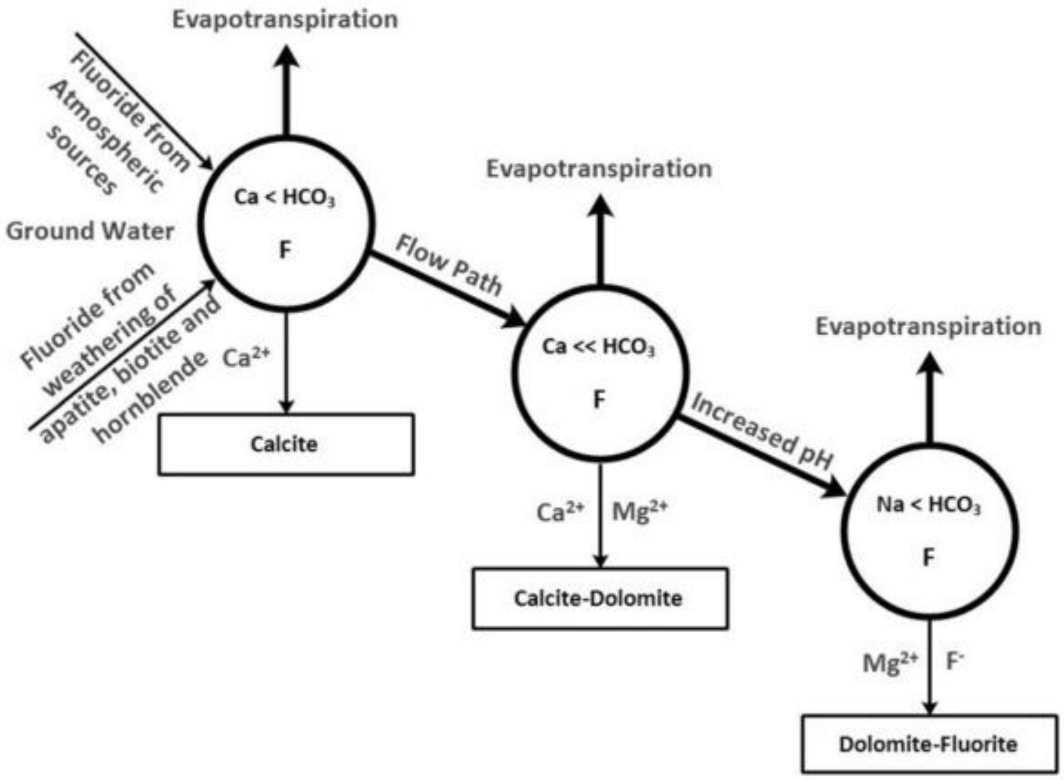

Fig. 3.4: Mechanism of formation of fluoride in groundwater (Source: Mukherjee and Singh, 2018)

Fluorite is the mineral that most strongly influences fluoride concentrations in natural water. Because fluorite's solubility product is very low, water with low calcium content should have a high fluoride concentration (Apambire et al., 1997). Fluoride concentrations are always high in sodium bicarbonate and bicarbonate chloride groundwater. The water-soluble fluoride content of sodic surface soil treated with gypsum increases as the exchangeable sodium percentage increases (Chhabra et al., 1980). These findings, along with the exchange mechanism proposed, are significant in light of the reported excess fluoride in groundwater due to high sodicity of soil near major south Indian irrigation schemes, which causes fluorosis in nearby populations (Datta et al., 2000; Singh, 2000; Umar and Sami Ahmad, 2000). The fluoride-rich groundwater comes from an active geothermal system, where dissolved fluoride concentrations can exceed 1000 mg/L (Ozsvath, 2009; Edmunds and Smedley, 2005). However, Edmunds and Smedley (2005) reported that the most common type is high fluoride bearing groundwater that occurs in areas of active geothermic activity, which is alkali-chloride solutions with neutral pH and fluoride concentrations ranging from l-10 mg/L.

3.4. Global scenario of fluoride distribution in groundwater

More than 200 million people worldwide (Rasool et al., 2018) are estimated to rely on drinking water with fluoride concentrations that exceed the current WHO guideline of 1.5 mg/L (Susheela et al., 1999). Indoor air pollution caused by coal combustion may contribute significantly to daily fluoride intake in some areas (Ando et al., 1998; Chen et al., 1990; Lin and Liu, 2020).

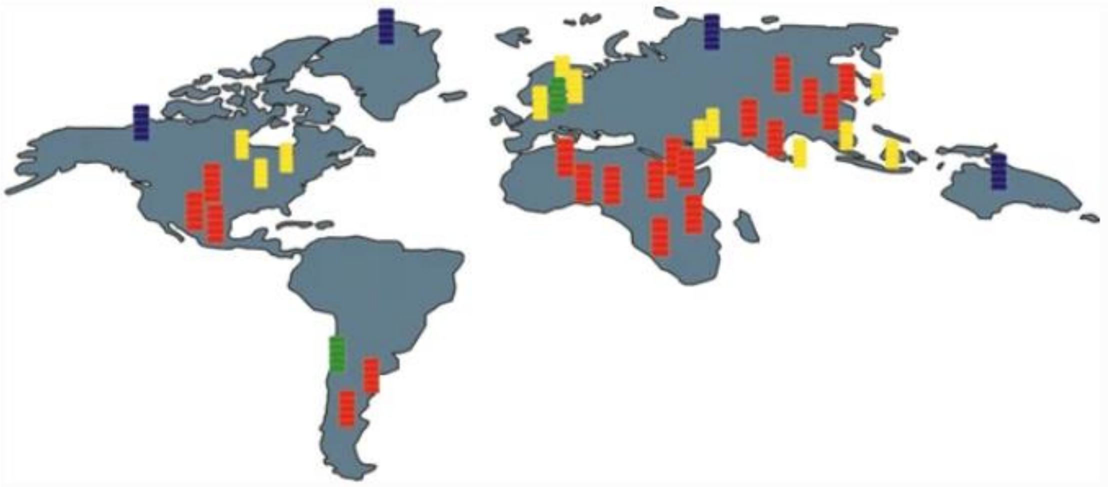

Fig. 3.5: Global distribution of fluoride (Ali et al., 2016).

Fluorosis, caused by high fluoride levels in drinking water, has been reported in a number of countries around the world, including India, China, Tanzania, Mexico, Argentina, and South Africa (Ali et al., 2016). The Global distribution of fluoride is shown in **Fig. 3.5.** In this figure, *Red bars* indicate highly affected areas; *Yellow bars* indicate moderately affected areas; *Green bars* shows the least affected areas; *Blue bars* shows lack of sufficient data. It is to be noted that in general highly affected areas are arid and semi-arid regions.

3.5. Indian scenario of fluoride distribution in groundwater

Fluoride was first discovered in India in the Nellore district of Andhra Pradesh in 1937 (Subba Rao, 2003). Since then, extensive research has been conducted in various parts of India to investigate fluoride-contaminated water sources and their effects on humans and animals. Fluorosis is currently estimated to be prevalent in 17 of India's 29 states and 7 union territories (Fig. 3.6). Andhra Pradesh, Assam, Bihar, Delhi, Gujarat, Haryana, Jammu and Kashmir, Karnataka, Kerala, Madhya Pradesh, Maharashtra, Orissa, Punjab, Rajasthan, Tamil Nadu, Uttar Pradesh, and West Bengal are among the fluoridated states (Mukherjee and Singh, 2018). Spatial distribution of fluoride in groundwater of India has been shown in **Fig.3.6.**

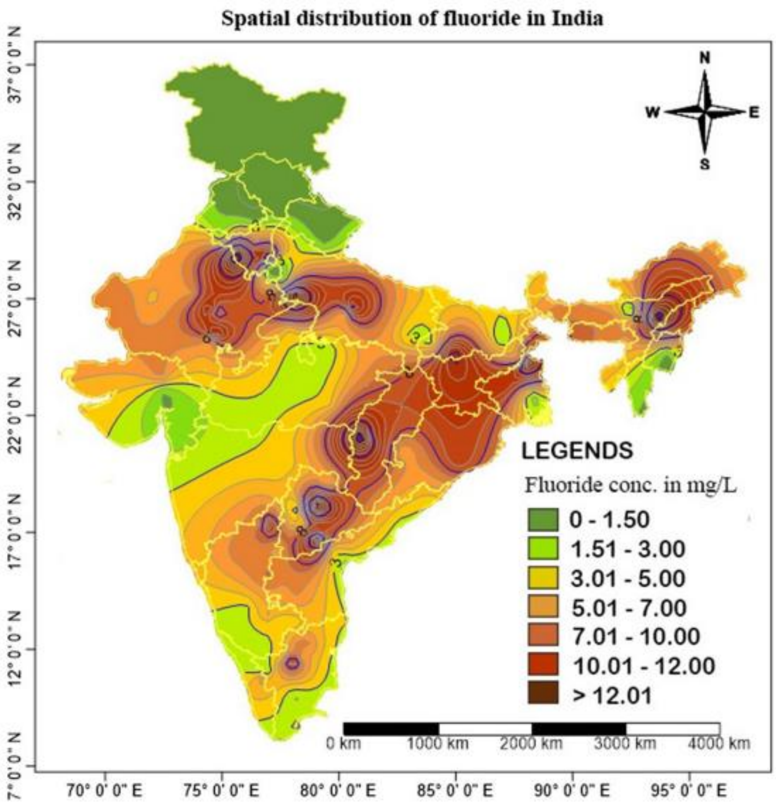

Fig 3.6: Spatial distribution of fluoride in India (Source: Mukherjee and Singh, 2018)

3.6. Fluoride distribution in groundwater of West Bengal

Mukherjee and Singh (2018) investigated a comprehensive study on the states of India. They have mentioned that West Bengal's lithology (**Fig. 3.7**) is distinguished by the Gondwana supergroup, the Singhbhum Group, the Baikunthapur formation, the Chalsa formation, the Lalgarh formation, and granitic gneiss.

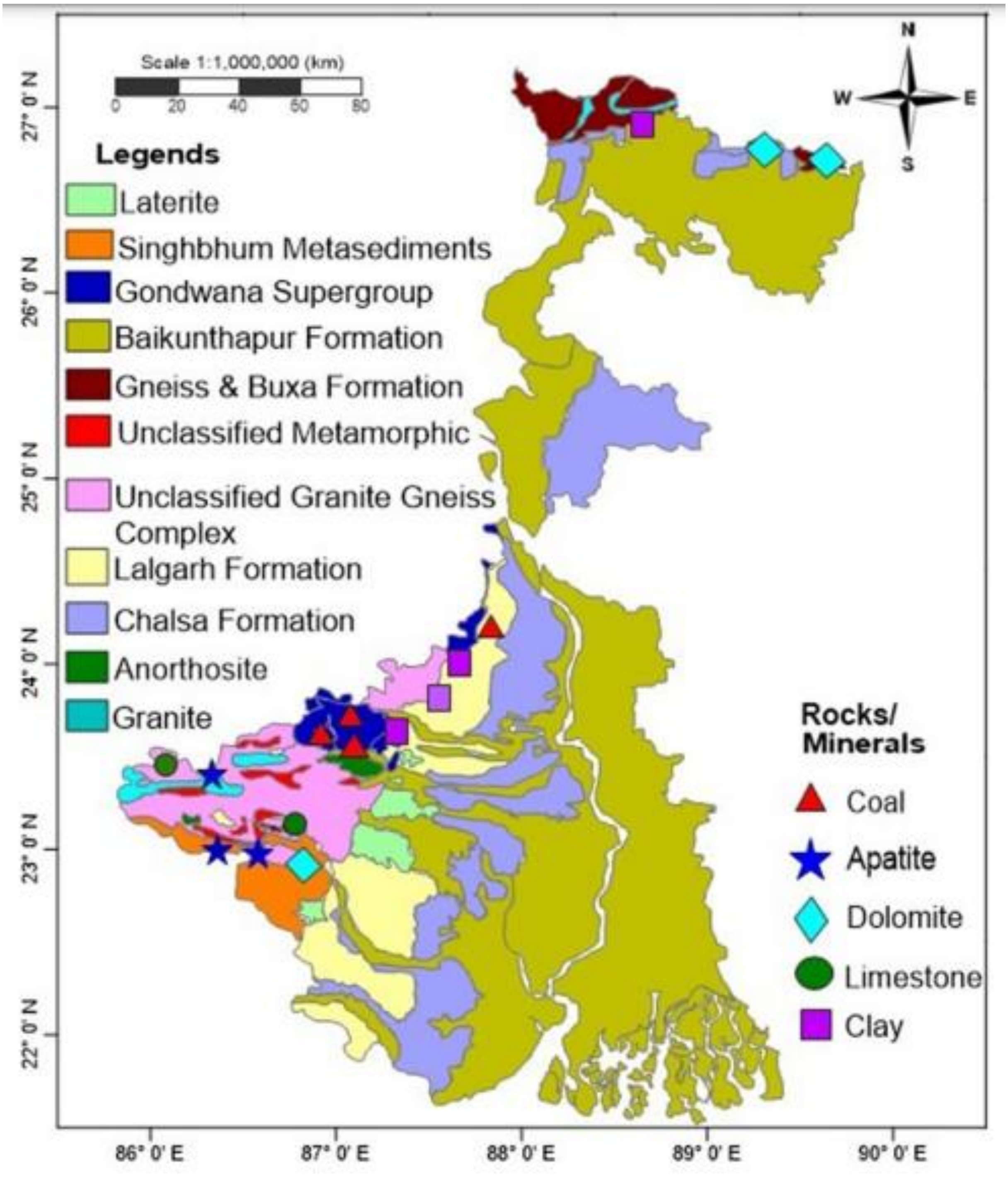

Fig. 3.7: Geological map of West Bengal (Source: Mukherjee and Singh, 2018)

According to Datta et al. (2014), the concentration of fluoride in West Bengal districts was within tolerable limits except in Nadia, 24 Parganas, Burdwan, Purulia, and Midnapur. Low fluoride concentrations (0.01 to 1.18 mg/L) were discovered in 17 blocks of Hooghly district (Kundu and Mandal 2009). As a result, the western part of the state (Birbhum, Bankura, and Purulia) is the worst-affected, with high fluoride concentrations in groundwater. **Fig. 3.8** shows spatial distribution of fluoride affected districts of West Bengal

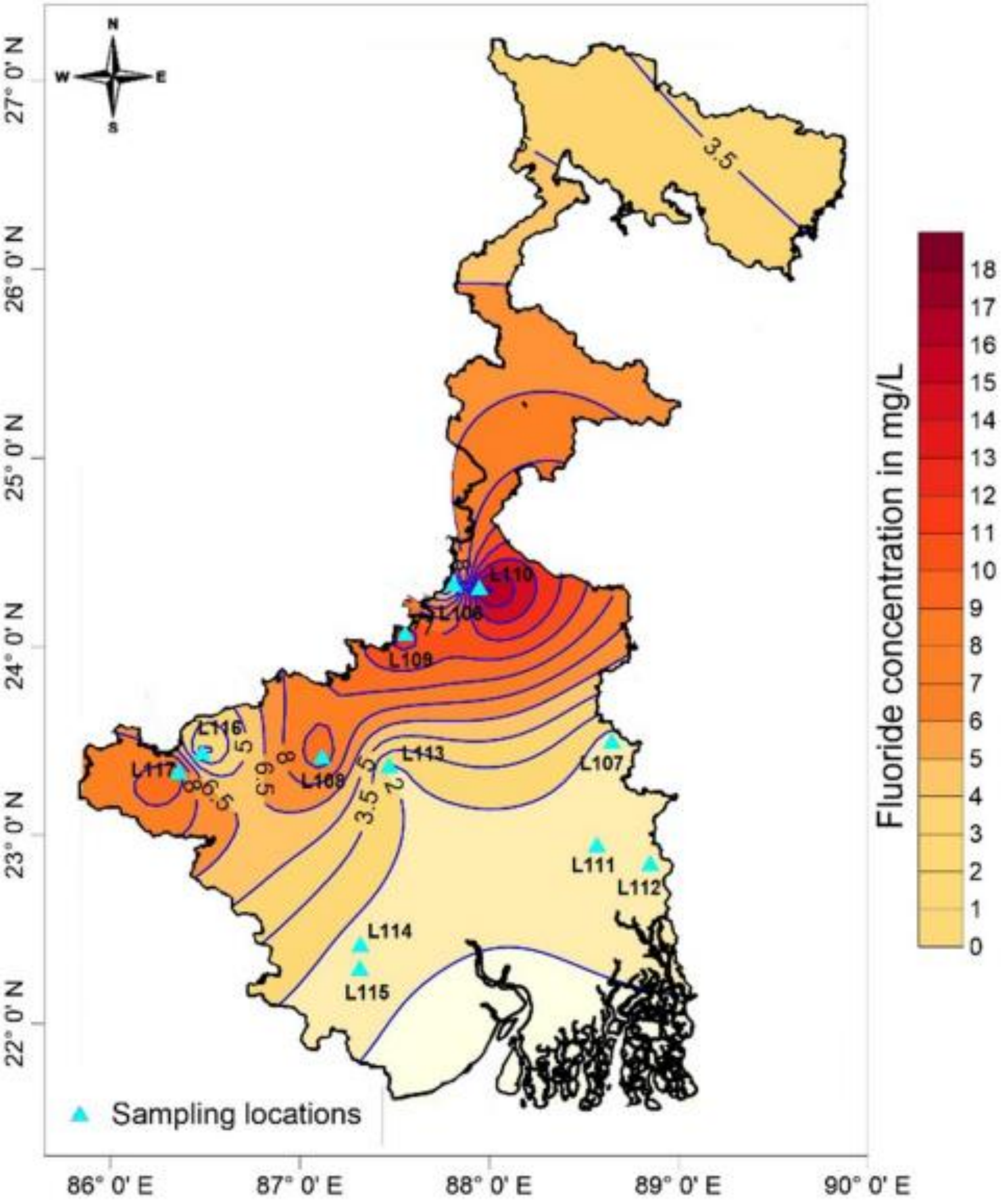

Fig. 3.8: Spatial distribution of fluoride affected districts of West Bengal (Mukherjee and Singh, 2018)

3.7. Toxicity, health impacts & permissible limits

Fluorosis is an endemic disease caused by long-term fluoride exposure. So far, two types of fluorosis have been identified: dental fluorosis (**Fig. 3.9**) and skeletal fluorosis (**Fig. 3.10**). Fluorosis occurs as a result of fluoride concentrations in drinking water that are both high (>1.5 mg/L) and low (0.6 mg/L), with known health effects and benefits for humans. Teeth mottling is characterized initially by opaque white patches on the teeth and progresses to dental fluorosis (brown to black staining of the teeth) followed by pitting of the tooth surfaces (Revelo-Mejía et al., 2021; Thylstrup and Fejerskov, 1978).

High levels of dental fluorosis are most common in children under the age of 12. Skeletal fluorosis is a bone disease caused solely by consuming more than 3 mg/L of fluoride (Cook et al., 2021; Srivastava and Flora, 2020). Mild cases of skeletal fluorosis cause minor complications. Skeletal fluorosis, on the other hand, causes excruciating pain as well as severe bone and joint damage in severe cases (Shashi et al., 2008). When the water supply contains more than 10 mg/L of fluoride, it can cause crippling skeletal fluorosis (Brouwer et al., 1988). Fluorosis severity is determined by the fluoride concentration in drinking water, daily intake, continuity and duration of exposure, and climatic conditions. Image of a patient's teeth suffering from mild fluorosis has been shown in **Fig. 3.9.**

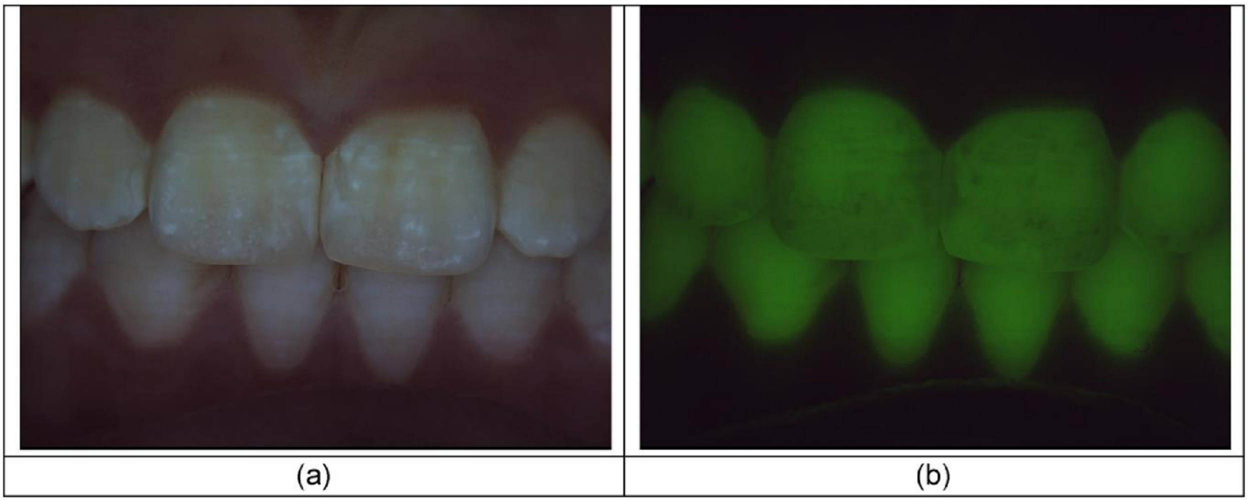

Fig. 3.9: Image of a patient suffering from mild fluorosis. a) Polarised white light image. b) Fluorescence image (Source: Liu et al., 2018).

Table 3.1: Effects of various concentrations of fluoride

Fluoride concentration (mg/L)	Effects
<1.0	Safe limit
1.0-3.0	Dental fluorosis
3.0-4.0	Stiffened and brittle bones and joints
4.0-6.0 and above	Deformities in knee and hip bones and finally paralysis making the person unable to walk or stand in straight posture, crippling fluorosis.

The various effects of fluoride intake against different concentrations has been shown in **Table 3.1**. To understand the level of severity, some images of affected patients have been shown in **Fig. 3.10.**

Fig. 3.10: Dental & skeletal fluorosis in affected people from Bankey Bazar and Rajauli

(Source: Mridha et al., 2021)

Because fluoride has two effects on human health, the World Health Organization (WHO) recommends that drinking water contain a minimum of 0.6 mg/L fluoride and a maximum of 1.5 mg/L fluoride (Saxena and Ahmed, 2001; WHO, 2008). This permissible limit varies according to a location's climatic conditions. As a result, each country in the world has different permissible limits based on geography, temperature, and humidity.

In drinking water, the US standard is between 0.6 and 0.9 mg/L, while India's standard is between 0.6 and 1.2 mg/L (ISI, 1983; Poonia et al., 2021), and it is the same in China (Li et al., 2009) and Bangladesh. In addition to fluorosis, excessive fluoride consumption frequently causes urinary tract manifestations, allergic manifestations, gastro intestinal problems, neurological and muscular problems, cancer, brain damage, Alzheimer's syndrome, and thyroid disorder (Ghosh et al., 2013; ISI, 1983).

3.8. Defluoridation technologies

To keep fluoride levels within the WHO allowable limit, various defluoridation techniques are used to treat fluoride-contaminated water. All defluoridation techniques are classified into two types: physical processes and chemical processes. Adsorption, ion exchange, and membrane separation techniques are examples of physical processes. Chemical coagulation-precipitation and electro-coagulation techniques are used in the chemical process. The following section provides a brief overview of each process.

3.8.1. Physical process

a) Adsorption method

Adsorption is a physical process that is inexpensive and simple to handle. Adsorbents should be economical, readily available, easy to handle, and have good fluoride adsorption behavior. Many adsorbents have been reported in the literature, including biological materials, natural clay materials, agricultural waste materials, metal oxides and hydroxides, and calcium and iron based adsorbents (Chiavola et al., 2019); Wan et al., 2021, Zhang et al., 2017). Plaster of Paris (Gopal and Elango, 2007), granular red mud (Pepper et al., 2017), pyrophyllite (Goswami and Purkait, 2011), PCB (Viswanathan et al., 2009), alumina (Alhassan et al., 2021), acidic alumina (Goswami and Purkait, 2012), calcium aluminates (Sakhare et al., 2012), etc.

Apart from these adsorbents, nano sized adsorbents such as nano alumina (Kumar et al., 2011), Fe-Al-Ce nano-adsorbents (Chen et al., 2009), and others (Ghosh et al., 2022) are used in water defluoridation. Despite the fact that many adsorbents have been reported in the literature, researchers are still looking for better, more efficient, and cost-effective adsorbents to aid in the treatment of fluoride-contaminated water.

b) Ion-exchange method

Adsorption and ion exchange are both physical processes. Fluoride can be removed from water supplies using a strongly basic anion-exchange resin containing quaternary ammonium functional groups in this method (Padungthon et al., 2014).

Meenakshi and Vishwanathan (2007) has deduced that fluoride ions replace the resin's chloride ions. This process is repeated until fluoride has occupied all of the sites on the resin. The resin is then backwashed with supersaturated water containing dissolved sodium chloride salt. The fluoride ions are then replaced by new chloride ions, causing the resin to be recharged and the process to begin again. The stronger electro negativity of fluoride ions drives the replacement of chloride ions from the resin. Indion FR10 and Ceralite IRA 400 resin were investigated as defluoridating agents. The same author has also investigated metal ion incorporation in ion exchange resin, which is used to remove fluoride from water.

c) Membrane based technologies

Membrane-based techniques such as reverse osmosis (RO), nano-filtration (NF), dialysis, and electro-dialysis are becoming increasingly popular in separation and purification technology. In recent years, the RO membrane process has emerged as a preferred alternative for providing safe drinking water without the issues associated with other traditional methods (Shenvi et al., 2015). RO is a physical process that removes contaminants from feed water by applying pressure to it and directing it through a semipermeable membrane. As a result of the applied pressure to the concentrated side of the membrane, which overcomes the natural osmotic pressure, the process is the inverse of natural osmosis. The size and electrical charge of ions are used to reject them by the RO membrane which ultimately generates water that is extremely pure. Ndiaye et al., (2005) investigated the removal of fluoride from effluents using the RO technique. When the RO membrane was fully regenerated after each set of experiments, the rejection of fluoride ion was typically greater than 98%. Cost, recovery, rejection, raw water characteristics, and pre-treatment are all factors that influence membrane selection. The process's efficiency is governed by various factors such as raw water characteristics, pressure, temperature, and timely monitoring & maintenance.

Shahmansouri and Bellona (2015) has reviewed nanofiltration technology in water treatment and they have mentioned that nano-filtration employs the same general principle as reverse osmosis. The membranes used for nano-filtration have slightly larger pores than those used for reverse osmosis and offer less resistance to solvent and solute passage. As a result, pressure requirements are much lower, energy requirements are lower, solute removal is less exhaustive, and flows are faster. The selectivity of nano-filtration over reverse osmosis is a distinct advantage, and much experimental and theoretical effort is being expended to gain a better understanding of the mechanism of solute retention in order to facilitate the production and selection of targeted membranes, as well as the optimization of conditions (Diawara, 2008). Although fluoride is a very small ion, it is more strongly hydrated than other monovalent anions due to its high charge density, and the consequent steric effects lead to fluoride being more strongly retained on nano-filtration membranes than competing monovalent anions such as chloride or nitrate, a particular advantage in defluoridation of brackish water (Diawara, 2008). Lhassani et al., (2001) investigated the selective demineralization of water via nano-filtration, particularly its application to the defluoridation of brackish water. Ceramic and polymeric membranes are commonly used in RO and NF techniques. However, the application of polymeric membrane exceeds that of ceramic membrane. Ceramic membranes are commonly used in MF and UF techniques.

3.8.2. Chemical process

Chemical processes include chemical coagulation precipitation, also known as the Nalgonda technique, and electro-coagulation.

a) Chemical coagulation-precipitation method

The most common method of removing fluoride from water is chemical precipitation. There are two steps to this process. Precipitation occurs in the first step by adding lime, and coagulation occurs in the second step by adding alum. When alum is added to water, it reacts with some of the alkalinity in the first reaction to form insoluble aluminum hydroxide [$Al(OH)_3$]. Alum reacts with fluoride ions in the water in the second reaction. The best fluoride removal occurs at pH levels ranging from 5.5 to 7.5 (Potgeiter, 1990; Waghmare and Arfin, 2015).

b) Electro-coagulation method

An applied potential generates the coagulant species in situ as the sacrificial metal anode (aluminium or iron) dissolves, while hydrogen is simultaneously evolved as the cathode in the electro-coagulation process (Garcia-Segura et al., 2017). Coagulation species aggregate suspended particles or precipitate contaminants and adsorb them. Tiny hydrogen and oxygen bubbles formed during water electrolysis collide with air bubbles, causing pollutant particles to float. The selection of an electrode material is influenced by a variety of factors such as cost, oxidation potential, inertness to the system under consideration, and so on. Carbon (Garcia-Segura et al., 2017), mild steel (Vasudevan et al., 2009), iron (Malakootian et al., 2010), titanium (Naje et al., 2015), and aluminium (Bazrafshan et al., 2012) are among the electrodes reported in various literatures. At favorable operating conditions, aluminium was reported to be very effective and successful in fluoride removal (Sandoval et al., 2021).

CHAPTER

4

ADSORPTION TECHNOLOGY

Adsorption was first used by a German physicist named Heinrich Kayser in 1881 (Gaur & Sharma, 2017). Adsorption is frequently described as a surface phenomenon in which particles adhere to the top layer of material. Adsorption is primarily caused by surface energy. In general, surface particles that can be partially exposed tend to attract other particles to their location.

Two components are required for the adsorption process,

- ***Adsorbate:*** A substance that adheres to the surface of another substance.
- ***Adsorbent:*** A substance's surface on which adsorbate adsorbs.

Meanwhile, we must distinguish between adsorption and absorption. The two processes use completely different mechanisms. Adsorption refers to the adhesion of atoms, ions, or molecules of a gas, liquid, or dissolved solid to a surface, whereas absorption is the process by which a material diffuses into a liquid or solid to form a solution (**Table 4.1**).

Table 4.1: Difference between absorption and adsorption

Absorption	Adsorption
1. Complete deposition of a substance in another substance is absorption	1. Deposition of a substance on the surface is known as adsorption.
2. It is not a surface phenomenon.	2. It is a surface process.
3. It is not spontaneous.	3. Adsorption of gas on solid is spontaneous.
4. It takes place uniformly throughout.	4. It does not take place uniformly.
5. Greater molecular interaction.	5. Less molecular interaction.
6. It involves the application of potential in the absorption of water by root hairs.	6. There is no involvement of potentials during adsorption.

The term sorption refers to both processes, whereas desorption refers to the opposite process. This process forms a film of the adsorbate (the molecules or atoms being accumulated) on the adsorbents' surface. Adsorption removal of excess fluoride from water includes physical, chemical, or ion exchange within the adsorption in which the fluoride is adsorbed on a fix bed packed with resign or other mineral particles. It is critical to distinguish between adsorption of a single compound and adsorption of multiple compounds. In the latter case, the different adsorbates will compete for adsorption sites, and the adsorption equilibrium and isotherm may differ significantly from those observed without competition. The initial concentration of the target adsorbate influences the resultant isotherm in a multi-component system.

The most important factors affecting adsorption are:

- Surface area of adsorbent
- Particle size of adsorbent; particle sizes reduce internal diffusion and mass transfer limitations to adsorbate penetration within the adsorbent (i.e. equilibrium is more easily achieved and nearly full adsorption capability can be attained).
- Affinity of the solute for the adsorbent
- Degree of ionization of the adsorbate molecule (more highly ionized molecules are adsorbed to a smaller degree than neutral molecules)
- pH

Because of its simplicity and wide range of adsorbents, adsorption is still one of the most widely used methods (Mahapatra et al., 2010). It is critical to distinguish between physical adsorption, which involves only weak intermolecular forces, and chemisorptions, which involve the formation of a chemical bond between the sorbent molecule and the adsorbent surface.

Adsorption of a gas on a solid is an exothermic reaction that occurs spontaneously. Heat of adsorption refers to the amount of heat released when a unit mass of a gas is adsorbed on the surface.

4.1.1. Difference between Physical Adsorption and Chemisorption (Source: Ruthven, 1984)

Physical Adsorption	***Chemisorption***
1. Physical forces are behind these type of adsorption.	1. Chemical forces are behind these type of adsorption.
2. The forces operating are weak Vander Waal's forces.	2. The forces are very strong & similar to a chemical bond.
3. These type of adsorption is multi-layered process.	3. This type of adsorption is mostly single layered phenomenon.
4. Physical adsorption is not specific and takes place all over the adsorbent.	4. Chemisorption is highly specific and takes place at reaction centres on the adsorbent.
5. The heat of adsorptions are low i.e. about 20-40 KJ mol^{-1}.	5. The heat of adsorptions are high i.e. about 40-400 KJ mol^{-1}.
6. The process is reversible.	6. The process is irreversible.
7. This type of adsorption decreases with increase of temperature.	7. This type of adsorption increases with increase of temperature.
8. Physisorption is affected by surface area, temperature, pressure, nature of adsorbate.	8. Chemisorption is affected by surface area, temperature, nature of adsorbate.
9. Energy of activation is low (20 – 40 KJ/mol)	9. Energy of activation is very high (40 – 400 KJ/mol)

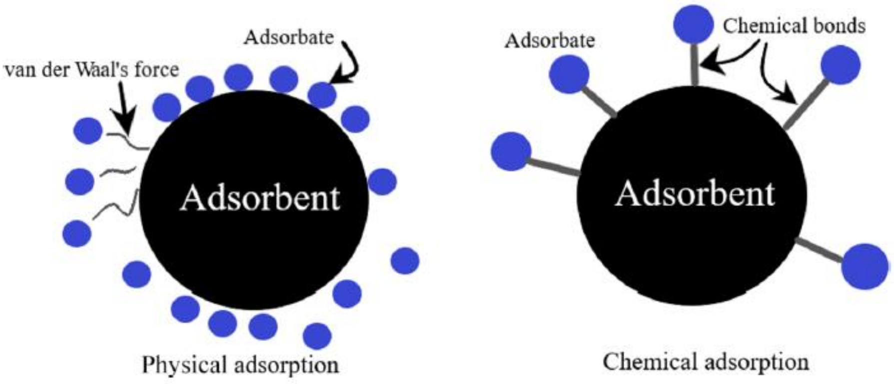

Fig. 4.1. Physical and chemical type of adsorption (Source: Moosavi et al., 2020)

4.1.2. Characteristics of physical adsorption

a) ***Low enthalpy of adsorption:*** Adsorption enthalpy is low because the attractive forces between the adsorbent and adsorbate molecules are weak (van der Waals forces), and thus the molar enthalpy of adsorption is low.

b) ***Reversible nature:*** Because the physical adsorption process is generally reversible, equilibrium is reached quickly. When we increase the pressure (or decrease the volume), the equilibrium shifts forward, resulting in increased adsorption. As a result, as the volume of the gas decreases, more gas is adsorbed when the pressure is increased. By lowering the pressure, gas can be removed.

c) ***Effect of temperature:*** Because the adsorption mechanism is exothermic, physisorption occurs commonly at low temperatures and decreases with increasing temperature, as per the Le-Chatelier principle. When the temperature rises, the kinetic energy of the gas molecules rises, and they leave the adsorbent's surface. As a result, increasing the temperature reduces the extent of adsorption.

d) ***Lack of specificity:*** Because it is not specific in nature, all gases are adsorbed to the same extent on all solids. Because van der Waals forces are universal, a given adsorbent surface does not demonstrate any preference for a specific gas.

e) ***Nature of adsorbate:*** Gases that are easily liquefied (i.e., possess higher critical temperatures) are easily adsorbed since van der Waals forces are stronger near critical temperatures.

f) ***State of adsorbate:*** The adsorbate is in the same state as in the bulk during physical adsorption.

4.1.3. Characteristics of chemical adsorption

a) ***Adsorption enthalpy*****:** Because the forces of attraction between adsorbent and adsorbate molecules are strong chemical bonds, the molar heat of adsorption is high.

b) ***Effect of temperature*****:** Chemical adsorption increases with temperature up to a certain point and then gradually decreases. A gas that is physically adsorbed at a low temperature may undergo chemisorption at a high temperature.

c) ***High selectivity:*** Chemical adsorption is the formation of chemical bonds between adsorbed molecules and the adsorbent's surface. As a result, it is extremely selective. Chemical adsorption is determined by the chemical properties of the gas and the adsorbent. For example, oxygen is adsorbed on metals as a result of oxide formation, and hydrogen is adsorbed on transition metals as a result of hydride formation.

d) ***State of adsorbate:*** Because this type of adsorption involves a chemical reaction, the state of the adsorbed molecules may differ from that of the bulk.

4.2. Advantages & Disadvantages of adsorption

Examples	**Adsorbents:**
	• Activated Alumina • Activated Carbon • Calcite • Activated saw dust • Activated coconut shell carbon and Activated fly ash, • Groundnut shell • Coffee husk • Rice husk • Water hyacinth • Bone charcoal • Activated soil sorbent, etc.
Advantage	• The process can remove fluoride up to 90% & arsenic up to 100% • Treatment is cost effective. • Easily available.
Disadvantage	• The process is highly dependent on pH • Presence of sulfate, phosphate or carbonate results in ionic competition.

4.3. Biochar as an adsorbent

Biochar has good potential to act as material for soil & water remediation (Vithanage et al., 2016). This is due to the fact that it shows favourable physio-chemical surface characteristics. The properties of arsenic adsorption are highly affected by temperature during pyrolysis, residence time, and feedstock and pyrolysis technology. It was observed that low pyrolytic temperature biochar are extra effective in arsenic sorption as compared to high temperature biochar. It was suggested that due to low surface area and mechanical properties, activated carbon is predominant in treating arsenic contamination in water. In a study by Xia et al., (2016), it was found that zinc impregnated biochar had the highest As

(III) adsorption potential at 26.6 mg/g. It was also reported in a publication by Rodriguez-Romero et al., (2020) that As (V) sorption potential decreases with an increase in pyrolysis temperature, although the surface area increases. Owing to the highest zinc amount, the highest sorption of As (V) is achieved at 400°C. Zhu et al., (2016) concluded that Bismuth impregnated biochar have high sorption capability to Arsenite, Phosphate, and dichromate. Arsenic removal was linked to ligand exchange.

4.4. Water hyacinth biochar

Eichhornia crassipes is the scientific name for water hyacinth (WH), which is one of the world's 30 most noxious, dreadful, and aquatic invasive weeds. It produces 14×10^7 daughter plants per year and covers 1.4 km^2 of water with 28×10^3 t of fresh biomass (Ruan et al., 2016). It causes severe problems such as flooding due to water body blockage (Malik, 2007). It has a significant impact on livelihood because of the decrease in fish population at various fish sites (Tellez et al., 2008), recreation, navigation (Chuang et al., 2011), irrigation system clogging, and sedimentation (Zhang et al., 2015). The drastic changes that occurred as an ecological and economic disaster (Villamagna and Murphy 2010), imparts a decrease in biodiversity (Plummer, 2005), and causes various diseases for humans such as malaria, filariasis (Mailu, 2001), dengue, and encephalitis due to the development of an abundance number of mosquitos and snails in low oxygen conditions over WH mat regions (Mironga, 2014).

The conventional methods (Harley et al., 1996) are defined as regular physical and mechanical removal of biomass from water bodies (Bordoloi et al., 2018). Various control methods, such as physical (Ram and Moolani; 2000), chemical (Howard et al., 1997), and biological (Ram and Moolani; 2000), have been proposed for WH control (Shabana and Mohamed, 2005). Because of its abundant availability at low cost, WH biomass (lignocellulosic biomass) can be used efficiently as an alternative energy source that is sustainable for waste management, economics, ecology, energy, and society (Bhattacharya et al., 2016). It is used as a potential feedstock for fertilisers, biofuels (Rahman, 2018), biochar (Masto et al., 2013), ethanol, natural gas, methane (Kalhorinia et al., 2013), xylitol, biogas, and compost production, but biochar production is a more focused and profitable path for the use of invasive WH (Bordoloi et al., 2019).

The concept of WH biomass (both leaf and stem) in the form of biochar is more relevant because it contains a higher proportion of cellulosic, hemicellulose, and lignin than other commonly obtained biomass such as rice straw, wood chips, sugarcane bagasse, and so on. Biochar has properties such as carbon-rich, porous substance, porous structure (Sohi et al., 2009), water retention time (McHenry, 2009), specific surface area that allows it to act as a long-term carbon sink and remove atmospheric CO_2 through photosynthesis (Lehman and Joseph et al., 2015). As a sustainable strategy for managing this aquatic invasive weed, biomass WH suffered a significant setback. Power generation biochar can be used to improve soil fertility, carbon storage, as an adsorbent in wastewater treatment, and for a variety of other purposes as a fuel (Sun et al., 2018).

Biochar is produced using a variety of methods known as bioenergy conversion biomass. Bioenergy conversion techniques are broadly classified into two types: biochemical and thermochemical conversion. The former is governed by biological catalysts and organisms, while the latter is governed by heat and chemical catalysts (Das and Veziroğlu, 2001). The first is less expensive and more environmentally friendly than the second, but the yield and hydrogen production rate in the case of biochemical are quite low, which is the major constraint thermochemical conversion and is the most popular and acceptable (Tripathi et al., 2016). The thermochemical method is divided into three steps: combustion, pyrolysis, and gasification.

Masto et al., (2013) performed extensive research on water hyacinth Biochar. Water hyacinth biochar (EBC) was analysed for its impact on soil activity. It was found that when biochar is produced at optimum temperature (300–350°C) and residence time (30–40 min), soil biochemical properties and maize seedling growth increased. Zhang et al., (2016) developed a new approach towards arsenate removal which was developed by magnetite modified water hyacinth biochar under this article. Magnetite biochar was prepared by co-precipitating Fe^{3+}/Fe^{2+} on water hyacinth biomass powder. It was then followed by slow pyrolysis at 250 and 450°C under nitrogen. It was reported that at a pyrolytic temperature of 250°C, the modified biochar (MW) showed maximum removal efficiency of As (V) in an aqueous medium. Moreover, the sorption efficiency was unaffected over a huge pH range from 3 to 10. The use of water hyacinth for biochar provides dual benefits of water hyacinth management as well as heavy metal removal. Liu et al., (2020) demonstrated that biochar made from water hyacinth not only controls this invasive species but also is effective in heavy metals removal. The study aimed to remove Cd^{2+} from an aqueous solution. The optimum pyrolysis temperature for biochar was reported to be >500°C.

Table 4.2: Performance evaluation of biochar derived from water hyacinth

Feedstock	*Amendments*	*Pollutants*	*Conditions*	*Sources*	*Outcomes*	*Reference(s)*
Water hyacinth	Fe_2O_3 & Fe_3O_4	P	Slow pyrolysis, 250°C, 450°C, 1 h	Eutrophic water	Q_{max} = 5.07 mg/g, pH = 3-9, Removal ~ 90%	Cai et al., 2017
Water hyacinth	Equiliberated with 0.1M HCl	Cd^{2+}	Slow pyrolysis, 250 - 550°C, 1 h	Contaminated water	Q_{max} = 70.3 mg/g, K = 0.11/mg, Removal ~ 100%	Zhang et al., 2015
Water hyacinth	Co-precipitation with Fe^{2+} & Fe^{3+}	As (V)	Slow pyrolysis, 250, 450°C, 1 h	Water	Q_{max} = 7.41mg/g, pH = 3-10 (unaffected), Removal ~ 100%	Zhang et al., 2016
Water hyacinth	-	Pb	Slow pyrolysis, 433°C, 2.65 h	Water	Q_{max} = 20.175 mg/g, pH = 5.5	Zhou et al., 2020
Water hyacinth	-	Cd^{2+}	Slow pyrolysis, 393°C, 2.42 h	Water	Q_{max} = 186.18 mg/g	Zhou et al., 2019
Water hyacinth	ZnO NP	Cr (VI)	Slow pyrolysis, 500 - 800°C, 0.17 - 14 h	Aqueous solution	Q_{max} = 43.48 mg/g, pH = Natural, Removal ~ 95%	Yu et al., 2018
Water hyacinth	Citric acid	Methylene Blue	Slow pyrolysis, 300°C, 0.17 - 14 h	Waste water	Q_{max} = 395 mg/g, pH = Natural, Removal ~ 90%	Xu et al., 2016
Water hyacinth	-	Arsenic	Grinder	Water	Removal ~ 90%	Govindaswamy et al., 2011
Water hyacinth	Co-precipitation with Fe^{2+} & Fe^{3+}	Arsenic	Slow pyrolysis, 400°C, 1 h	Water	Removal ~ 100%	This study
Water hyacinth	Co-precipitation with Fe^{2+} & Fe^{3+}	F^-	Slow pyrolysis, 400°C, 1 h	Water	Removal ~ 90%	This study

4.5. Characterization of biochar

Characterization is important for accounting/knowing the carbon form present/available in biochar, which is granted for soil stability, as well as estimating the charcoal potential for desired biochar purposes (Brewer et al., 2009). The detailed characterization is discussed in detail below.

4.5.1. Elemental and Proximate Characterisation

Different analytical methods have been used using ASTM standards to characterize the WH biomass and identify physicochemical properties such as elemental analysis (on free dry ash basis, wt. percent) such as carbon (C), hydrogen (H), nitrogen (N), sulphur (S), oxygen (O) by difference, proximate analysis (wt%) analyzed by standards such as moisture content (ASTM D3173), ash (ASTM D3175) (Rahman et al., 2018), volatiles matters VM (ASTM D3174) as well as fixed carbon FC (by difference) and further, biochemical components like protein, carbohydrate, lipids and also high heating value (HHV). Other techniques such as ISO, BS, and DIN are used to standardize the proximate analysis (Manya, 2012). All of these characteristics have a significant impact on product quality and distribution. Moisture content has a strong effect on heat transfer in the process, with significant effects on product distribution. The appropriate moisture content availability should be less than 10% wt (Choudhary et al., 2014). The presence of a high percentage of VM (around 65.6 wt%) in biomass indicates a high probability of bio-oil and syngas formation (Harman- Ware et al., 2013). A low ash content is a good sign for biochar products and has a positive effect on production efficiency and bio-oil and biochar quality.

High ash content, on the other hand, causes slagging and fouling, which affects biomass conversion and also reduces combustible compounds due to the negative influence of the heating value of the bio-oil. For increased biochar yield and carbon sequestration, the FC content of biomass WH should be around 20.3 wt%. The most suitable and favourable condition for biochar production is a carbon content of 33.33 wt%. The limited value of NOx and SOx in the biochar after pyrolysis is ensured by the promising value of nitrogen and sulphur content (0.7 wt%) and (0.4 wt%). The higher the oxygen content (59.3 wt%), the lower the heating values of bio-oil in comparison to fossil fuels (Choudhury et al., 2014).

4.5.2. Textural and Morphological Characterisation

The scanning electron microscope (SEM) is a useful tool for determining the structure, surface topography, surface area, and porosity of soil, which aids in identifying the water holding capacity in the soil, nurturing microorganisms (Batista et al., 2018), nutrient retention (Yu et al., 2018), and improving fertilizer efficiency, among other things. (SEM-X-ray energy dispersive spectroscopy) SEM-EDX reveals the composition of biochar particles (Liu et al., 2017). In the case of EBC, SEM images revealed puffy surfaces. When WH biomass is heated, micropores form on the surface due to the release of volatiles, whereas trapped volatiles expand the microstructure within the biomass. The resulting EBC has a high surface area and porosity. Two properties well suited as WH biomass have good water retention property for increasing soil water holding capacity, increased fertilizer used efficiency harboring microorganisms and nutrient retention, etc. (Masto et al., 2013). The SEM–EDX shows the composition of biochar particles. C, N, O, K, Cl, P, Mg, N, Si are the primary elemental compositions. The textual characterization of biochar made from WH biomass is experimentally determined by N_2 adsorption at 77 K and CO_2 adsorption (González et al., 2009) at 273 K, which is based on a certain surface area and distribution of pore size and is primarily determined by two factors: first, the nature of the biomass feedstock and the operating conditions of pyrolysis (mostly maximal temperature). Furthermore, the BET equation can be used to easily calculate specific surface area, and the Dubinin Radushkevich method can be used to calculate micropore volume (Gregg and Sing, 1982). CO_2 adsorption is also used to estimate the narrow micropore volume (Plaza et al., 2010).

4.5.3. Characterisation of surface functionality

Fourier transform infrared (FTIR) spectroscopy is used to investigate SF. This is used to investigate feedstock as biomass and their biochar with respect to distinct crest temperatures, which is useful in analysing vibrational frequency changes of functional groups and gradual loss of functional group lingo-cellulosic (OH straighten peak occurred at 3,400 cm^{-1}, responsible for effective feedstock's spec) (Brewer et al., 2009). Other spectral peaks have absorption bands assigned to them. The FTIR spectra are as follows: 1321 for aromatic C-H stretch; 1616 and 1427 for aromatic ring stretching of C=C-C; 1032 for C-O-C stretch connected with -OH bend cellulose, hemicelluloses, and lignin; and also 877 and 782 for aromatic C-H for a plane, bend. At high temperatures, the distinct spectra show high intensities absorption bands in the case of aromatics, whereas at low temperatures, an increase in aromatic C is reported (Coates, 2000). The peak characteristics of the carbonyl groups have also been observed in the limit of 1,660,725 cm^{-1}. The required position of the respective groups is dependent on the presence of an aromatic ring.

In surface analysis, X-ray photoelectron spectroscopy (XPS) is used. The XPS abroad-scan spectrum generally shows two major peaks at 285 eV and 530 eV in the form of C (C1s) and O (O1s) (Cheng et al., 2006). The highest-resolution spectra of C1s and O1s are used to identify carbon and oxygen forms on the surface of biochar (Gao et al., 2012). In the case of the C1s spectrum, various energies in the form of binding involve to CC, CO, CH, C=C, C=O, and COO stretches; whereas in the case of the O1s spectrum, distinct energies are set by signal peaks to O=C and OC stretches (Nguyen et al., 2009).

4.5.4. Characterisation of inorganic fraction

First, an inorganic fraction containing carbonaceous materials was isolated using two techniques: low and medium temperature ashing in oxygen plasma at 100-150°C and in air at 600°C. Following that, inorganic species were examined using techniques such as inductively coupled plasma mass spectrometry (ICP-MS), inductively coupled plasma atomic emission spectroscopy (ICP-AES), X-ray diffraction (XRD), and X-ray fluorescence (XRF) (Bahng et al., 2009). At low concentrations, ICP-MS detects metals and distinct nonmetals associated with non-interfered low-background isotopes. ICP-AES is used to determine the absolute concentration of inorganic elements (such as Al, Fe, K, Ca, P, Mg, Si, and so on) (Suárez-Garca et al., 2002). XRF spectrometry is used to determine the ash compositions using the weight fraction of oxides. XRD is used to determine the identity of crystalline minerals in ash (Liao et al., 2007).

4.5.5. Thermal characterisation

Thermogravimetric analysis (TGA)/derivative thermogravimetric (DTG) is a device used to collect data on thermal material degradation (Gasco et al., 2012). It also aids in understanding biochar thermal stability when extraction steps are skipped (Enders et al., 2012). TGA is useful in determining the thermal stability of biochar while avoiding extraction steps. The DTG curve is used to calculate weight loss. Through the DTG curve, absorbed water loss and partial dehydration of cellulosic structural parts; hemicellulose and cellulose degradation and remained cellulose and lignin degradation occurred with varying temperature (Girisuta et al., 2008). The comparison of TGA/DTG, DSC curves in WH biomass and biochar shows the

DTG characteristic curve shifted to high temperature (Zhou et al., 2009), organic carbon stability in WH biochar, and availability of high ash content in biochar as compared to WH biomass. The lignin reaction peak has shifted to a low-temperature zone at higher temperatures, which strongly promotes cellulose decomposition reaction due to catalytic potassium behaviour (Nowakowski and Jones, 2005), and the presence of potassium also influenced char formation. The availability of a high potassium content aids in the dissolution/degradation of cellulose and lignin and also influences thermal stability (Masto et al., 2013).

4.6. Adsorption Isotherms

There are various types of adsorption equilibrium models that differ in complexity and the number of parameters required. An adsorption isotherm is an equation that relates to the amount of a substance attached to a surface to its concentration in the gas phase or solution at a fixed temperature.

The Langmuir (1918) and Freundlich (1906) isotherms are the two most commonly used models.

4.6.1. Freundlich adsorption isotherm

By assuming a heterogeneous surface with a non-uniform distribution of heat of adsorption over the surface, the Freundlich isotherm is derived. According to the Freundlich equation, sorption energy decreases exponentially as an adsorbent's sorption centers are completed. Freundlich isotherm is an empirical equation which encompasses the heterogeneity of sites and the exponential distribution of sites and their energy. It is empirical expression that encompasses the heterogeneity of the surface and the exponential distribution of sites and their energies. The Freundlich isotherm can be derived assuming a logarithmic decrease in the enthalpy of adsorption with the increase in the fraction of occupied sites. The Freundlich isotherm is generally better suited to describe adsorption in aqueous solutions than the Langmuir isotherm. It has been shown that the Freundlich equation can be derived from the Langmuir equation if a logarithmic decrease of the differential adsorption enthalpy with increasing solid-phase concentration is assumed, corresponding to the behavior of a heterogeneous adsorbent surface. It is important to note that the Freundlich equation can only be used to describe experimental data within a limited concentration range where the constants are valid. To describe adsorption outside of this range, other isotherms have to be derived in experiments within other concentration ranges.

The Freundlich model is commonly given by the non-linear equation (Freundlich, 1906):

$$q_e = k_f C_e^{\frac{1}{n}} \qquad \text{(Eq. 4.1)}$$

A linear form of Freundlich equation is:

$$\log q_e = \log k_f + \frac{I}{n} \log C_e \qquad \text{(Eq. 4.2)}$$

where, C_e is the final adsorbate concentration, q_e is the adsorption capacity at equilibrium, k_f is the freundlich constant and n is the freundlich exponent.

$$\text{Slope} = \frac{1}{\text{n}} \qquad \text{(Eq.4.3)}$$

$$\text{Intercept} = \log \text{k}_\text{f} \qquad \text{(Eq. 4.4)}$$

The amount of gas adsorbed on the m gram of adsorbent is represented by x, K and n are adsorption constants, and 'p' is pressure n, which is always greater than one.

The adsorption obeys the Freundlich adsorption isotherm when the adsorbate forms a monomolecular layer on the surface of the adsorbent.

The Freundlich adsorption isotherm has a significant drawback in that it fails at high pressure. It couldn't account for the multi-layered adsorption process.

4.6.2. Langmuir Adsorption Isotherm

The Langmuir isotherm is the equilibrium distribution of sorbate ions between the solid and liquid phases (Kumar et al., 2011). It is assumed that the surface of the adsorbents is uniform so that all the adsorption sites are equal, adsorbed molecules will not interact, all adsorption occurs through the same mechanism and at the maximum adsorption only a monolayer is formed. Langmuir isotherm model assumes uniform energies of adsorption onto the surface without interaction of adsorbate in the plane of the surface where adsorbate molecules can be chemically bound.

The Langmuir adsorption isotherm model is predicated on the following assumptions:

- The gas adsorbed behaves optimally in a vapour phase, and only monolayer adsorption occurs. Adsorption cannot continue beyond the monolayer.

- The solid's surface is homogeneous. It is a homogeneous adsorption with constant sorption activation energy and enthalpies in each molecule.

- The adsorbate molecule has no lateral interactive force. Even if the adsorbed molecules are adjacent to each other, no interactions (lateral and steric hindrance) occur.

- Adsorption can only occur at a limited number of definite localized sites that are similar and equal. The adsorbed gas molecules have a specific location.

It is also assumed that the reaction is in a constant free-energy change for all sites and a maximum of one adsorbate molecule can be bound to each site (monolayer coverage). The Langmuir equation which is in most cases only applicable for small concentration ranges since the Langmuir equation resumes that homogeneous structure of the adsorbent surface, i.e. it is assumed as all sites of adsorption energetically equal (Langmuir, 1918).

The Langmuir in its nonlinear equation is commonly expressed as follows (Kumar et al., 2011)

$$q_e = \frac{q_{max}\, k_L C_e}{1+k_L C_e} \qquad \text{(Eq. 4.5)}$$

The linear Langmuir isotherm allows the calculation of adsorption capacities and the Langmuir isotherm in its linear form is represented by:

$$\frac{1}{q_e} = \frac{1}{k_L q_{max}} \cdot \frac{1}{C_e} + \frac{1}{q_{max}} \qquad \text{(Eq. 4.6)}$$

Where the Q_o is the amount of adsorbate at complete monolayer coverage (mg/g) and gives the maximum sorption capacity of sorbent, C_e is equilibrium concentration of adsorbate (mg/L) and k_L (L/mg) is Langmuir isotherm constant that relates to the energy of adsorption and q_e is an adsorption capacity at equilibrium. The Langmuir constants Q_o and k_L can be calculated from the slope and intercept of the plot C_e/q_e versus C_e respectively. The feasibility of a Langmuir isotherm can be expressed in terms of a dimensionless constant separation factor, R_L. (Weber, 1974), which is expressed as:

$$R_L = \frac{1}{1+C_i k_L} \qquad \text{(Eq. 4.7)}$$

Where k_L is the Langmuir isotherm constant and C_o is the initial concentration of adsorbate (mg/L). The R_L values lying between 0 and 1 indicate the conditions are favourable for adsorption (**Table 4.3**)

$$Slope = \frac{1}{k_L q_{max}} \quad \text{(Eq. 4.8)}$$

$$\text{Intercept} = \frac{1}{\text{q}_{\text{max}}} \quad \text{(Eq. 4.9)}$$

Table 4.3: Favourability of Langmuir isotherm model (source: Weber, 1974)

R_L	Type of Isotherm
$R_L>1$	Unfavourable
$R_L= 1$	Linear
$0<R_L<1$	Favourable
$R_L= 0$	Irreversible

4.7. Adsorption kinetics

During an adsorption process, adsorbate would diffuse from the bulk phase to the hydrodynamic boundary layer surrounding the adsorbent, then through the film boundary to the surface (film diffusion). The adsorbate molecules could then diffuse into the particles' interiors (inter particle diffusion). Finally, the adsorbate molecules are adsorbed onto the final adsorption sites via energetic interactions between the paired molecules and sites (Khamwichit et al., 2022).

The kinetic model is suitable for the experimental data if

- The line of graph is passing through all the dots.
- If the value of q_e (experimental) and q_e (calculated) are close to each other.
- If value of $R^2 \sim 1$

4.7.1. Pseudo first order adsorption model

In general, the pseudo-first order (PFO) model assumes that adsorption capacity is a direct proportion of the difference between the concentration at any contact time and the equilibrium value, and that the occupation rate of adsorbent sites is directly proportional to the number of unoccupied sites. As a result of the assumption of physisorption control, the pseudo-first order kinetic model was developed (Dutta et al., 2015). Eq. (4.10), also known as the Lagergren equation (Ho and McKay, 1999), shows the linear form of the pseudo-first order model.

$$\ln(q_e - q_t) = \ln q_e - k_1 t \qquad \text{(Eq. 4.10)}$$

where, q_e (mg/g) is the amount of metal ions adsorbed at equilibrium and k_1 (min^{-1}) is the pseudo-first order rate constant. A linear plot of ln (q_e – q) against time can be used to analyze the rate constant k_1.

$$\text{Intercept} = \ln q_e \qquad \text{(Eq. 4.11)}$$

$$\text{Slope} = k_1 t \qquad \text{(Eq. 4.12)}$$

The higher the value of k_1, the quicker is the adsorption rate (Maliyekkal et al., 2006).

4.7.2. Pseudo second order adsorption model

The model assumes that the rate-determining step is chemisorption (Ho and McKay, 1999). Eq. (4.13) shows the model's linear form, where k_2 is the equilibrium rate constant of pseudo-second order adsorption (g/mg/min) (Khamwichit et al., 2022).

$$\frac{t}{q_t} = \frac{1}{k_2 q_e^2} + \frac{1}{q_e} t \qquad \text{(Eq. 4.13)}$$

where, q_t (mg/g) is the amount of metal ions adsorbed at time t (minutes) and k_2 (min^{-1}) is the pseudo-second order rate constant. A linear plot of $\frac{t}{q_t}$ against time can be used to analyze the rate constant k_2.

The slope and intercept of the linear plot of $\frac{t}{q_t}$ against t were used to calculate the values of q_e and k_2.

$$\text{Intercept} = \frac{1}{k_2 q_e^2} \qquad \text{(Eq. 4.14)}$$

$$\text{Slope} = \frac{1}{q_e} \qquad \text{(Eq. 4.15)}$$

The lesser the value of k_2, the quicker is the adsorption rate (Maliyekkal et al., 2006).

CHAPTER 5

MATERIALS & METHODS

Materials and methods chapter covers all the materials used while performing the experiments carried out in order to meet the objectives. All chemical reagents used in this study were of analytical grade purchased from reputed industries.

5.1. Materials required

a) *Chemicals*

- Fluoride standard 100 mg/L (Orion 940907, Thermo Scientific)
- TISAB III [Total Ionic Strength Adjustment Buffer] (Orion 940911, Thermo Scientific)
- Arsenate standard 1000 mg/L as $Na_2HAsO_4.7H_2O$ (Merck, St. Louis, USA)
- Arsenite standard as As_2O_3 (Merck, St. Louis, USA)
- Solution of 1.25% sodium borohydride (Merck, Schuchardt, Germany)
- Sodium hydroxide (Merck, Bombay, India)
- 5.0 M HCl (Merck, Bombay, India)
- Sodium Fluoride as NaF (Loba chemie, India)
- Iron (III) chloride anhydrous (Merck, Bombay, India)
- Iron (II) sulfate heptahydrate (Merck, Bombay, India)
- Hydrogen Peroxide 30% (Merck, Bombay, India)
- Nitric acid 69%
- Hydrochloric acid 35%
- Calcium oxide powder (Merck, Bombay, India)

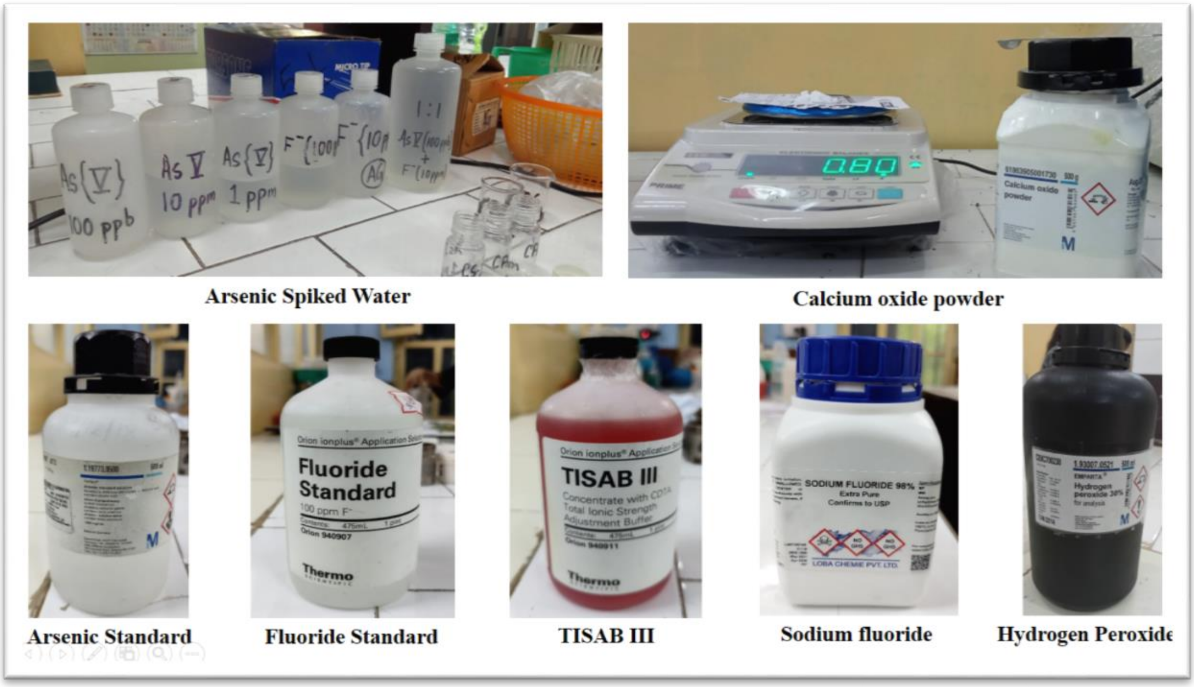

Arsenic Spiked Water

Calcium oxide powder

Arsenic Standard

Fluoride Standard

TISAB III

Sodium fluoride

Hydrogen Peroxide

Fig. 5.1: Various chemicals used during research work

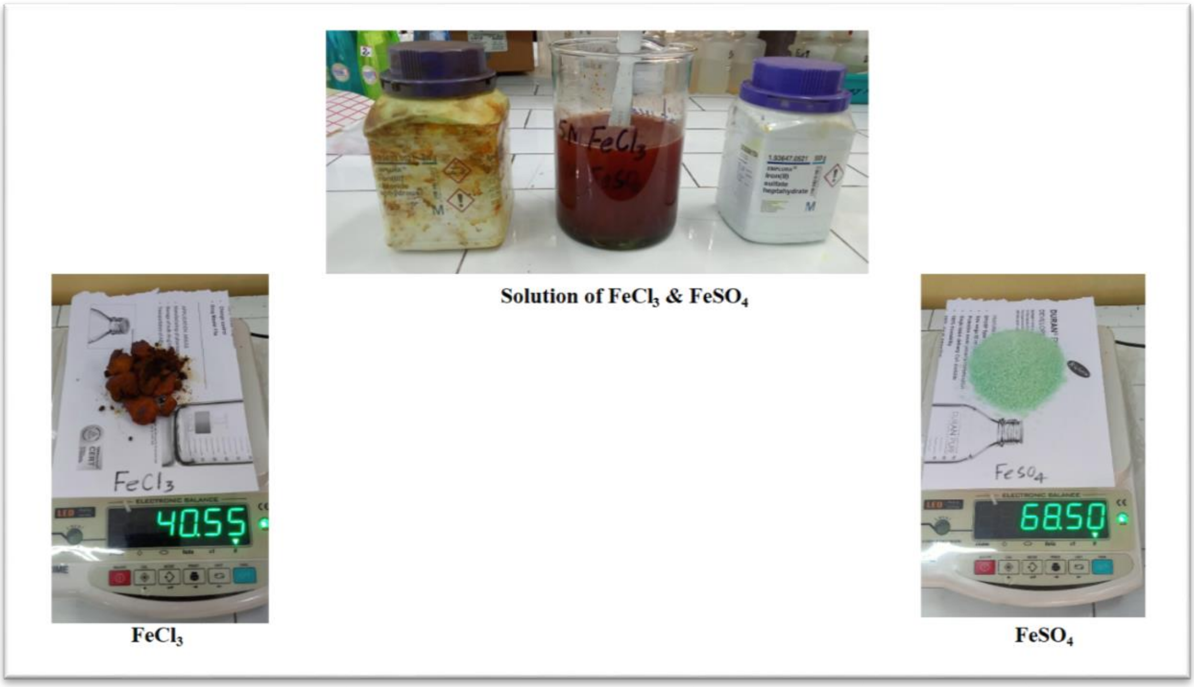

Solution of $FeCl_3$ & $FeSO_4$

$FeCl_3$

$FeSO_4$

Fig. 5.2: Various chemicals used during research work

b) Instruments

- pH/ISE meter (Orion Star A214)
- pH meter CL 46+ (Toschon Industries, Ajmer, India)
- Fine Balance (Mettler AE240)
- Fine Balance (Prime, India)
- Spinix Orbital shaker (Tarsons)
- Universal hot air oven (Labtech, India)
- Muffle furnace (Selec TC344)
- FI-HG-AAS [Flow Injection-Hydride Generation-Atomic Absorption Spectrometer] (Varian Model AA 140 AAS, USA)
- Gas flame photometer (G-301, HPG)
- UV-VIS Spectrophotometer (Orion aquamate 8000, Thermo Scientific)
- Fine Balance (Mettler AE240)
- Spinix Orbital shaker (Tarsons)
- Grinder (Rex500, Bajaj)
- Centrifuge (Remi R-8C)
- Distillation unit (Rivotek)
- Filtration unit (Suction filter)

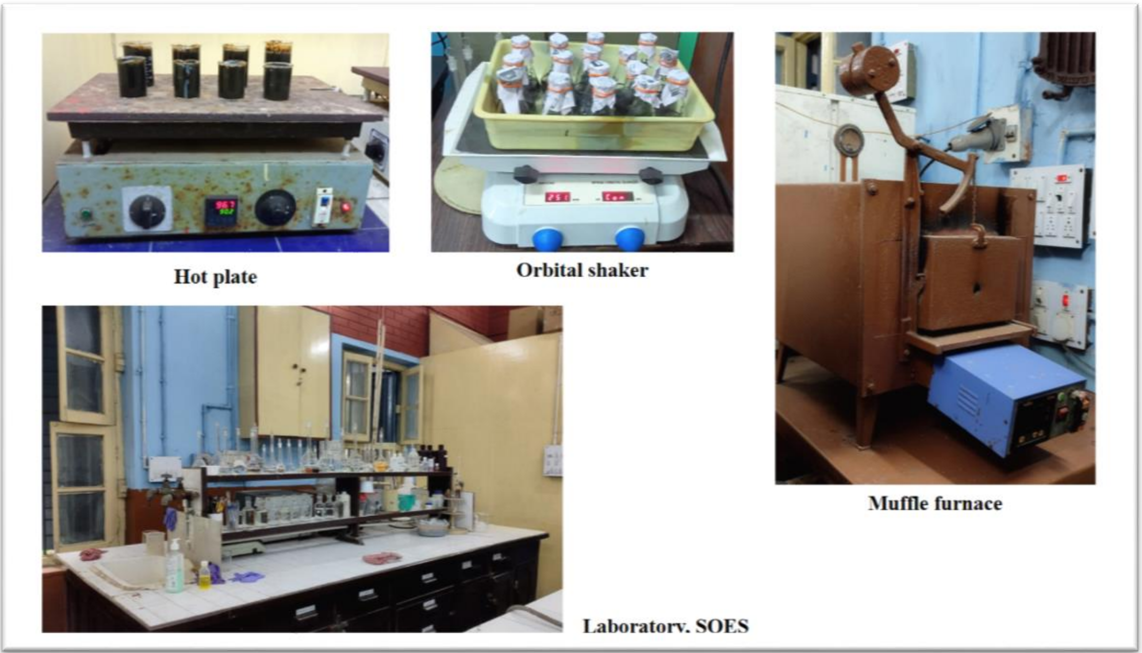

Hot plate

Orbital shaker

Muffle furnace

Laboratory, SOES

Fig. 5.3: Various instruments used during research work

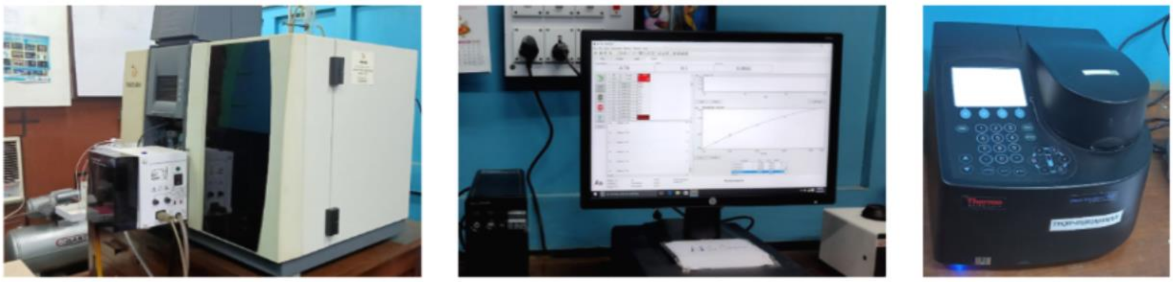

AAS **AAS - Computer** **UV-VIS Spectrophotometer**

Fluoride meter **pH meter** **Gas flame photometer** **Centrifuge**

Fig. 5.4: Various instruments used during research work

Grinder **Weighing balance** **Hot air oven**

Distillation unit **Suction filter unit**

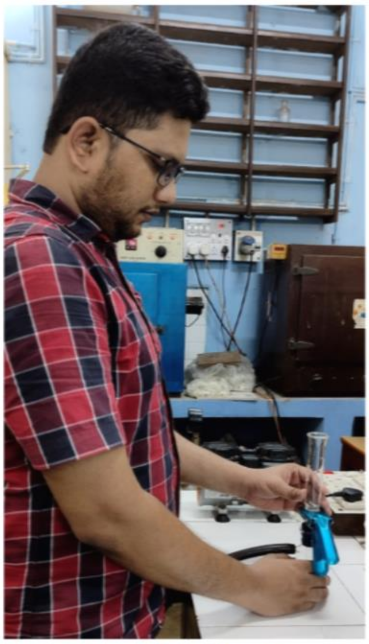

Performing suction filter of sample

Fig. 5.5: Various instruments used during research work

c) Glassware

- Conical flasks (Borosil)
- Glass beakers (Borosil)
- Measuring cylinder (Borosil)
- Glass tubes (Borosil)

Conical flask **Conical flask with samples for trials** **Glass beakers**

Glass tubes **Conical flask with samples for trials** **Glass beakers**

Fig. 5.6: Various glassware used during research work

d) Miscellaneous

- Double distilled water
- Filter paper (Whatman 42)
- Plastic containers (15 ml, 250 ml)
- Ziploc® bags
- Plastic trays
- Filter paper, Whatman 42 (GE Healthcare Life sciences)
- Plastic containers (15 ml, 250 ml)
- Eichhornia crassipes (Water hyacinth)
- A pair of scissors
- Micropipette 5 ml (Accupipet)
- Micropipette 1 ml (Eppendorf Research plus)

- pH indicator paper (Merck, Mumbai, India)
- Mortar pestle
- Crucibles
- Centrifuge tubes
- Microfilters (0.45 µm)
- Dessicators
- Fine sieve 0.16 mm (Filtra, Barcelona)

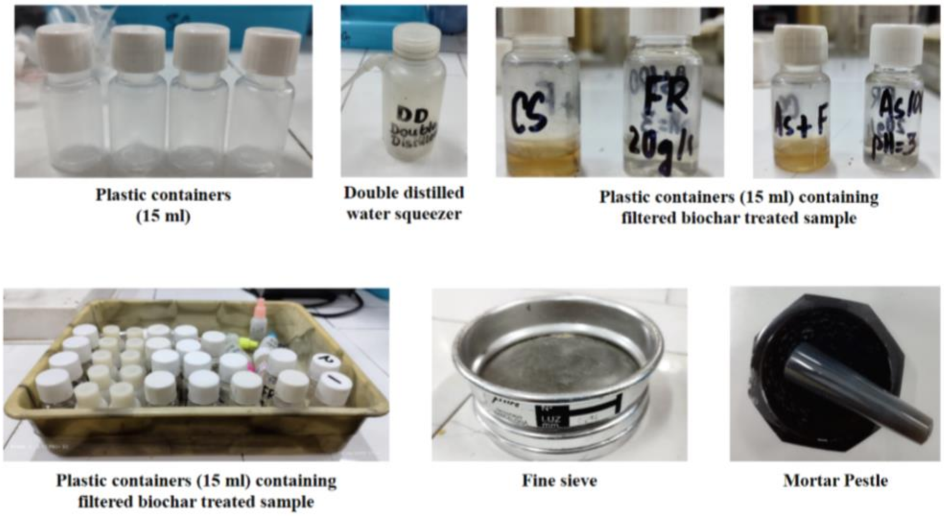

Plastic containers (15 ml)

Double distilled water squeezer

Plastic containers (15 ml) containing filtered biochar treated sample

Plastic containers (15 ml) containing filtered biochar treated sample

Fine sieve

Mortar Pestle

Fig. 5.7: Miscellaneous equipment used during research work

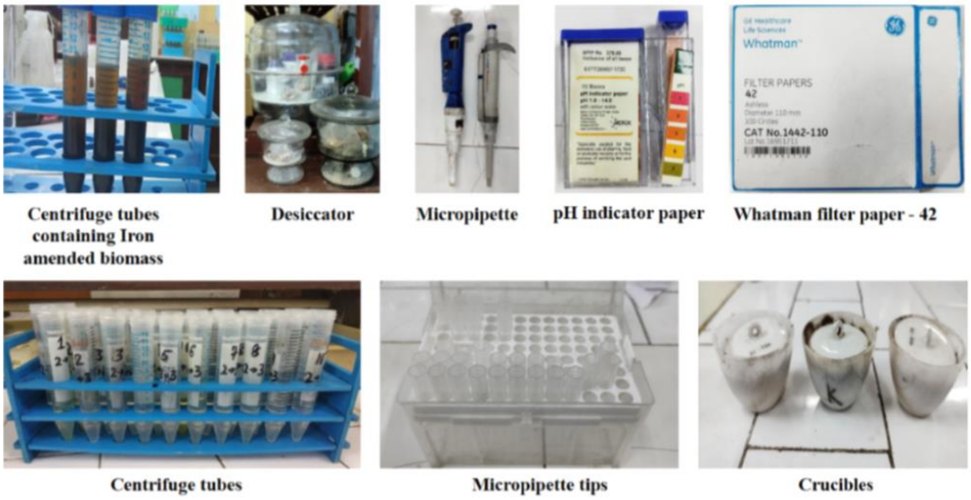

Centrifuge tubes containing Iron amended biomass

Desiccator

Micropipette

pH indicator paper

Whatman filter paper - 42

Centrifuge tubes

Micropipette tips

Crucibles

Fig. 5.8: Miscellaneous equipment used during research work

5.2. Biochar Preparation

A brief scheme of the methodology has been illustrated in Fig. 5.9 to meet the objectives as discussed in the previous chapter**.**

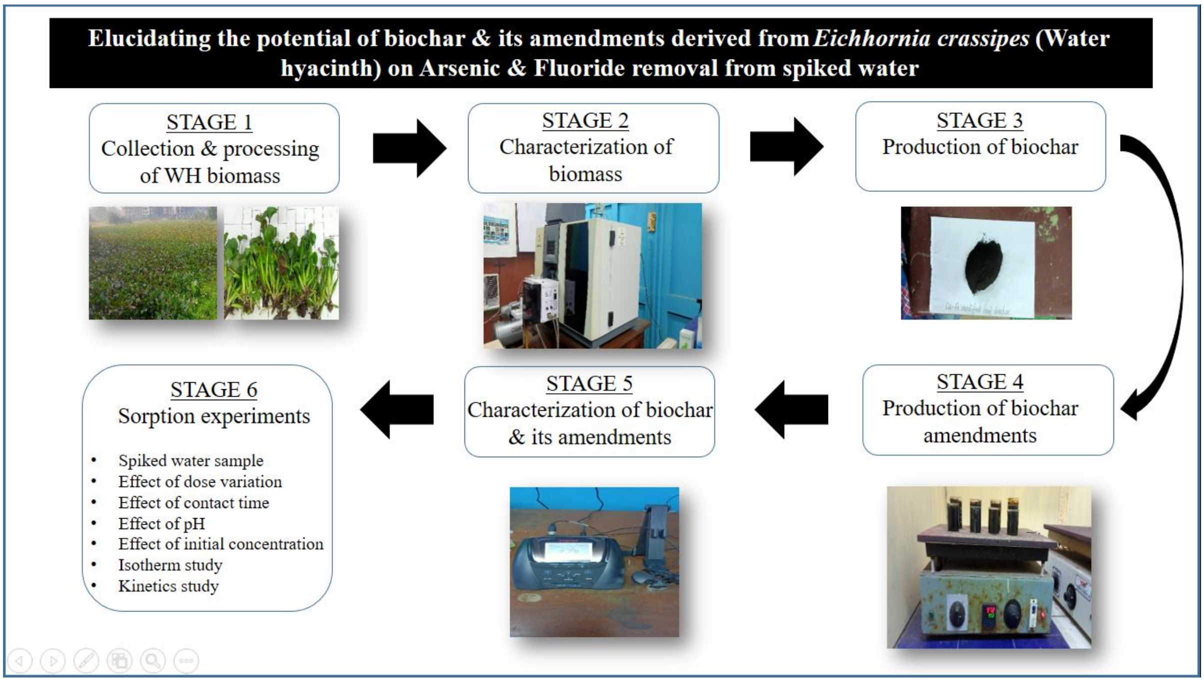

Fig. 5.9: A brief scheme of methodology to prepare biochar

5.2.1. Water hyacinth: collection & processing of biomass

Water hyacinth (*Eichhornia crassipes*) biomass was collected from a pond near Talbanda, North 24 Parganas, West Bengal, India (Geo-reference: 22°42´2.54´´N, 88°26´21.6´´E). The collected biomass was placed in plastic bags and transported to the lab for further analysis and experimentation.

In the lab, the biomass was thoroughly cleaned under tap water to remove dirt, mud, and other biological matter. The roots, stem, stolons and leaves were separated (stolons were included in the stem) using a pair of stainless steel scissors. The stem and leaves were kept in plastic trays and washed with tap water. Then they were soaked in distilled water and kept overnight at room temperature. The roots were soaked in 5-L glass beaker, mixed using hand and kept overnight at room temperature to let go of any pigments, tannins, and other symbiotic growth on its surface. Next day, the water was drained and all the 3 parts were rinsed thrice with distilled water until the wash water was visibly clear. They were chopped with a pair of scissors to reduce its size to about 30 – 50 mm in length. Initial weights of the chopped roots, stem and leaves were noted.


Water hyacinth

Fig. 5.10: Water hyacinth (*Eichhornia crassipes)* in the field

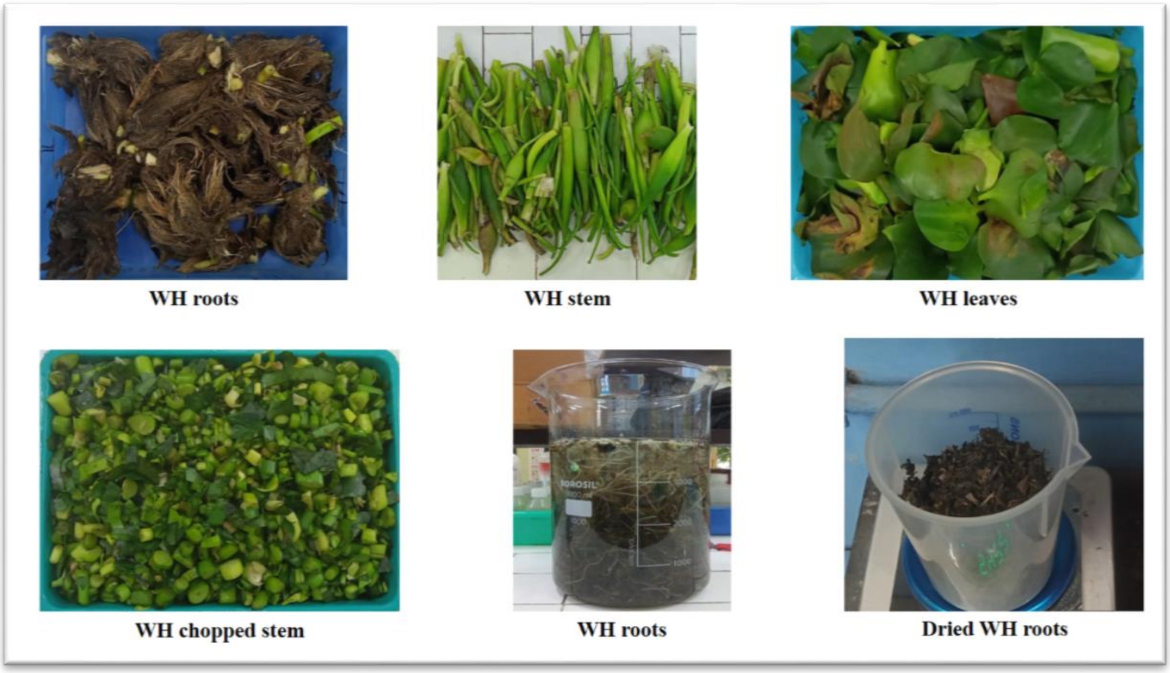
WH roots **WH stem** **WH leaves**
WH chopped stem **WH roots** **Dried WH roots**

Fig. 5.11: Processing of water hyacinth in the lab

Fig. 5.12: Water hyacinth (*Eichhornia crassipes)* in the lab

After sun drying for 3 days, the chopped biomass was kept in hot air oven for 72 h until completely dried. The moisture free biomass was then grinded in a stainless steel jar of a commercial grinder at 12000 rpm to get fine grained biomass. Grinded biomass was kept separately in polyethylene Ziploc® bags at room temperature and labelled as Roots (R), Stem (S) & Leaf (L).

5.2.2. Characterization of biomass

Biomass was characterized for its length, weight and chemical properties. Initial length and weight of individual parts of the biomass was taken. Biomass was digested following the established procedure to determine the chemical properties viz. Total arsenic.

Total arsenic was analysed after acidic digestion of the biomass sample (about 0.5 g each) where a mixture of concentrated nitric acid and 30% (v/v) hydrogen peroxide was added in a proportion of 2:1. The solution thus prepared was kept overnight at room temperature for complete digestion of samples. Following day, the digested samples were fumed out until volume reduces to about 0.1 ml by keeping it on a hot plate at 90°C. The final volume of the evaporated samples were made upto 5 ml using double distilled water followed by filtration by a suction filter (Millipore 45 µm). The filtrate was stored in 15 ml plastic bottles at 4°C until analysis was done. The details of the procedure for digestion is described elsewhere (Das et al., 1995; Chowdhury et al., 2018; Joardar et al., 2021; Roychowdhury, 2010).

5.2.3. Production of biochar

Weighed quantity of Roots, Stem & Leaves were separately put in porcelain crucible which was placed inside muffle furnace under limited supply of oxygen. The limited supply of oxygen was maintained by wrapping the crucible with aluminium foil. The furnace was set at a temperature of 400°C (with uniform rise of 20°C/min) and the samples were kept there for 1 h. After 1 h, the crucible was taken out and cooled to room temperature. The produced biochar was weighed and the biochar recovery from the biomass was noted. The biochar was named as RBC (Root biochar), SBC (Stem biochar), LBC (Leaves biochar) and put inside Ziploc® bags which was stored in desiccator for further experimentation.

The optimum temperature and time for pyrolysis of water hyacinth has been taken from elsewhere (Masto et al., 2013; Zhang et al., 2016).

5.2.4. Preparation of biochar amendments

In order to enhance the percentage removal of selective ions from the spiked water the biochar was modified as follows:-

a) Iron modified biochar
b) Calcium-Iron modified biochar
c) Calcium modified biochar

The amendments were done in consultation with various reference journals mentioned as and where required. pH of the prepared biochar was kept in the range of 5.5 to 6.5 (pH to be checked by adding biochar to distilled water, 1:20 w/v).

a) Iron modified biochar

700 ml stock solution of Iron (II) sulphate heptahydrate (278.02 g/mol) and Ferric (III) chloride (162.2 g/mol) was prepared in molar ratio of 0.5:0.5. (Zhang et al., 2016). Dried R, S, L was dipped in the prepared solution (1:15 w/v). pH was raised to 10 by adding 8 (M) NaOH and stirring on hot plate at 90°C for 2h. The glass beaker was then wrapped with aluminium foil with perforation and left on an orbital shaker (50 rpm) at room temperature overnight (Wu et al., 2018).

For iron impregnated WH biochar preparation, solid residue was separated by centrifugation (3000 rpm for 10 minutes). Then, it was subjected to slow pyrolysis at 400°C for 1 h. The prepared biochar was allowed to cool at room temperature and then rinsed with deionized water, left to dry at 65°C for 5 hours in crucibles. It was then finely grounded using mortar pestle to pass 0.16 mm sieve and then stored in Ziploc® bags, marked as FR (Iron modified roots biochar), FS (Iron modified stem biochar), and FL (Iron modified leaves biochar) and placed in desiccator for further experimentation.

b) Calcium-Iron modified biochar

For Ca-Fe modified WH biochar preparation, Calcium Oxide powder (56 g/mol) was mixed (CaO mass: dried biomass = 0.16) with the prepared stock solution of Iron salts (Agrafioti et al., 2014). The Ca-Fe modified mixture will then be pyrolysed at 400°C for 1 h. The prepared biochar was rinsed with deionized water, left to dry at 65°C for 5 hours in crucibles. It was then grounded to pass 0.16 mm sieve and then stored in Ziploc® bags and placed in desiccator for further experimentation.

c) Calcium modified biochar

R, S, and L were immersed in 50ml CaO solution prepared by dissolving Calcium Oxide powder (56 g/mol) in distilled water (CaO mass: dried biomass = 0.16) (Agrafioti et al., 2014). It was then kept on hot plate at 90°C for 6 h for complete drying. Then, it was put inside porcelain crucible and subjected to slow pyrolysis at 400°C for 1h. The prepared biochar was rinsed with deionized water and left to dry at 65°C for 5 hours. Subsequently, it was grounded to pass 0.16 mm sieve and then stored in Ziploc® bags and placed in desiccator for further experimentation.

Fig. 5.13: Modified and dried water hyacinth biomass

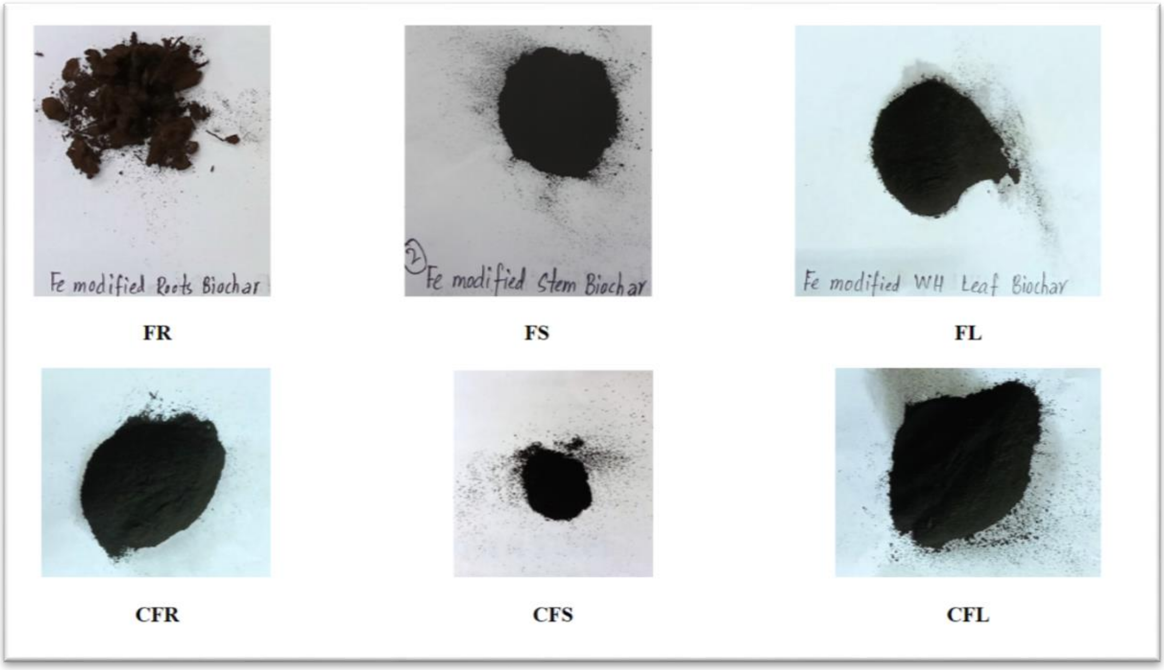

Fig. 5.14: Amended water hyacinth biochar

5.3. Removal of As (V) from spiked water

A brief scheme of the work for the fulfillment of Arsenic removal is discussed below:

5.3.1. Preparation of spiked water sample

Double distilled water was used to prepare spiked water samples of various concentrations. Arsenate standard 1000 mg/L as $Na_2HAsO_4.7H_2O$ was used to prepare 0.1 mg/L, 0.5 mg/L, and 1 mg/L of Arsenate solution which was kept in 250 ml plastic container in refrigerated condition (4°C).

5.3.2. Effect of adsorbent dose variation

The percentage removal of Arsenate ion from the spiked water sample was studied by varying the adsorbent dosage of the prepared sample. The adsorbent used was FR and dosage under consideration was 5 g/L, 10 g/L, 20 g/L, 30 g/L, and 50 g/L. Other parameters were kept constant viz. Arsenate concentration: 0.1 mg/L; Contact time: 15 min; Temperature: 30°C; pH: 5 in an orbital shaker at a speed of 250 rpm.

5.3.3. Effect of contact time

The percentage removal of Arsenate ion from the spiked water sample was studied by varying the contact time of the prepared sample. The adsorbent used was FR and the time was varied as 5 min, 15 min, 30 min, 45 min, 1 h, 2 h, 4 h, 24 h. Other parameters were kept constant viz. Arsenate concentration: 0.1 mg/L; FR Dose: 20 g/L; Temperature: 30°C; pH: 5 in an orbital shaker at a speed of 250 rpm.

5.3.4. Effect of pH

The percentage removal of Arsenate ion from the spiked water sample was studied by varying the pH of the prepared sample. The adsorbent used was FR and the pH was varied as 3, 5, 7, 9, and 12. Other parameters were kept constant viz. Arsenate concentration: 0.1 mg/L; FR Dose: 20 g/L; Temperature: 30°C for a contact time of 15 minutes in an orbital shaker at a speed of 250 rpm

5.3.5. Effect of Initial concentration

The percentage removal of Arsenate ion from the spiked water sample was studied by varying the initial concentration of Arsenate in the spiked water sample. The adsorbent used was R, FR, CR, CFR, S, FS, CS, CFS, L, FL, CL, and CFL and the initial concentration was varied as 0.1 mg/L, 0.5 mg/L, and 1 mg/L. Other parameters were kept constant viz. Adsorbent Dose: 20 g/L; pH: 5; Temperature: 30°C for a contact time of 15 minutes in an orbital shaker at a speed of 250 rpm.

5.4. Defluoridation trials

A brief scheme of the work for the fulfillment of defluoridation is discussed below:

5.4.1. Preparation of spiked water sample

Double distilled water was used to prepare spiked water samples of various concentrations. Sodium Fluoride (NaF) was used to prepare 5 mg/L, and 10 mg/L of Fluoride solution which was kept in 250 ml plastic container in refrigerated condition (4°C).

5.4.2. Effect of adsorbent dose variation

The percentage removal of Fluoride ion from the spiked water sample was studied by varying the adsorbent dosage of the prepared sample. The adsorbent used was FL and dosage under consideration was 5 g/L, 10 g/L, 20 g/L, 30 g/L, and 50 g/L. Other parameters were kept constant viz. Fluoride concentration: 10 mg/L; Contact time: 15 min; Temperature: 30°C; pH: 5 in an orbital shaker at a speed of 250 rpm.

5.4.3. Effect of contact time

The percentage removal of Fluoride ion from the spiked water sample was studied by varying the adsorbent dosage of the prepared sample. The adsorbent used was FL and the time was varied as 5 min, 15 min, 30 min, 45 min, 1 h, 2 h, 4 h, and 24 h. Other parameters were kept constant viz. Fluoride concentration: 10 mg/L; FL Dose: 20 g/L; Temperature: 30°C; pH: 5 in an orbital shaker at a speed of 250 rpm.

5.4.4. Effect of pH

The percentage removal of Fluoride ion from the spiked water sample was studied by varying the adsorbent dosage of the prepared sample. The adsorbent used was FL and the pH was varied as 3, 5, 7, 9, and 12. Other parameters were kept constant viz. Fluoride concentration: 10 mg/L; FL Dose: 20 g/L; Temperature: 30°C for a contact time of 15 minutes in an orbital shaker at a speed of 250 rpm

5.4.5. Effect of Initial concentration

The percentage removal of Arsenate ion from the spiked water sample was studied by varying the initial concentration of Arsenate in the spiked water sample. The adsorbent used was R, FR, CR, CFR, S, FS, CS, CFS, L, FL, CL, and CFL and the initial concentration was varied as 5 mg/L, and 10 mg/L. Other parameters were kept constant viz. Adsorbent Dose: 20 g/L; pH: 5; Temperature: 30°C for a contact time of 15 minutes in an orbital shaker at a speed of 250 rpm

CHAPTER 6

RESULTS & DISCUSSIONS

Total 15 numbers of water hyacinth plant containing Roots, Stem, Leaves & Stolons was obtained. The initial observations about the obtained water hyacinth biomass has been tabulated in **Table 6.1**. It was observed that the roots stored the highest arsenic (4960.86 µg/kg) among all the parts of the plant. 95.03% of weight of root biomass was reduced upon drying, 96.82% for stem biomass, and 88.41% for leaf biomass.

Table 6.1: Characterization of water hyacinth biomass

Parts of Plant	Nos.	Initial length (cm)	Initial weight (g)	Final weight (g)	Reduction in weight (%)	Total arsenic (µg/kg)
Roots	15	54	664	33	95.03	4960.86
Stem	15	10	1700	54	96.82	1380.81
Leaves	15	9	406	47	88.41	76.34

6.1. Biochar Yield

Initial & final weights were taken in order to get an idea about the quantity of biochar obtained from the biomass. A very low yield of biochar was noted for stem (1.75%), followed by roots (3.13%) and (5.91%) for leaves.

Table 6.2 shows the ultimate yield of biochar obtained from water hyacinth biomass. The yield of biochar is an important parameter for cost analysis at industrial scale.

Table 6.2: Yield of biochar derived from water hyacinth biomass

Parts of plant	Initial weight of Biomass (g)	Weight of biochar (g)	Ultimate Yield (%)
Roots	663.95	20.79	3.13
Stem	1700.18	29.7	1.75
Leaves	405.51	23.97	5.91

6.2. Removal of As (V) from spiked water

6.2.1. Effect of adsorbent dose variation

Initial Arsenate Conc. (C_i) = 100 µg/L, Mixing time = 15 min, pH = 5, Temp. = 30°C, Mixing speed = 250 rpm

Table 6.3: Removal efficiency of arsenic against variation in adsorbent dose

ADSORBENT	ADSORBENT DOSE (g/L)	FINAL ARSENATE CONC. (µg/L) [C_e]	REMOVAL (C_i - C_e)	REMOVAL EFFICIENCY (%)
FR	5	0.12	99.88	99.88
FR	10	0.05	99.95	99.95
FR	20	0.01	99.99	99.99
FR	30	0.01	99.99	99.99
FR	50	0.01	99.99	99.99

To investigate the effect of adsorbent dosage on arsenate adsorption efficiency, the amount of adsorbent (FR) was varied (5 - 50) g/L while maintaining initial arsenate at 100 µg/L and pH (5). The solution was shaked at a constant speed of 250 rpm. **Table 6.3** and **Figure 6.1** shows that increasing the adsorbent dosage from (5 to 50) g/L, increases the percentage arsenate removal by adsorbent from 99.88% to 99.99%.

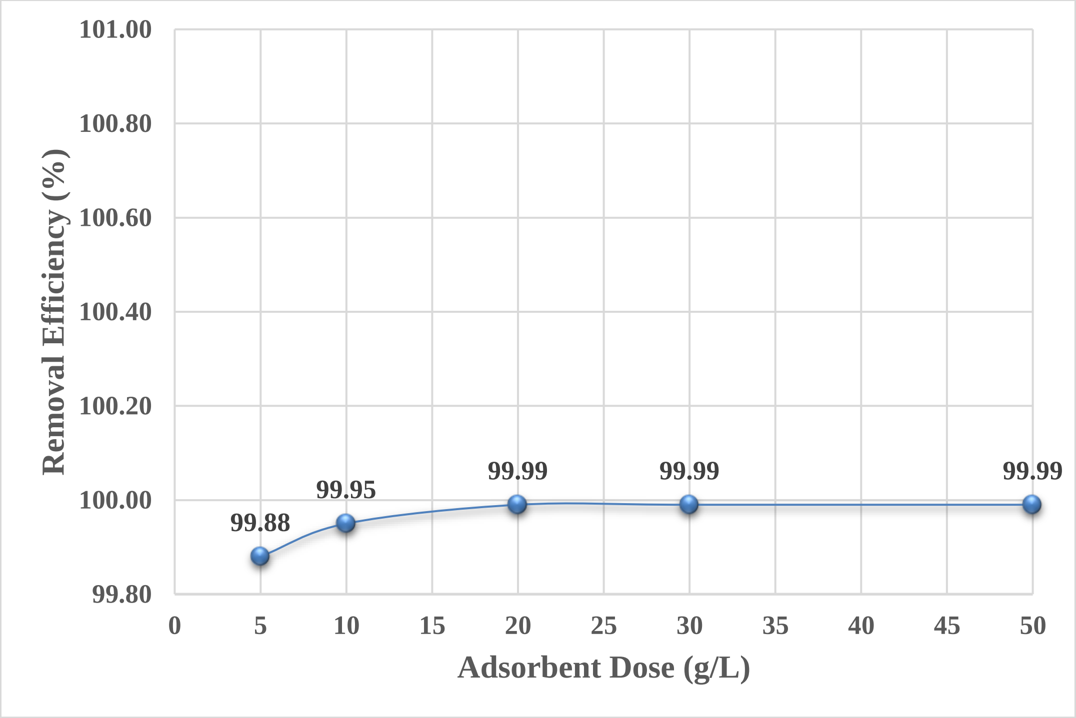

Fig. 6.1: Effect of adsorbent dose on adsorption of As (V) on FR

6.2.2. Effect of contact time

Initial Arsenate Conc. (C_i) = 100 µg/L, Adsorbent dose = 20 g/L, pH = 5, Temp. = 30°C, Mixing speed = 250 rpm

Table 6.4: Removal efficiency of arsenic against variation in mixing time

ADSORBENT	TIME (h)	FINAL ARSENATE CONC. (µg/L) [C_e]	REMOVAL (C_i - C_e)	REMOVAL EFFICIENCY (%)
FR	5 min	3.84	96.16	96.16
FR	15 min	0.00	100.00	100.00
FR	30 min	0.00	100.00	100.00
FR	45 min	0.00	100.00	100.00
FR	1	0.00	100.00	100.00
FR	2	0.00	100.00	100.00
FR	4	0.00	100.00	100.00
FR	24	0.00	100.00	100.00

The adsorption of arsenate ion on FR as a function of contact time was investigated at an initial arsenate ion concentration of 100 µg/L, pH 5, and adsorbent dose of 20 g/L. The solution was shaked at a constant speed of 250 rpm.

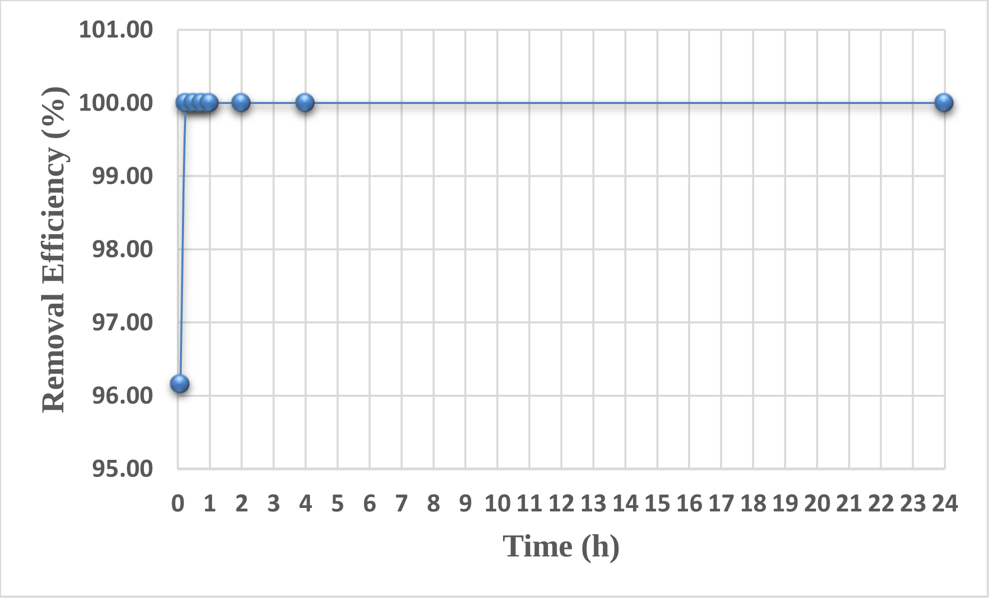

Fig. 6.2: Effect of contact time on adsorption of As (V) on FR

Table 6.4 and **Figure 6.2** shows that as contact time increases from 5 min to 1440 minutes, the percentage of arsenate removed increases from 96.16% to 100%. The time of equilibrium was considered as 15 min for batch adsorption experiments because desirable removal was almost achieved at this time duration.

6.2.3. Effect of pH

Initial Arsenate Conc. (C_i) = 100 µg/L, Adsorbent dose = 20g/L, Mixing time = 15 min, Temp. = 30°C, Mixing speed = 250 rpm

Table 6.5: Removal efficiency of arsenic against variation in pH

ADSORBENT	pH	FINAL ARSENATE CONC. (µg/L) [C_e]	REMOVAL (C_i - C_e)	REMOVAL EFFICIENCY (%)
FR	3	0.00	100.00	100.00
FR	5	0.00	100.00	100.00
FR	7	0.00	100.00	100.00
FR	9	0.12	99.88	99.88
FR	12	15.27	84.73	84.73

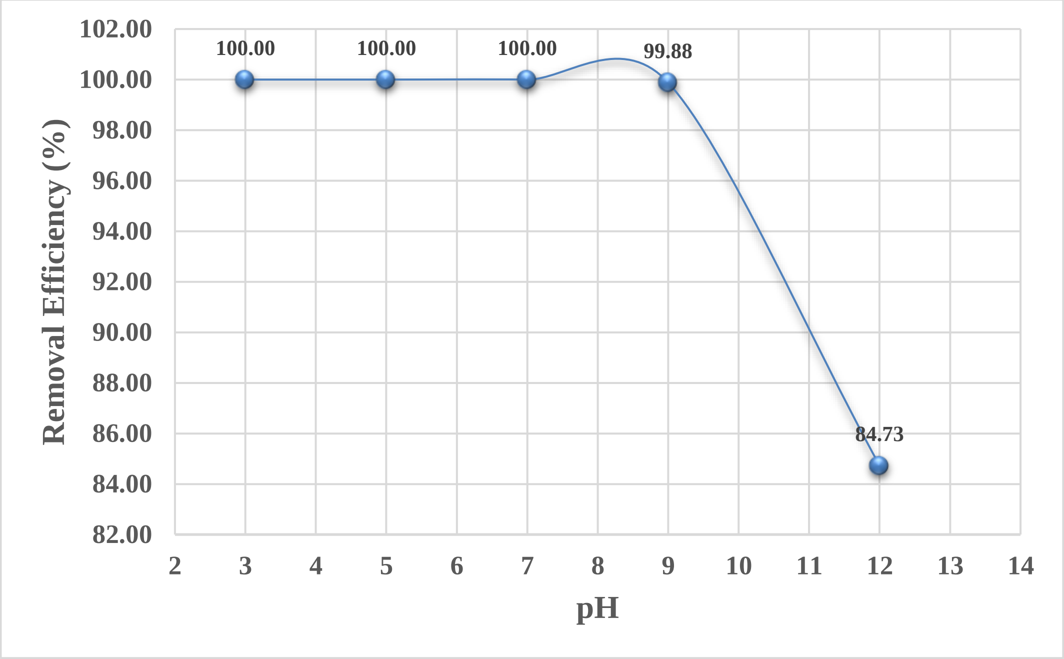

Fig. 6.3: Effect of pH on adsorption of As (V) on FR

The effect of pH on As (V) depletion by FR was investigated and shown in **Table 6.5** and **Figure 6.3**. With pH ranging from 3 to 12, As (V) removal percentage remained consistently greater than 90% after equilibrium (Figure 6.3), indicating that pH has no effect on As (V) removal till pH 9. However, As (V) removal decreased rapidly as pH increased above 9, most likely due to increased competition between OH and $HAsO_4^{2-}$ for adsorption sites on negatively charged adsorbent. The fact that there was little decrease in As (V) removal from aqueous solution by the magnetic biochar prepared in this study until pH increased to >9 indicated that prepared magnetic biochar (FR) has a broad applicability for most As-containing water.

6.2.4. Effect of Initial concentration

Dose = 20g/L, Mixing time = 15 min, pH = 5, Temp. = 30°C, Mixing speed = 250 rpm

Table 6.6: Removal efficiency of arsenic against variation in initial concentration

ADSORBENT	Initial Conc. (μg/L)	FINAL ARSENATE CONC. (μg/L) [C_e]	REMOVAL ($C_i - C_e$)	REMOVAL EFFICIENCY (%)
R	100	31.25	68.75	68.75
	500	161.60	338.40	67.68
	1000	395.20	604.80	60.48
FR	100	0.78	99.22	99.22
	500	1.65	498.35	99.67
	1000	8.52	991.48	99.148
CR	100	6.80	93.20	93.20
	500	24.80	475.20	95.04
	1000	91.60	908.40	90.84
CFR	100	0.85	99.15	99.15
	500	7.58	492.42	98.484
	1000	12.74	987.26	98.726
S	100	75.85	24.15	24.15
	500	265.20	234.80	46.96
	1000	657.80	342.20	34.22
FS	100	0.00	100.00	100.00
	500	3.79	496.21	99.242
	1000	0.00	1000.00	100
CS	100	12.05	87.95	87.95
	500	56.30	443.70	88.74
	1000	102.80	897.20	89.72
CFS	100	0.72	99.28	99.28
	500	13.80	486.20	97.24
	1000	70.15	929.85	92.985
L	100	44.75	55.25	55.25
	500	275.30	224.70	44.94
	1000	381.00	619.00	61.9
FL	100	2.37	97.63	97.63
	500	1.82	498.18	99.636
	1000	0.00	1000.00	100
CL	100	17.45	82.55	82.55
	500	105.30	394.70	78.94
	1000	188.30	811.70	81.17
CFL	100	0.72	99.28	99.28
	500	8.43	491.57	98.314
	1000	16.85	983.15	98.315

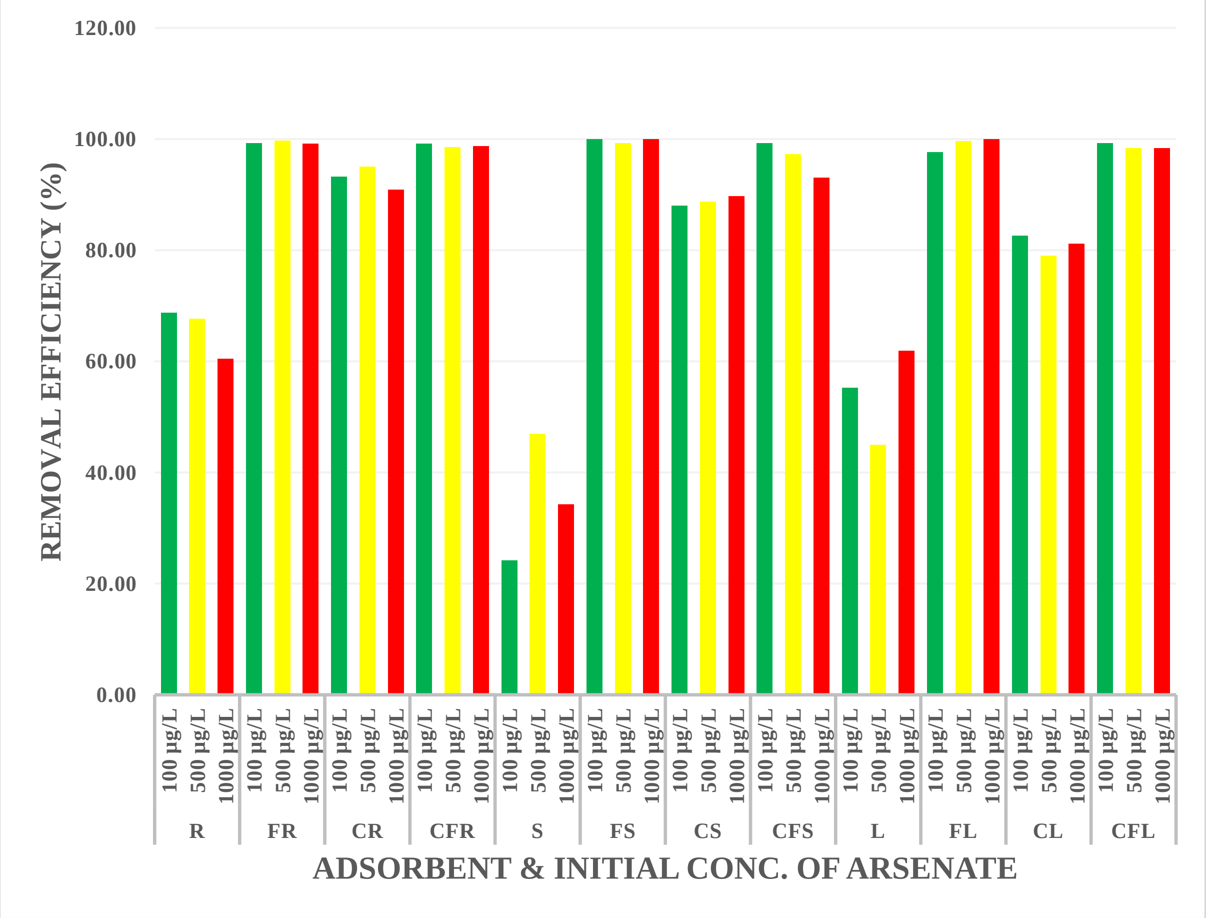

Fig. 6.4: Effect of initial As (V) concentration on adsorption of As (V) on FR

The effect of initial concentration on the percentage removal of As (V) by various adsorbent was investigated by varying the initial concentration from (100, 500, 1000) µg/L while maintaining all other parameters constant, such as pH (5), adsorbent dose (20 g/L), and contact time (15 min) while shaking at a speed of 250 rpm. **Table 6.6** and **Figure 6.4** shows that increasing the initial arsenate concentration has very less effect on the percentage removal of arsenate ions while significant increase in the adsorption capacity (q_e) was observed.

6.2.5. Adsorption Isotherms

The Langmuir isotherm describes the monolayer adsorption of pollutants onto the adsorbent surface with a finite number of adsorption sites, whereas the Freundlich isotherm supports the fact that adsorption occurs on the adsorbent's heterogeneous surface (Sierra et al., 2020).

a) Langmuir adsorption isotherm

Table 6.7: Calculation of Langmuir adsorption isotherm for As (V)

AD (g/L)	W (g/10ml)	C_e (µg/L)	$(C_i - C_e)$	$1 / C_e$	q_e (µg/g) = $(C_i - C_e)$ * V / W	$1 / q_e$
5	0.0521	0.12	99.88	8.33333	19.1708253	0.052
10	0.1046	0.05	99.95	20	9.5554493	0.105
20	0.2014	0.01	99.99	100	4.9647468	0.201
30	0.3024	0.01	99.99	100	3.3065476	0.302
50	0.5149	0.01	99.99	100	1.9419305	0.515

where,

AD = Adsorbent dose (g/L)

C_i = Initial arsenic concentration = 100 µg/L

C_e = Final arsenic concentration (µg/L)

V = Volume taken = 10 ml = 0.01 L

q_e = Adsorption capacity at equilibrium (µg/g)

Q_{max} = Maximum adsorption rate (µg/g)

W = Mass of adsorbent taken (g)

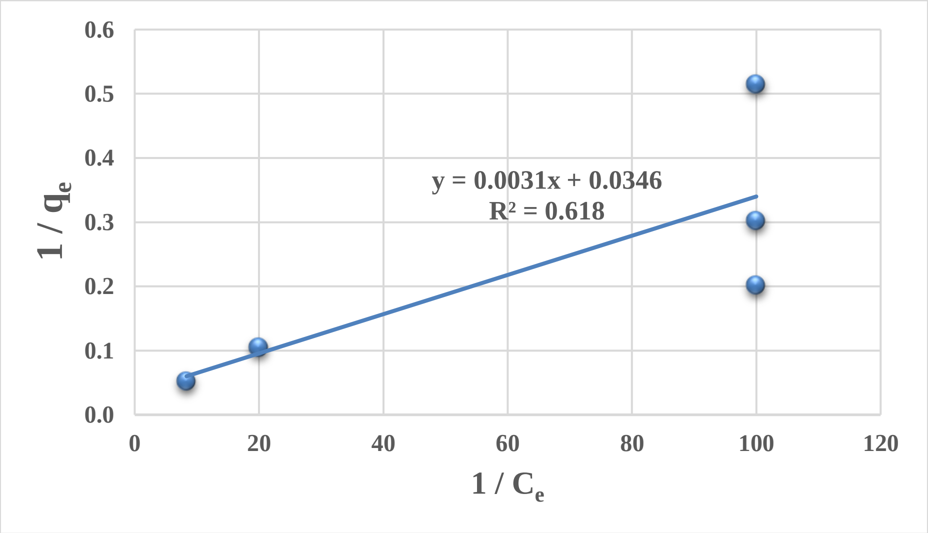

Fig. 6.5: Langmuir plot for removal of As (V) at 100 µg/L, pH = 5, Temp. of 30°C, Contact time of 15 min. and varied adsorbent dosage / 10 ml volume

Table 6.8: Langmuir isotherm parameters for As (V) sorption onto FR

Isotherm	*Parameters*	*Value*
Langmuir	**Intercept**	0.0346
	Slope	0.0031
	Q_{max} (µg/g)	28.90
	K_L	11.16
	R_L	0.01
	R^2	0.618

b) Freundlich adsorption isotherm

By assuming a heterogeneous surface with a non-uniform distribution of heat of adsorption over the surface, the Freundlich isotherm is derived. According to the Freundlich equation, sorption energy decreases exponentially as an adsorbent's sorption centres are completed.

Table 6.9: Calculation of Freundlich adsorption isotherm for As (V)

AD (g/L)	**W (g/10ml)**	**C_e (µg/L)**	**$(C_i - C_e)$**	**Log_{10} C_e**	**q_e (µg/g) = $(C_i - C_e) * V / W$**	**Log_{10} Q_e**
5	0.0521	0.12	99.88	-0.9208	19.1708253	1.28264
10	0.1046	0.05	99.95	-1.301	9.5554493	0.98025
20	0.2014	0.01	99.99	-2	4.9647468	0.6959
30	0.3024	0.01	99.99	-2	3.3065476	0.51937
50	0.5149	0.01	99.99	-2	1.9419305	0.28823

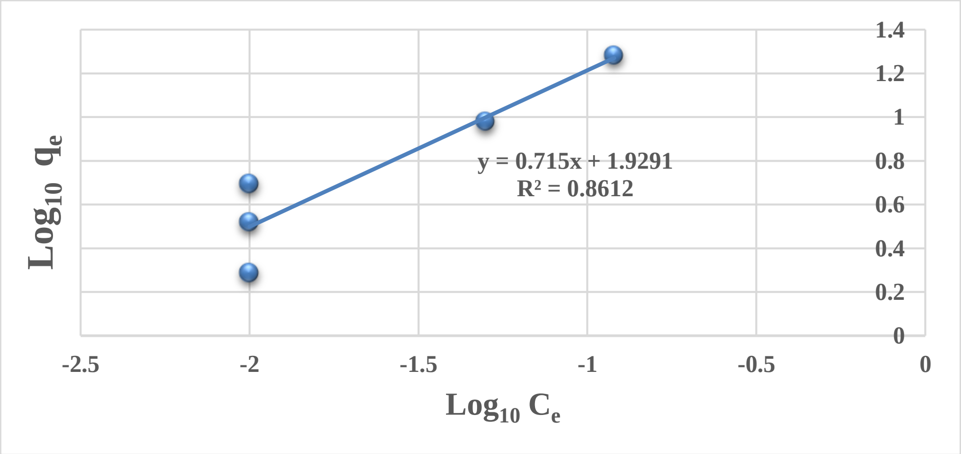

Fig. 6.6: Freundlich plot for removal of As (V) at 100 µg/L, pH = 5, Temp. of 30°C, Contact time of 15 min. and varied adsorbent dosage / 10 ml volume

Table 6.10: Freundlich isotherm parameters for As (V) sorption onto FR

Isotherm	*Parameters*	*Value*
Freundlich	**Intercept**	1.9291
	Slope	0.715
	n	1.40
	K_f (µg/g)	84.94
	R^2	0.8612

From the plot, the values of n and K_f were calculated as 1.40 and 84.94 µg/g, respectively, at R^2 value 0.8612. The values of n greater than 1 shows favourable condition for adsorption.

The results shown in **Table 6.1** & **6.2** show that Freundlich' s isotherm was the best fit because the linear regression coefficient (R^2 > 0.8612) of this isotherm was found to be higher than that of the Langmuir isotherm (R^2 > 0.618), confirming the heterogeneous adsorption of arsenate on adsorbent (FR). The maximum adsorption capacity of FR for As (V) was observed to be 84.94 µg/g.

6.2.6. Adsorption kinetics

a) Pseudo first order adsorption model

Table 6.11: Calculation of pseudo first order adsorption model for As (V)

AD (g/L)	**W (g/10ml)**	**Time (min)**	**C_e (µg/L)**	**$(C_i - C_e)$**	**q_t (µg/g) = $(C_i - C_e)$ * V / W**	**$Log_e (q_e - q_t)$**
20	0.2084	5	3.84	96.16	4.6142035	-1.152657117
20	0.2058	15	0.81	99.19	4.8197279	-2.204804251
20	0.2056	30	0.00	100	4.8638132	-2.715274678
20	0.2098	45	0.00	100	4.7664442	-1.810601262
20	0.2084	60	0.00	100	4.7984645	-2.028478436
20	0.2075	120	0.00	100	4.8192771	-2.200724671
20	0.2088	240	0.00	100	4.7892720	-1.960926547
20	0.2078	1440	0.00	100	4.8123195	-2.139782277

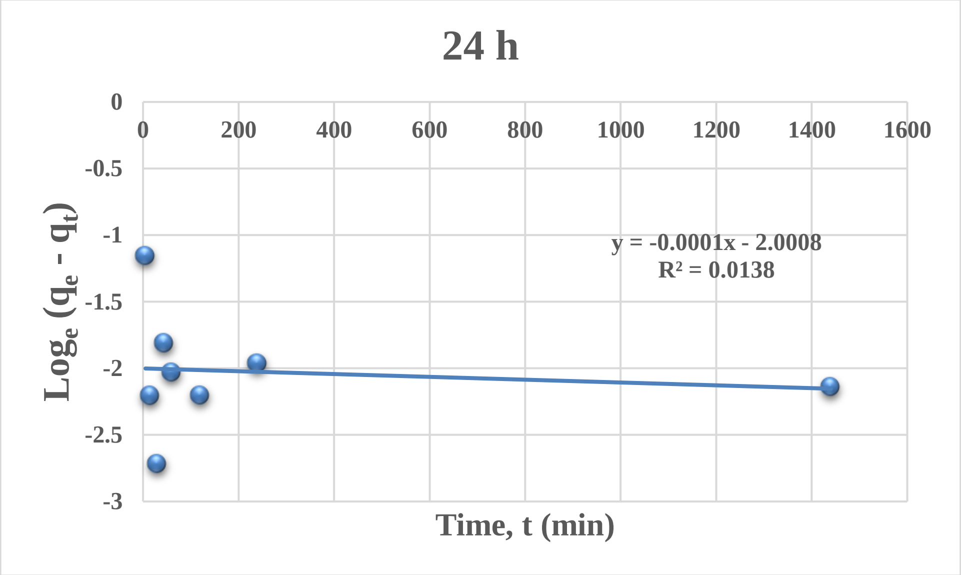

Fig. 6.7: Pseudo 1st order reaction plot for removal of As (V) at 100 µg/L, Dosage = 20 g/L, pH = 5, Temp. of 30°C, and varied contact time up to 24 h

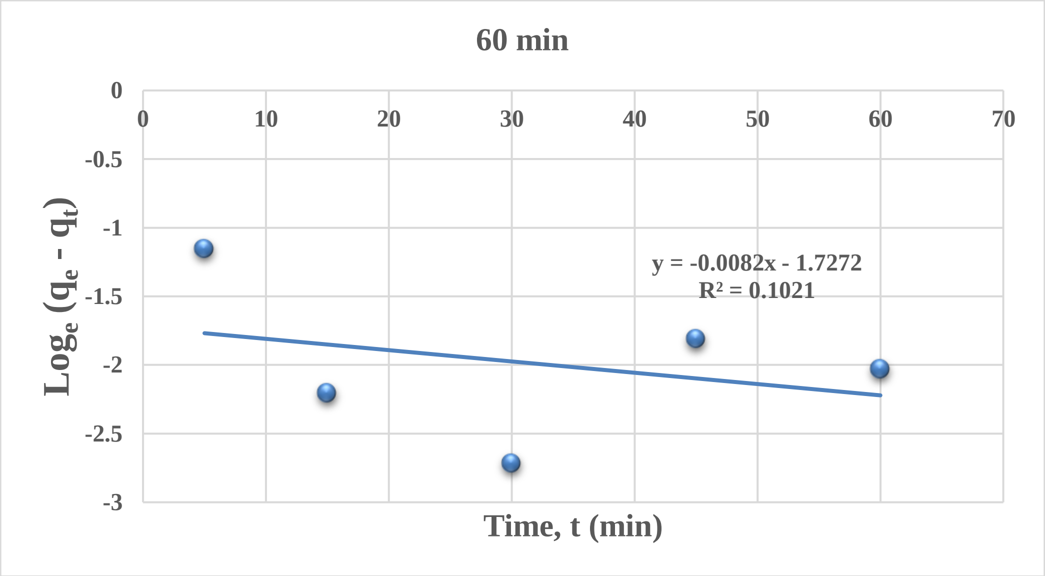

Fig. 6.8: Pseudo 1st order reaction plot for removal of As (V) at 100 µg/L, Dosage = 20 g/L, pH = 5, Temp. of 30°C, and varied contact time up to 1 h

Table 6.12: Pseudo 1st order model (24 h) of As (V)

Intercept	**Slope**	**q_e**	**K_1**	**R^2**
-2.0008	-0.0001	0.14	-6.94E-08	0.0138

Table 6.13: Pseudo 1st order model (1 h) of As (V)

Intercept	**Slope**	**q_e**	**K_1**	**R^2**
-1.7272	-0.0082	0.18	-0.000137	0.1021

b) Pseudo second order adsorption model

Table 6.14: Calculation of pseudo second order adsorption model for As (V)

AD (g/L)	**W (g/10ml)**	**Time (min)**	**C_e (µg/L)**	**(C_i - C_e)**	**q_t (µg/g) = (C_i - C_e) * V / W**	**t / q_t**
20	0.2084	5	3.84	96.16	4.6142035	1.0836106
20	0.2058	15	0.81	99.19	4.8197279	3.1122089
20	0.2056	30	0.00	100	4.8638132	6.1680000
20	0.2098	45	0.00	100	4.7664442	9.4410000
20	0.2084	60	0.00	100	4.7984645	12.5040000
20	0.2075	120	0.00	100	4.8192771	24.9000000
20	0.2088	240	0.00	100	4.7892720	50.1120000
20	0.2078	1440	0.00	100	4.8123195	299.2320000

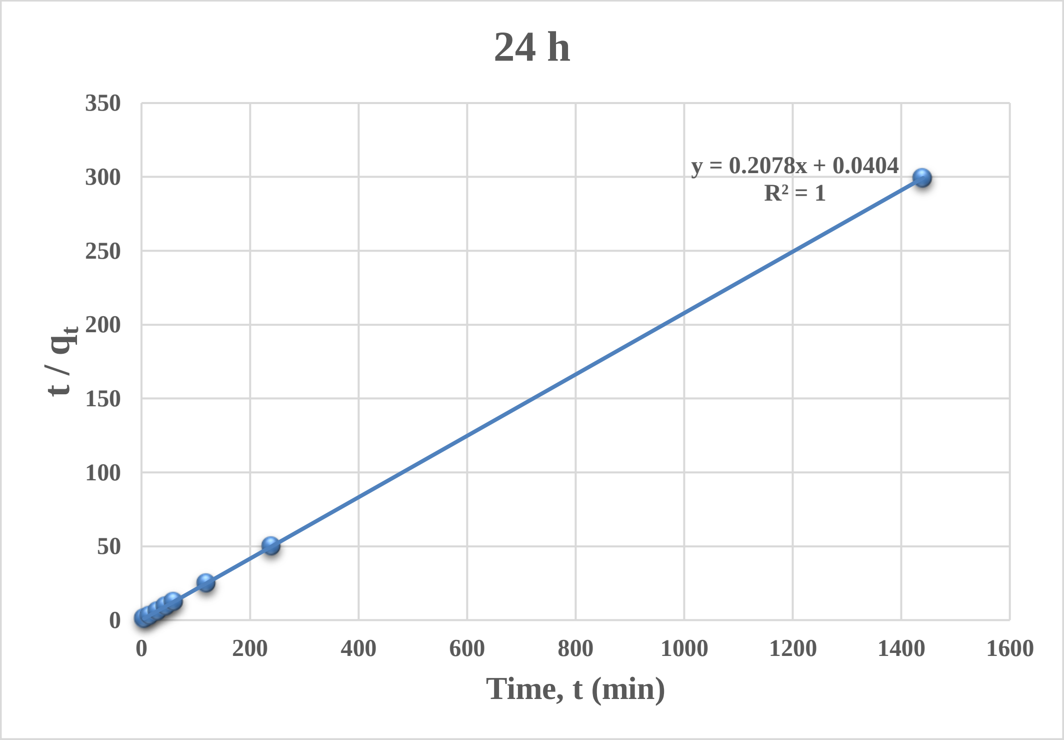

Fig. 6.9: Pseudo 2nd order reaction plot for removal of As (V) at 100 µg/L, Dosage = 20 g/L, pH = 5, Temp. of 30°C, and varied contact time up to 24 h

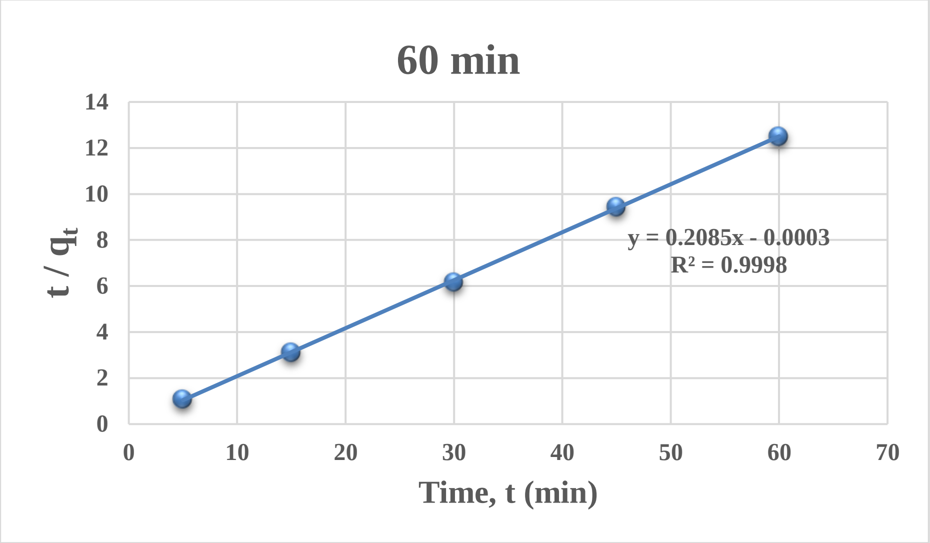

Fig. 6.10: Pseudo 2nd order reaction plot for removal of As (V) at 100 µg/L, Dosage = 20 g/L, pH = 5, Temp. of 30°C, and varied contact time upto 1 h

Table 6.15: Pseudo 2nd order model (24 h) of As (V)

Intercept	**Slope**	**q_e**	**K_2**	**R^2**
0.0404	0.2078	4.81	1.0688327	1

Table 6.16: Pseudo 2nd order model (1 h) of As (V)

Intercept	**Slope**	**q_e**	**K_2**	**R^2**
-0.0003	0.2085	4.8	-144.9075	0.9998

Adsorption kinetic curves for As (V) onto FR are shown separately in **Graphs 6.7, 6.8, 6.9, and 6.10**. Fast and maximum arsenic adsorption was observed with the FR in the first 5 minutes, and equilibrium was reached within 30 minutes. This fast-kinetic behavior indicates that the adsorption process was dependent on the available binding sites on FR for arsenic species uptake. After 30 minutes, the adsorbent surface became saturated with adsorbate, and dynamic equilibrium was reached.

The pseudo first and second order rate equations were used in this study to further evaluate the kinetic parameters of arsenic adsorption on FR. The fitting of two kinetic models to the As (V) equilibrium data is shown in Graphs 6.7, 6.8, 6.9, and 6.10, and the results of respective kinetic parameters are shown in consecutive tables. Because it had a higher value of linear regression coefficient ($R^2 > 0.998$, in all cases) than the pseudo 1st order model ($R^2 > 0.0138$, in all cases), the pseudo 2nd order kinetics was found to be the best fitted model in explaining the kinetics of As(V) adsorption on FR.

6.3. Defluoridation from spiked water

6.3.1. Effect of adsorbent dose variation

Initial Fluoride Conc. (C_i) = 10 mg/L, Mixing time = 15 min, pH = 5, Temp. = 30°C, Mixing speed = 250 rpm

Table 6.17: Removal efficiency of fluoride against variation in adsorbent dose

ADSORBENT	ADSORBENT DOSE (g/L)	FINAL FLUORIDE CONC. (mg/L) [C_e]	REMOVAL (C_i - C_e)	REMOVAL EFFICIENCY (%)
FL	5	4.24	5.76	57.6
FL	10	2.72	7.28	72.8
FL	20	1.68	8.32	83.2
FL	30	1.55	8.45	84.5
FL	50	1.47	8.53	85.3

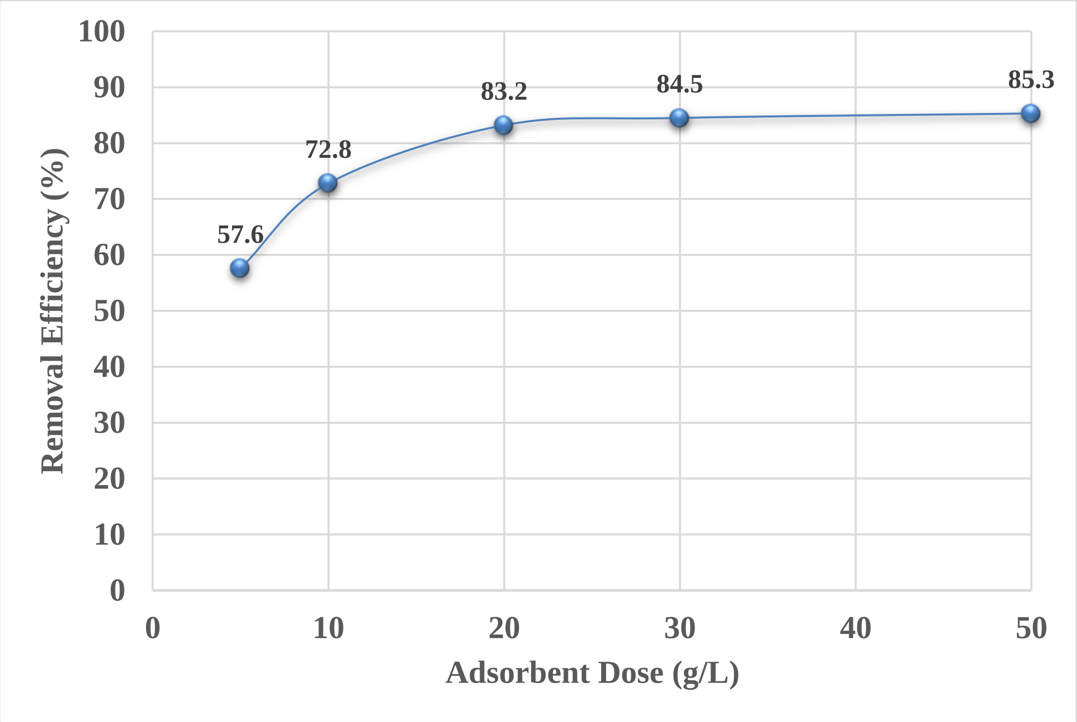

Fig. 6.11: Effect of Adsorbent dose on adsorption of F^- on FL.

To investigate the effect of adsorbent dosage on fluoride adsorption efficiency, the amount of adsorbent (FL) was varied (5 - 50) g/L while maintaining initial fluoride at 10 mg/L and pH (5). **Table 6.17** and **Figure 6.11** shows that increasing the adsorbent dosage from (5 to 50) g/L, increases the percentage fluoride removal by adsorbent from 57.6% to 85.3%.

6.3.2. Effect of contact time

Initial Fluoride Conc. (C_i) = 10 mg/L, Adsorbent dose = 20 g/L, pH = 5, Temp. = 30°C, Mixing speed = 250 rpm

Table 6.18: Removal efficiency of fluoride against variation in mixing time

ADSORBENT	TIME (h)	FINAL FLUORIDE CONC. (mg/L) [C_e]	REMOVAL (C_i - C_e)	REMOVAL EFFICIENCY (%)
FL	5 min	1.81	8.19	81.9
FL	15 min	1.54	8.46	84.6
FL	30 min	1.38	8.62	86.2
FL	45 min	1.14	8.86	88.6
FL	1	1.09	8.91	89.1
FL	2	1.05	8.95	89.5
FL	4	1.01	8.99	89.9
FL	24	0.971	9.03	90.29

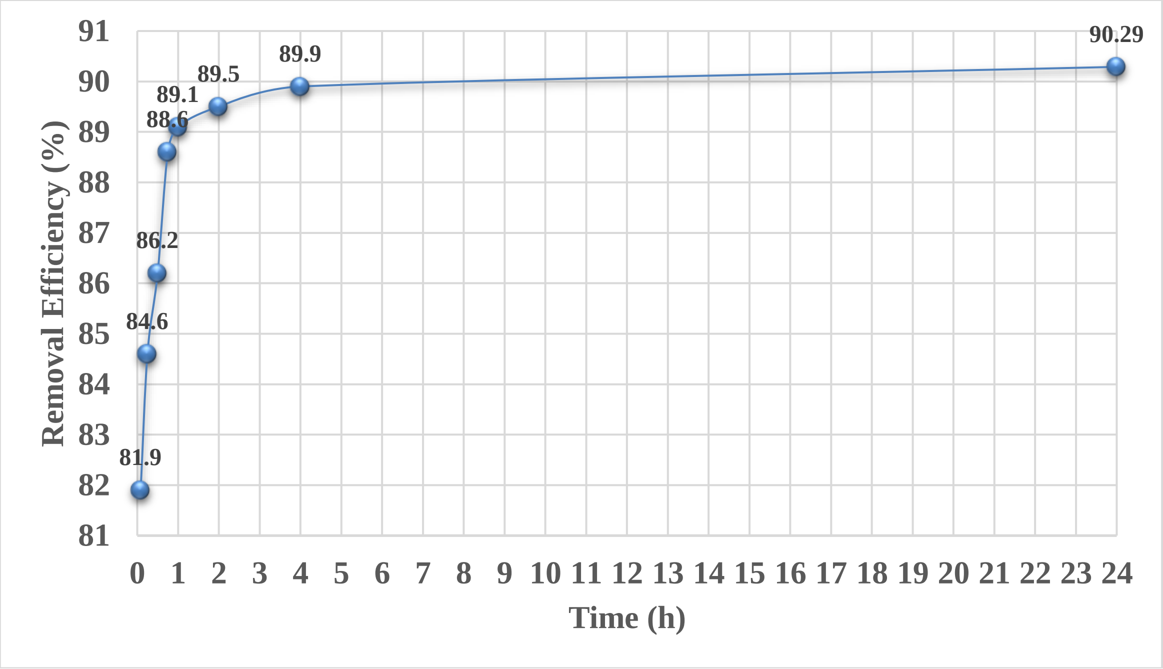

Fig. 6.12: Effect of contact time on adsorption of F^- on FL.

Two parameters, namely initial concentration and contact time, should have a significant impact on drinking water defluoridation. The adsorption of fluoride ion on FL as a function of contact time was investigated at an initial fluoride ion concentration of 10 mg/L, pH 5, and adsorbent dose of 20 g/L. The solution was mixed at a constant speed of 250 rpm.

Table 6.18 and **Figure 6.12** shows that as contact time increases from 5 min to 1440 minutes, the percentage of fluoride removed increases from 81.9% to 90.29%. It was also discovered that the removal percentage was slow at first and eventually reached a maximum at 60 minutes of contact time, after which there was very minor change in the removal percentage. This was caused by the saturation of all active sites on the adsorbent. The time of equilibrium however was considered as 15 min for batch adsorption experiments because desirable removal was almost achieved at this time duration.

6.3.3. Effect of pH

Initial Fluoride Conc. (C_i) = 10 mg/L, Adsorbent dose = 20 g/L, Mixing time = 15 min.,
Temp. = 30°C, Mixing speed = 250 rpm

Table 6.19: Removal efficiency of fluoride against variation in pH

ADSORBENT	pH	FINAL FLUORIDE CONC. (mg/L) [C_e]	REMOVAL (C_i - C_e)	REMOVAL EFFICIENCY (%)
FL	3	3.85	6.15	61.5
FL	5	1.68	8.32	83.2
FL	7	5.30	4.70	47
FL	9	5.10	4.90	49
FL	12	7.20	2.80	28

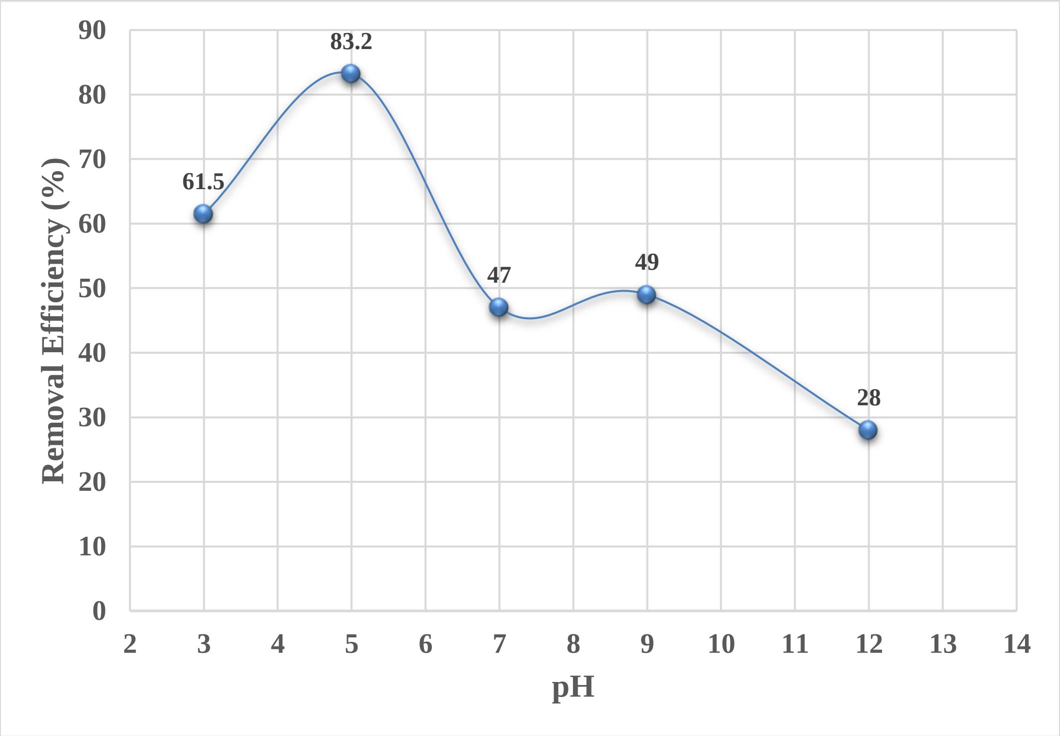

Fig. 6.13: Effect of pH on adsorption of F^- on FL

The pH of the medium has been discovered to influence the adsorption process. Different batch experiments at different pH (3–12) were performed to determine the optimum pH at which adsorption is maximum. **Table 6.19** and **Figure 6.13** shows that the removal percentage of fluoride ion is low at very low pH (at value 3.08) about 61.5%. As the pH increased from 3 to 5, the removal percentage increased from 61.5% to 83.2%, then decreased as the pH increased further. As a result, the optimal pH at which adsorption achieves maximum value could be in the range of 4 - 6.

Depending on the pH of the water, fluorine can exist as HF and F^- (fluoride ion). As the pH increases from (4 to 5), two phenomena could have occurred:

a) The concentration of fluoride ion (F^-) becomes greater than that of HF, and

b) Protonation of the functional group of adsorbent occurs to form charged functional group and protonation of metal oxides and hydroxides occurs, making the surface of the adsorbent positively charged, which attracts the negatively charged fluoride ions present in water, resulting in high removal percentage.

As the pH rises above 5, two phenomena could have occurred:

a) Fluorine in water now exists entirely as fluoride ion (F), and

b) Ferric salts become negatively charged, resulting in competition for active sites by ions and electrostatic repulsion of anionic fluoride ion (F) by negatively charged adsorbent surface, resulting in a reduction in removal percentage.

The concentration of protons in water is very high at very low pH (3–4), which results in

a) Protonating the functional group of adsorbent as well as ferric salts and

b) Fluorine in water now mostly exists in the form of hydrogen fluoride (HF).

As a result, the number of binding sites is reduced. Furthermore, HF is stabilized through the formation of more stable intermolecular hydrogen bonding, which inhibits fluoride ion adsorption from its aqueous solution.

6.3.4. Effect of Initial concentration

Dose = 20 g/L, pH = 5, Time = 15 min., Temp. = 30°C, Shaker = 250 rpm

Table 6.20: Removal efficiency of fluoride against variation in initial conc. of fluoride

ADSORBENT	Initial Conc. (mg/L)	FINAL FLUORIDE CONC. (mg/L) [C_e]	REMOVAL (C_i - C_e)	REMOVAL EFFICIENCY (%)
R	5	1.52	3.48	69.6
	10	3.00	7.00	70
FR	5	3.82	1.18	23.6
	10	7.45	2.55	25.5
CR	5	1.58	3.42	68.4
	10	2.83	7.17	71.7
CFR	5	3.45	1.55	31
	10	6.67	3.33	33.3
S	5	2.89	2.11	42.2
	10	5.79	4.21	42.1
FS	5	2.86	2.14	42.8
	10	5.59	4.41	44.1
CS	5	1.76	3.24	64.8
	10	3.43	6.57	65.7
CFS	5	2.22	2.78	55.6
	10	4.46	5.54	55.4
L	5	3.88	1.12	22.4
	10	7.71	2.29	22.9
FL	5	0.963	4.04	80.74
	10	1.62	8.38	83.8
CL	5	1.68	3.32	66.4
	10	3.51	6.49	64.9
CFL	5	4.34	0.66	13.2
	10	8.52	1.48	14.8

The effect of initial concentration on the percentage removal of fluoride ion by various adsorbent was investigated by varying the initial concentration from (5 and 10) mg/L while maintaining all other parameters constant, such as pH (5), adsorbent dose (20 g/L), and contact time (15 min) while mixing at a speed of 250 rpm. Table 6.20 and Figure 6.14 shows that increasing the initial fluoride concentration has very less effect on the percentage removal of fluoride ions while significant increase in the adsorption capacity (q_e) was observed.

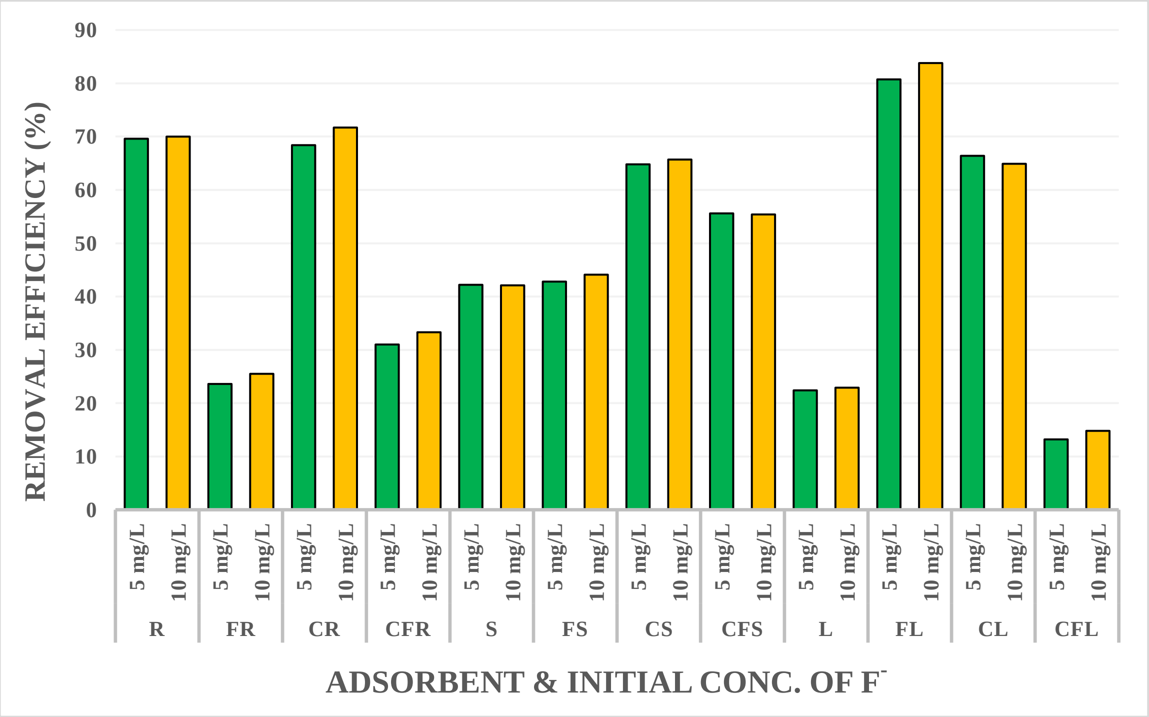

Fig. 6.14: Effect of initial concentration on adsorption of F^- on FL

6.3.5. Adsorption Isotherms

a) Langmuir adsorption isotherm

Table 6.21: Calculation of Langmuir adsorption isotherm for fluoride

AD (g/L)	W (g/10ml)	C_e (mg/L)	$(C_i - C_e)$	$1 / C_e$	q_e (mg/g) = $(C_i - C_e) * V / W$	$1 / q_e$
5	0.0507	4.24	5.76	0.23585	1.1360947	0.880
10	0.1008	2.72	7.28	0.36765	0.7222222	1.385
20	0.2091	1.68	8.32	0.59524	0.3978957	2.513
30	0.3006	1.55	8.45	0.64516	0.2811045	3.557
50	0.5024	1.47	8.53	0.68027	0.1697850	5.890

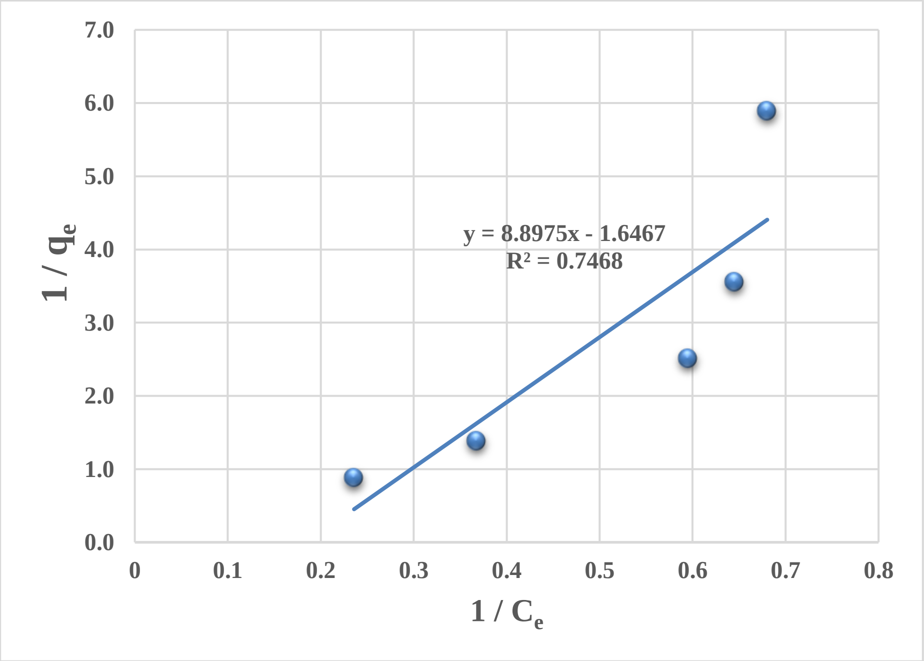

Fig. 6.15: Langmuir plot for removal of F^- at 10 mg/L, pH = 5, Temp. of 30°C, Contact time of 15 min. and varied adsorbent dosage / 10 ml volume

Table 6.22: Langmuir Isotherm Parameters for fluoride sorption onto FL

Isotherm	*Parameters*	*Value*
Langmuir	**Intercept**	-1.6467
	Slope	8.8975
	q_{max} (mg/g)	-0.607275156
	K_L	-0.185074459
	R_L	-1.175440914
	R^2	0.7468

b) Freundlich adsorption isotherm

Table 6.23: Calculation of Freundlich adsorption isotherm for fluoride

AD (g/L)	W (g/10ml)	C_e (mg/L)	(C_i - C_e)	Log_{10} C_e	q_e (mg/g) = (C_i - C_e) * V / W	Log_{10} q_e
5	0.0507	4.24	5.76	0.62737	1.1360947	0.05541
10	0.1008	2.72	7.28	0.43457	0.7222222	-0.1413
20	0.2091	1.68	8.32	0.22531	0.3978957	-0.4002
30	0.3006	1.55	8.45	0.19033	0.2811045	-0.5511
50	0.5024	1.47	8.53	0.16732	0.1697850	-0.7701

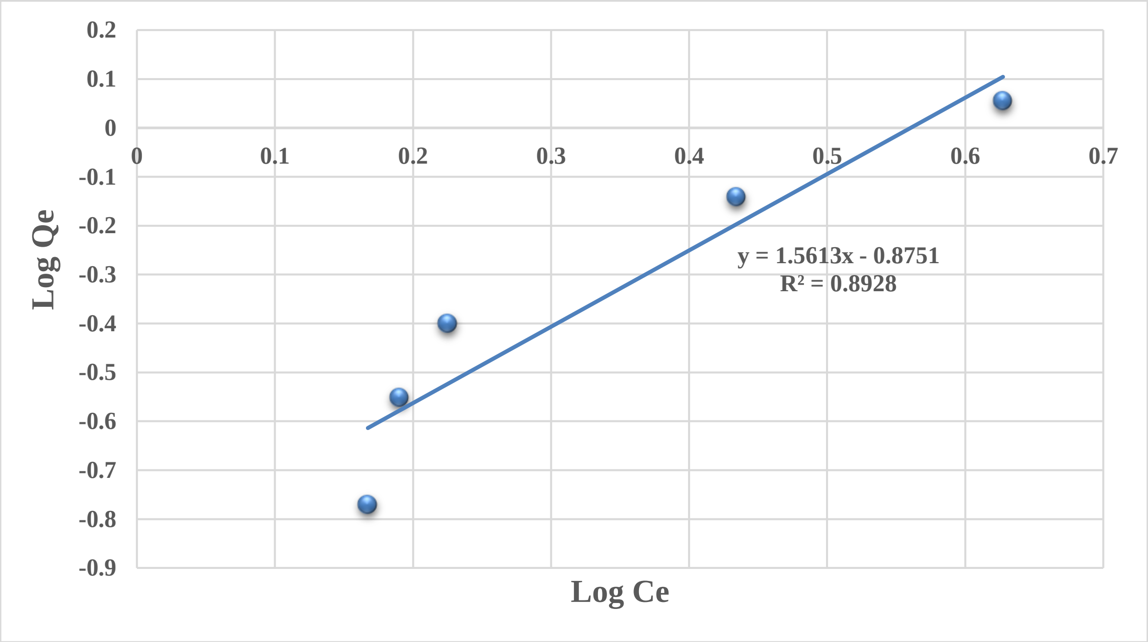

Fig. 6.16: Freundlich plot for removal of F$^-$ at 10 mg/L, pH = 5, Temp. of 30°C, Contact time of 15 min. and varied adsorbent dosage / 10 ml volume

From the plot, the values of n and K_f were calculated as 1.40 and 84.94 μg/g, respectively, at R^2 value 0.8612. The values of n greater than 1 shows favourable condition for adsorption.

Table 6.24: Freundlich Isotherm Parameters for fluoride sorption onto FL

Isotherm	*Parameters*	*Value*
Freundlich	**Intercept**	-0.8751
	Slope	1.5613
	n (mg/g)	0.640491898
	K_f	0.133321441
	R^2	0.8928

6.3.6. Adsorption kinetics

a) Pseudo first order adsorption model

Table 6.25: Calculation of pseudo first order adsorption model for fluoride

AD (g/L)	W (g/10ml)	Time (min)	C_e (mg/L)	$(C_i - C_e)$	q_t (μg/g) = $(C_i - C_e)$ * V / W	$Log_e (q_e - q_t)$
20	0.2099	5	1.81	8.19	0.3901858	-4.438453315
20	0.2089	15	1.54	8.46	0.4049785	#NUM!
20	0.2081	30	1.38	8.62	0.4142239	#NUM!
20	0.2085	45	1.14	8.86	0.4249400	#NUM!
20	0.2098	60	1.09	8.91	0.4246902	#NUM!
20	0.2096	120	1.05	8.95	0.4270038	#NUM!
20	0.2078	240	1.01	8.99	0.4326275	#NUM!
20	0.2088	1440	0.971	9.03	0.4324234	#NUM!

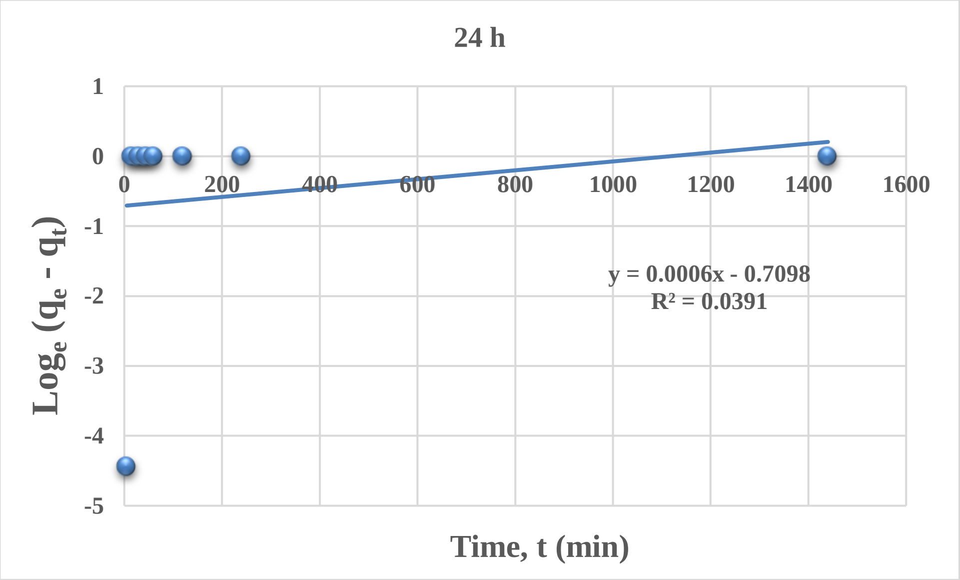

Fig. 6.17: Pseudo 1st order reaction plot for removal of F$^-$ at 10 mg/L, Dosage = 20 g/L, pH = 5, Temp. of 30°C, and varied contact time up to 24 h

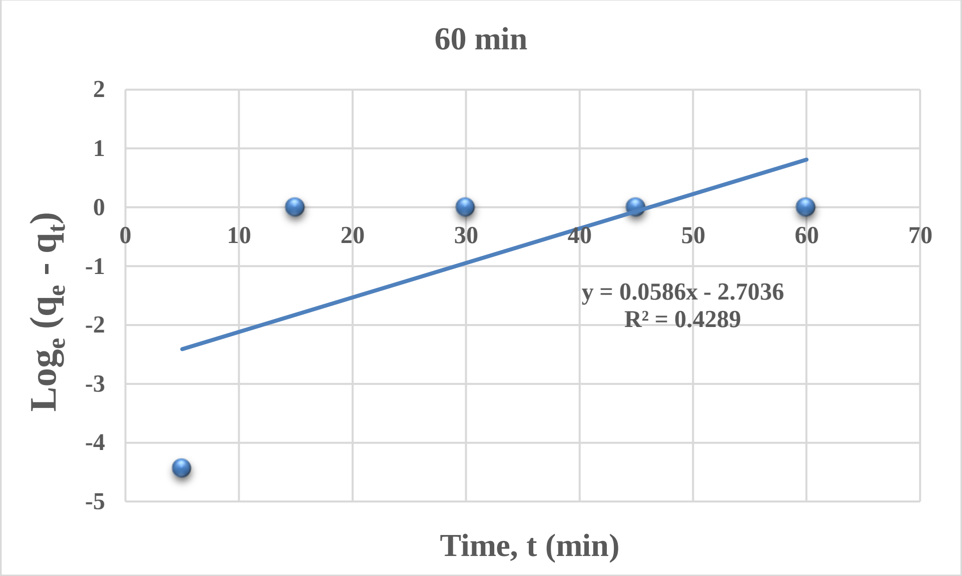

Fig. 6.18: Pseudo 1st order reaction plot for removal of F^- at 10 mg/L, Dosage = 20 g/L, pH = 5, Temp. of 30°C, and varied contact time up to 1 h

Table 6.26: Pseudo 1st order model (24 h) of fluoride

Intercept	**Slope**	**q_e**	**K_1**	**R^2**
-0.7098	0.0006	0.491743	4.16667E-07	0.0391

Table 6.27: Pseudo 1st order model (1 h) of fluoride

Intercept	**Slope**	**q_e**	**K_1**	**R^2**
-2.7036	0.0586	0.066964	4.06944E-05	0.4289

b) Pseudo second order adsorption model

Table 6.28: Calculation of pseudo second order adsorption model for fluoride

AD (g/L)	**W (g/10ml)**	**Time (min)**	**C_e (mg/L)**	**$(C_i - C_e)$**	**q_t (µg/g) = $(C_i - C_e)$ * V / W**	**t / q_t**
20	0.2099	5	1.81	8.19	0.3901858	12.8144078
20	0.2089	15	1.54	8.46	0.4049785	37.0390071
20	0.2081	30	1.38	8.62	0.4142239	72.4245940
20	0.2085	45	1.14	8.86	0.4249400	105.8972912
20	0.2098	60	1.09	8.91	0.4246902	141.2794613
20	0.2096	120	1.05	8.95	0.4270038	281.0279330
20	0.2078	240	1.01	8.99	0.4326275	554.7497219
20	0.2088	1440	0.971	9.029	0.4324234	3330.0697752

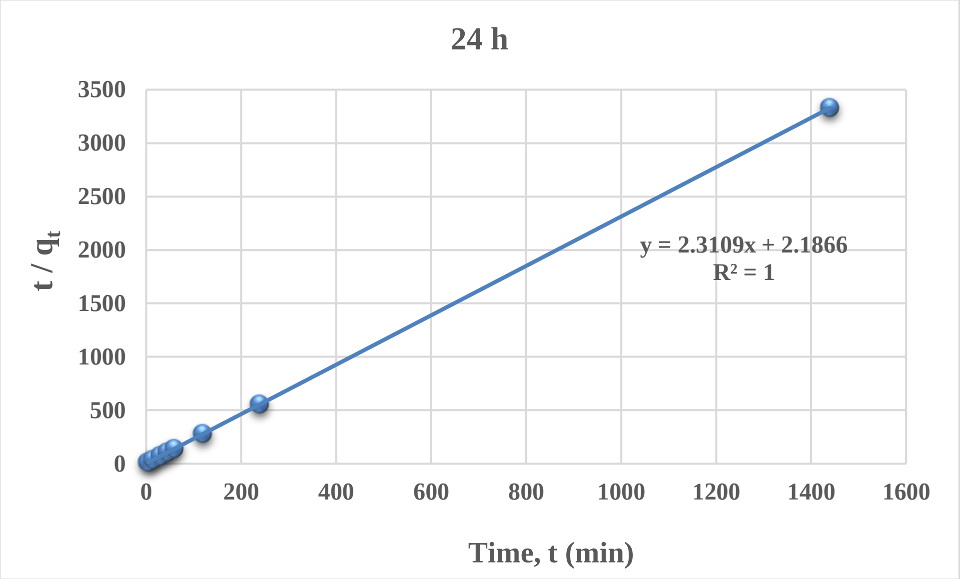

Fig. 6.19: Pseudo 2nd order reaction plot for removal of F^- at 10 mg/L, Dosage = 20 g/L, pH = 5, Temp. of 30°C, and varied contact time up to 24 h

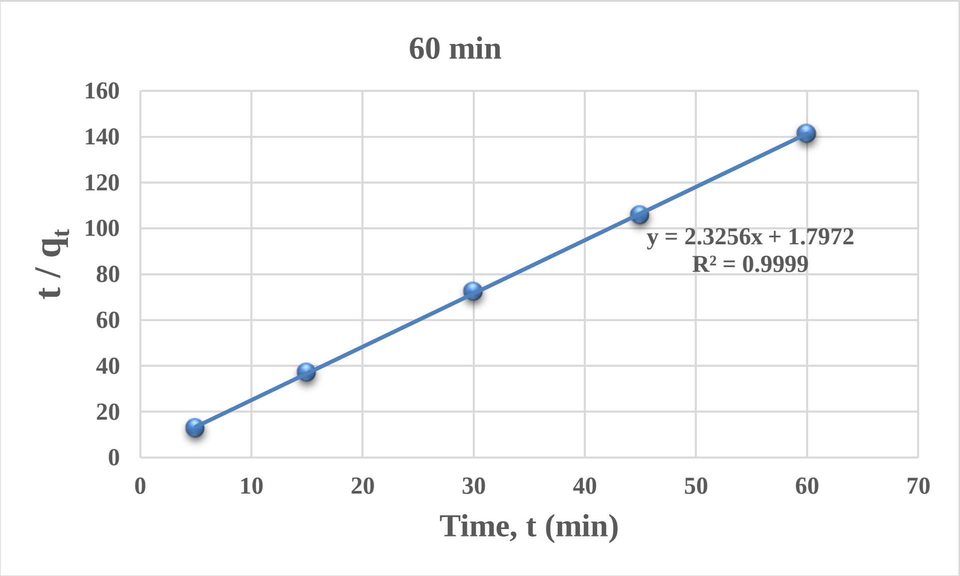

Fig. 6.20: Pseudo 2nd order reaction plot for removal of F^- at 10 mg/L, Dosage = 20 g/L, pH = 5, Temp. of 30°C, and varied contact time up to 1 h

Table 6.29: Pseudo 2nd order model (24 h) of fluoride

Intercept	Slope	q_e	K_2	R^2
2.1866	2.3109	0.432732	2.44227	1

Table 6.30: Pseudo 2nd order model (1 h) of fluoride

Intercept	Slope	q_e	K_2	R^2
1.7972	2.3256	0.429997	3.00936	0.9999

Adsorption kinetic curves for F^- onto FL are shown separately in **Figures 6.17, 6.18, 6.19, and 6.20**. Fast and maximum fluoride adsorption was observed with the FL in the first 30 minutes, and equilibrium was reached within 60 minutes. This fast-kinetic behavior indicates that the adsorption process was dependent on the available binding sites on FL for fluoride species uptake. After 60 minutes, the adsorbent surface became saturated with adsorbate, and dynamic equilibrium was reached.

The pseudo first and second order rate equations were used in this study to further evaluate the kinetic parameters of arsenic adsorption on FL. The fitting of two kinetic models to the F^- equilibrium data is shown in Figures 6.17, 6.18, 6.19, and 6.20, and the results of respective kinetic parameters are shown in consecutive tables 6.25, 6.26, 6.27, 6.28, 6.29, 6.30. Because it had a higher value of linear regression coefficient ($R^2 > 0.999$, in all cases) than the pseudo 1st order model ($R^2 > 0.01391$, in all cases), the pseudo 2nd order kinetics was found to be the best fitted model in explaining the kinetics of F^- adsorption on FL.

CHAPTER

7

SUMMARY & FUTURE SCOPE

Biochar was produced from parts of *Eichhornia crassipes (*water hyacinth) and it was amended with iron salts, calcium salts, and iron & calcium salts. The impregnation of biochar with these salts especially iron salts has been observed to increase the sorption efficiency of the biochar against adsorbate.

7.1. Summary

The sorption experiments have shown that FR is an excellent adsorbent against As (V) with maximum specific uptake from Freundlich isotherm is 84.94 µg of As (V) /g of FR with the increase in adsorbent dosage from 5 g/L to 50 g/L in 15 minutes at pH – 5.0 and temperature 30°C. The R^2 value from Freundlich isotherm curve ($R^2 \sim 0.8612 < 1$) indicates Freundlich as a desirable sorption model compared to Langmuir's. The optimum conditions for sorption of As (V) from spiked water is listed in the **Table 7.1**.

Table 7.1: Optimum conditions for sorption of As (V) from spiked water

Parameters	Value
Adsorbate	As (V)
Adsorbent	FR (Iron modified water hyacinth roots biochar)
Initial As (V) Concentration	1000 mg/L
Adsorbent Dosage	20 g/L
Optimum time	15 minutes
Optimum pH	5.0
Optimum temperature	Room temperature (30°C)
Orbital Shaking	250 rpm
Removal efficiency	> 99%

The sorption experiments have also shown that FL is an excellent adsorbent against F^- with maximum specific uptake from Freundlich isotherm is 0.64 mg of F^- /g of FL with the increase in adsorbent dosage from 5 g/L to 50 g/L in 15 minutes at pH – 5.0 and temperature 30°C. The R^2 value from Freundlich isotherm curve ($R^2 \sim 0.8928 < 1$) indicates Freundlich as a desirable sorption model compared to Langmuir's. The optimum conditions for sorption of F^- from spiked water is listed in the **Table 7.2.**

Table 7.2: Optimum conditions for sorption of F^- from spiked water

Parameters	**Value**
Adsorbate	F^-
Adsorbent	FL (Iron modified water hyacinth leaves biochar)
Initial F^- Concentration	10 mg/L
Adsorbent Dosage	50 g/L
Optimum time	30 minutes
Optimum pH	5.0
Optimum temperature	Room temperature (30°C)
Orbital Shaking	250 rpm
Removal efficiency	> 85%

7.2. Future scope of the work

- Characterization of the biochar viz. surface area, pore volume, pore size, SEM, XRD, EDX, TGA, and FTIR has not been done and can be conducted to specify the reasons behind the effectiveness of produced biochar.
- Other amendments of biochar can also be prepared such as with Aluminium salts to check its efficacy against Fluoride adsorption.
- The methodology of biochar amendment was to mix the salts with dried biomass and then subject it to slow pyrolysis, however other methodology where biochar is first

prepared and then it is mixed with desired salts and then slow pyrolysis for doping is also an open area of research.

- Column study has not been conducted and can be studied further.
- Reusability of biochar is an important parameter while using biochar at an industrial scale. This parameter can be tested further as per standard protocol.
- Performance of biochar in presence of other competitive ions has not been tested.
- Spiked water was used to test for the efficacy of the biochar, action of biochar on groundwater remediation of arsenate and fluoride has not been tested and is an area for further research.
- The test was conducted only on As (V) removal using produced biochar, however the efficacy of biochar against As (III) removal is an area of further research.
- Research at lab scale is fruitful only when it is benefitting the whole masses and its applicability at industrial is verified. This is an area of further work.
- The biochar was tested for its efficacy on removal of contaminants from water, however its efficacy on soil can also be checked.

REFERENCES

Acharyya, S. K., Lahiri, S., Raymahashay, B. C., & Bhowmik, A. (2000). Arsenic toxicity of groundwater in parts of the Bengal basin in India and Bangladesh: the role of Quaternary stratigraphy and Holocene sea-level fluctuation. *Environmental Geology, 39*(10), 1127-1137.

Acharyya, S. K., Shah, B. A., Ashyiya, I. D., & Pandey, Y. (2005). Arsenic contamination in groundwater from parts of Ambagarh-Chowki block, Chhattisgarh, India: source and release mechanism. *Environmental Geology*, *49*(1), 148-158.

Agrafioti, E., Kalderis, D., & Diamadopoulos, E. (2014). Ca and Fe modified biochars as adsorbents of arsenic and chromium in aqueous solutions. *Journal of Environmental Management, 146*, 444-450.

Aguilar, D. (2010). Groundwater reform in India: An equity and sustainability dilemma. *Tex. Int'l LJ*, *46*, 623.

Ahmad, M., Dora, S. L., Chakraborty, M. K., Arya, P. K., & Gupta, A. (2007). Hydrological study of limestone mining area, Vijayraghovgarh, Katni. *Indian Journal of Environmental Protection*, *27*(11), 980.

Ahsan, N., Lee, D. G., Kim, K. H., Alam, I., Lee, S. H., Lee, K. W., & Lee, B. H. (2010). Analysis of arsenic stress-induced differentially expressed proteins in rice leaves by two-dimensional gel electrophoresis coupled with mass spectrometry. *Chemosphere*, *78*(3), 224-231.

Alhassan, S. I., Huang, L., He, Y., Yan, L., Wu, B., & Wang, H. (2021). Fluoride removal from water using alumina and aluminum-based composites: A comprehensive review of progress. *Critical Reviews in Environmental Science and Technology*, *51*(18), 2051-2085.

Ali, S., Thakur, S. K., Sarkar, A., & Shekhar, S. (2016). Worldwide contamination of water by fluoride. *Environmental Chemistry Letters*, *14*(3), 291-315.

Ando, M., Tadano, M., Asanuma, S., Tamura, K., Matsushima, S., Watanabe, T., & Cao, S. (1998). Health effects of indoor fluoride pollution from coal burning in China. *Environmental Health Perspectives, 106*(5), 239-244.

Apambire, W. B., Boyle, D. R., & Michel, F. A. (1997). Geochemistry, genesis, and health implications of fluoriferous groundwaters in the upper regions of Ghana. *Environmental Geology, 33*(1), 13-24.

Ayoob, S., & Gupta, A. K. (2006). Fluoride in drinking water: a review on the status and stress effects. *Critical Reviews in Environmental Science and Technology*, *36*(6), 433-487.

Bahng, M. K., Mukarakate, C., Robichaud, D. J., & Nimlos, M. R. (2009). Current technologies for analysis of biomass thermochemical processing: A review. *Analytica Chimica Acta*, *651*(2), 117-138.

Bano, R., Khayyam, U., & Khalid, S. (2020). Effects of increasing soil fluoride on the growth of vegetation in the vicinity of brick kilns: a case study from Rawalpindi, Pakistan. *Polish Journal of Environmental Studies*, *29*(2), 1535-1544.

Barbier, O., Arreola-Mendoza, L., & Del Razo, L. M. (2010). Molecular mechanisms of fluoride toxicity. *Chemico-Biological Interactions*, *188*(2), 319-333.

Batista, A. H., Melo, V. F., Gilkes, R., & Roberts, M. (2018). Identification of heavy metals in crystals of sand and silt fractions of soils by scanning electron microscopy (SEM EDS/WD-EPMA). *Revista Brasileira de Ciência do Solo*, *42*.

Bazrafshan, E., Ownagh, K. A., & Mahvi, A. H. (2012). Application of electrocoagulation process using iron and aluminum electrodes for fluoride removal from aqueous environment. *E-Journal of Chemistry*, *9*(4), 2297-2308.

Bhattacharya, P., Chatterjee, D., & Jacks, G. (1997). Occurrence of arsenic-contaminated groundwater in alluvial aquifers from delta plains, eastern India: Options for safe drinking water supply. *International Journal of Water Resources Development*, *13*(1), 79-92.

Bhattacharya, A., Sadhukhan, A. K., Ganguly, A., & Chatterjee, P. K. (2016). Dilute Acid Induced Changes on Microscopic and Tomographic Structure of Water Hyacinth [Eichhornia Crassipes (Mart.) Solms] Biomass during Bioconversion Process to Xylitol. *Indian Journal of Science and Technology*, *9*(6), 1-9.

Bindal, S., & Singh, C. K. (2019). Predicting groundwater arsenic contamination: Regions at risk in highest populated state of India. *Water Research*, *159*, 65-76.

BIS. (2012). Indian Standard Specifications for Drinking Water. IS: 10500. Bureau of Indian Standards, New Delhi, India.

Bloom, D. E. (2011, January). Population dynamics in India and implications for economic growth. St. Gallen, Switzerland: WDA-Forum, University of St. Gallen.

Bobba, A. G., Singh, V. P., & Bengtsson, L. (1997). Sustainable development of water resources in India. *Environmental Management*, *21*(3), 0367-0393.

Bordoloi, S., Garg, A., Sreedeep, S., Lin, P., & Mei, G. (2018). Investigation of cracking and water availability of soil-biochar composite synthesized from invasive weed water hyacinth. *Bioresource Technology*, *263*, 665-677.

Bordoloi, S. (2019). *Physio-biochemical properties of water hyacinth based Bio-materials and its application in soil amendment* (Doctoral dissertation).

Boyle, R. W., & Jonasson, I. R. (1973). The geochemistry of arsenic and its use as an indicator element in geochemical prospecting. *Journal of Geochemical Exploration*, *2*(3), 251-296.

Britannica, T. Editors of Encyclopaedia (2020, October 26). Arsenic. Encyclopaedia Britannica.

Brewer, C. E., Schmidt-Rohr, K., Satrio, J. A., & Brown, R. C. (2009). Characterization of biochar from fast pyrolysis and gasification systems. *Environmental Progress & Sustainable Energy: An Official Publication of the American Institute of Chemical Engineers*, *28*(3), 386-396.

Brouwer, I. D., De Bruin, A., Dirks, O. B., & Hautvast, J. G. A. J. (1988). Unsuitability of World Health Organisation guidelines for fluoride concentrations in drinking water in Senegal. *The Lancet*, *331*(8579), 223-225.

Cai, R., Wang, X., Ji, X., Peng, B., Tan, C., & Huang, X. (2017). Phosphate reclaim from simulated and real eutrophic water by magnetic biochar derived from water hyacinth. *Journal of Environmental Management*, *187*, 212-219.

Camacho, L. M., Ponnusamy, S., Campos, I., Davis, T. A., & Deng, S. (2015). Evaluation of novel modified activated alumina as adsorbent for arsenic removal. In *Handbook of Arsenic Toxicology* (pp. 121-136). Academic Press.

Camargo, J. A., & Alonso, Á. (2006). Ecological and toxicological effects of inorganic nitrogen pollution in aquatic ecosystems: a global assessment. *Environment International*, *32*(6), 831-849.

Cebrian, M. E., Albores, A., Aguilar, M., & Blakely, E. (1983). Chronic arsenic poisoning in the north of Mexico. *Human Toxicology*, *2*(1), 121-133.

Čerňanský, S., Urík, M., Ševc, J., & Khun, M. (2007). Biosorption and biovolatilization of arsenic by heat-resistant fungi (5 pp). *Environmental Science and Pollution Research*, *14*(1), 31-35.

Chand, D. (1999). Fluoride and human health-Cause for concern. *Indian Journal of Environmental Protection*, *19*, 81-89.

Chakraborti, D., Biswas, B. K., Chowdhury, T. R., Basu, G. K., Mandal, B. K., Chowdhury, U. K., & Rathore, K. C. (1999). Arsenic groundwater contamination and sufferings of people in Rajnandgaon district, Madhya Pradesh, India. *Current Science*, *77*(4), 502-504.

Chakraborti, D., Singh, E. J., Das, B., Shah, B. A., Hossain, M. A., Nayak, B., & Singh, N. R. (2008). Groundwater arsenic contamination in Manipur, one of the seven North-Eastern hill states of India: a future danger. *Environmental Geology*, *56*(2), 381-390.

Chakraborti, D., Ghorai, S. K., Das, B., Pal, A., Nayak, B., & Shah, B. A. (2009). Arsenic exposure through groundwater to the rural and urban population in the Allahabad-Kanpur track in the upper Ganga plain. *Journal of Environmental Monitoring*, *11*(8), 1455-1459.

Chakraborti, D., Singh, S. K., Rashid, M. H., & Rahman, M. M. (2011). Arsenic: occurrence in groundwater. *Encyclopedia of Environmental Health*, *2*, 1e17.

Chakraborti, D., Das, B., & Murrill, M. T. (2011). Examining India's groundwater quality management. *Environ. Sci. Technol.* 2011, 45, 1, 27–33

Chakraborti, D., Rahman, M. M., Das, B., Nayak, B., Pal, A., Sengupta, M. K., & Quamruzzaman, Q. (2013). Groundwater arsenic contamination in Ganga–Meghna–Brahmaputra plain, its health effects and an approach for mitigation. *Environmental Earth Sciences*, *70*(5), 1993-2008.

Chaudhary, V., Jacks, G., & Gustafsson, J. E. (2002). An analysis of groundwater vulnerability and water policy reform in India. *Environmental Management and Health,* 13 (2), 175-193.

Chen, B. H., Hong, C. J., Pandey, M. R., & Smith, K. R. (1990). Indoor air pollution in developing countries. *World Health Statistics Quarterly 1990; 43 (3): 127-138.*

Chen, L., Wu, H. X., Wang, T. J., Jin, Y., Zhang, Y., & Dou, X. M. (2009). Granulation of Fe–Al–Ce nano-adsorbent for fluoride removal from drinking water by spray coating on sand in a fluidized bed. *Powder technology*, *193*(1), 59-64.

Chen, A. Y. Y., & Olsen, T. (2016). Chromated copper arsenate–treated wood: a potential source of arsenic exposure and toxicity in dermatology. *International Journal of Women's Dermatology*, *2*(1), 28-30.

Cheng, R. C., Liang, S., Wang, H. C., & Beuhler, M. D. (1994). Enhanced coagulation for arsenic removal. *Journal-American Water Works Association*, *86*(9), 79-90.

Cheng, C. H., Lehmann, J., Thies, J. E., Burton, S. D., & Engelhard, M. H. (2006). Oxidation of black carbon by biotic and abiotic processes. *Organic geochemistry, 37*(11), 1477-1488.

Chhabra, R., Singh, A., & Abrol, I. P. (1980). Fluorine in sodic soils. *Soil Science Society of America Journal*, *44*(1), 33-36.

Chiavola, A., D'Amato, E., & Boni, M. R. (2019). Comparison of different iron oxide adsorbents for combined arsenic, vanadium and fluoride removal from drinking water. *International Journal of Environmental Science and Technology*, *16*(10), 6053-6064.

Choudhury, N. D., Chutia, R. S., Bhaskar, T., & Kataki, R. (2014). Pyrolysis of jute dust: effect of reaction parameters and analysis of products. *Journal of Material Cycles and Waste Management*, *16*(3), 449-459.

Chowdhury, U. K., Biswas, B. K., Chowdhury, T. R., Samanta, G., Mandal, B. K., Basu, G. C., & Chakraborti, D. (2000). Groundwater arsenic contamination in Bangladesh and West Bengal, India. *Environmental Health Perspectives*, *108*(5), 393-397.

Chowdhury, N. R., Das, R., Joardar, M., Ghosh, S., Bhowmick, S., & Roychowdhury, T. (2018). Arsenic accumulation in paddy plants at different phases of pre-monsoon cultivation. *Chemosphere*, *210*, 987-997.

Chuang, Y. S., Lay, C. H., Sen, B., Chen, C. C., Gopalakrishnan, K., Wu, J. H., ... & Lin, C. Y. (2011). Biohydrogen and biomethane from water hyacinth (Eichhornia crassipes) fermentation: effects of substrate concentration and incubation temperature. *International Journal of Hydrogen Energy*, *36*(21), 14195-14203.

Chutia, P., Kato, S., Kojima, T., & Satokawa, S. (2009). Arsenic adsorption from aqueous solution on synthetic zeolites. *Journal of Hazardous Materials*, *162*(1), 440-447.

Coates, G. W. (2000). Precise control of polyolefin stereochemistry using single-site metal catalysts. *Chemical Reviews*, *100*(4), 1223-1252.

Cook, F. J., Seagrove-Guffey, M., Mumm, S., Veis, D. J., McAlister, W. H., Bijanki, V. N., & Whyte, M. P. (2021). Non-endemic skeletal fluorosis: causes and associated secondary hyperparathyroidism (case report and literature review). *Bone*, *145*, 115839.

CREED, J. (1997). Speciation of arsenic compounds in drinking water by capillary electrophoresis with hydrodynamically modified electroosmotic flow detected through hydride generation inductively coupled plasma mass spectrometry with a membrane gas–liquid separator. *Journal of Analytical Atomic Spectrometry*, *12*(7), 689-695.

Das, A., Joardar, M., Chowdhury, N. R., De, A., Mridha, D., & Roychowdhury, T. (2021). Arsenic toxicity in livestock growing in arsenic endemic and control sites of West Bengal: risk for human and environment. *Environmental Geochemistry and Health*, *43*(8), 3005-3025.

Das, D., Chatterjee, A., Mandal, B. K., Samanta, G., Chakraborti, D., & Chanda, B. (1995). Arsenic in ground water in six districts of West Bengal, India: the biggest arsenic calamity in the world. Part 2. Arsenic concentration in drinking water, hair, nails, urine, skin-scale and liver tissue (biopsy) of the affected people. *Analyst*, *120*(3), 917-924.

Das, D., Samanta, G., Mandal, B. K., Chowdhury, T. R., Chanda, C. R., Chowdhury, P. P., & Chakraborti, D. (1996). Arsenic in groundwater in six districts of West Bengal, India. *Environmental Geochemistry and Health*, *18*(1), 5-15.

Das, S., Metha, B. C., Das, P. K., Srivastava, S. K., & Samanta, S. K. (1998). Source of High Fluoride in Ground Water around Anugul, Dhenkenal District, Orissa. *Pollution Research*, *17*, 385-392.

Das, S., Mehta, B. C., Das, P. K., Srivastava, S. K., & Samanta, S. K. (1999). Sources of high fluoride in ground water around Anugul, Dhenkenal district, Orissa. *Pollution Research*, *18*(1), 21-28.

Das, D., & Veziroğlu, T. N. (2001). Hydrogen production by biological processes: a survey of literature. *International Journal of Hydrogen Energy*, *26*(1), 13-28.

Datta, K. K., De Jong, C., & Singh, O. P. (2000). Reclaiming salt-affected land through drainage in Haryana, India: a financial analysis. *Agricultural Water Management*, *46*(1), 55-71.

Datta, A. S., Chakrabortty, A., De Dalal, S. S., & Lahiri, S. C. (2014). Fluoride contamination of underground water in West Bengal, India. *Fluoride*, *47*(3), 241-8.

Dey, U., Chatterjee, S., & Mondal, N. K. (2016). Isolation and characterization of arsenic-resistant bacteria and possible application in bioremediation. *Biotechnology reports*, *10*, 1-7.

Diawara, C. K. (2008). Nanofiltration process efficiency in water desalination. *Separation & Purification Reviews*, *37*(3), 302-324.

Dutta, A., Diao, Y., Jain, R., Rene, E. R., & Dutta, S. (2015). Adsorption of cadmium from aqueous solutions onto coffee grounds and wheat straw: equilibrium and kinetic study. *J. Environ. Eng*, *142*(9), C4015014.

Dwivedi, A., & Jain, M. K. (2014). Fly ash–waste management and overview: A Review. *Recent Research in Science and Technology*, *6*(1).

Edmunds, W. M., & Smedley, P. L. (1996). Groundwater geochemistry and health: an overview. *Geological Society, London, Special Publications*, *113*(1), 91-105.

Edmunds, W.M., & Smedley, P.L. (2005). Fluoride in natural waters. In O. Selinus (Ed.), Essentials of medical geology (pp. 311-336). Dordrecht: Springer.

Edwards, M. (1994). Chemistry of arsenic removal during coagulation and Fe–Mn oxidation. *Journal-American Water Works Association*, *86*(9), 64-78.

Egyedi, K., & Pataky, E. (1978). Dermatologic aspects of arsenic poisoning caused by drinking water. *Dermatosen in Beruf und Umwelt. Occupation and Environment*, *26*(2), 54-56.

Elcik, H., Celik, S. O., Cakmakci, M., & Özkaya, B. (2016). Performance of nanofiltration and reverse osmosis membranes for arsenic removal from drinking water. *Desalination and Water Treatment*, *57*(43), 20422-20429.

Enders, A., & Lehmann, J. (2017). Proximate analyses for characterising biochar. *Biochar: a guide to analytical methods*, 9-22.

EPA Report. 1976. National interim primary drinking water regulation. EPA publication no. EPA-570/9-76-003.

Ferreccio, C., & Sancha, A. M. (2006). Arsenic exposure and its impact on health in Chile. *Journal of Health, Population and Nutrition*, 164-175.

Fields, K. A., Chen, A. H., & Wang, L. (2000). *Arsenic removal from drinking water by coagulation/filtration and lime softening plants*. Washington: National Risk Management Research Laboratory, Office of Research and Development, US Environmental Protection Agency.

Freundlich, H. M. F. (1906). Over the adsorption in solution. *J. Phys. chem*, *57*(385471), 1100-1107.

Fuwa, K. (1986). Analytical chemistry and biogeochemistry of fluorine: an historical view. In *Studies in Environmental Science* (Vol. 27, pp. 3-14). Elsevier.

Gao, Y., Wang, X. H., Yang, H. P., & Chen, H. P. (2012). Characterization of products from hydrothermal treatments of cellulose. *Energy*, *42*(1), 457-465.

Garcia-Segura, S., Eiband, M. M. S., de Melo, J. V., & Martínez-Huitle, C. A. (2017). Electrocoagulation and advanced electrocoagulation processes: A general review about the fundamentals, emerging applications and its association with other technologies. *Journal of Electroanalytical Chemistry*, *801*, 267-299.

Garrison, T. S., Ellis, R. (2022). Oceanography:An Invitation to Marine Science. Brazil: Cengage Learning.

Gaur, G., & Sharma, S. (2017). Study of Biosorbents for Removal of Dyes and Metals. *Asian Journal of Chemistry*, *29*(6).

Ghosh, A., Mukherjee, K., Ghosh, S. K., & Saha, B. (2013). Sources and toxicity of fluoride in the environment. *Research on Chemical Intermediates*, *39*(7), 2881-2915.

Ghosh, S., Malloum, A., Igwegbe, C. A., Ighalo, J. O., Ahmadi, S., Dehghani, M. H., & Mubarak, N. M. (2022). New generation adsorbents for the removal of fluoride from water and wastewater: A review. *Journal of Molecular Liquids, 346,* 118257.

Girisuta, B., Danon, B., Manurung, R., Janssen, L. P. B. M., & Heeres, H. J. (2008). Experimental and kinetic modelling studies on the acid-catalysed hydrolysis of the water hyacinth plant to levulinic acid. *Bioresource technology*, *99*(17), 8367-8375.

Gleick, P. H. (1993). *Water in Crisis: A Guide to the World's Fresh Water Resources* (Illustrated ed.). Oxford University Press.

González, J. F., Román, S., Encinar, J. M., & Martínez, G. (2009). Pyrolysis of various biomass residues and char utilization for the production of activated carbons. *Journal of Analytical and Applied Pyrolysis*, *85*(1-2), 134-141.

Gopal, V., & Elango, K. P. (2007). Equilibrium, kinetic and thermodynamic studies of adsorption of fluoride onto plaster of Paris. *Journal of Hazardous Materials*, *141*(1), 98-105.

Goswami, A., & Purkait, M. K. (2011). Kinetic and equilibrium study for the fluoride adsorption using pyrophyllite. *Separation Science and Technology*, *46*(11), 1797-1807.

Goswami, A., & Purkait, M. K. (2012). The defluoridation of water by acidic alumina. *Chemical Engineering Research and Design*, *90*(12), 2316-2324.

Govindaswamy, S., Schupp, D. A., & Rock, S. A. (2011). Batch and continuous removal of arsenic using hyacinth roots. *International journal of phytoremediation*, *13*(6), 513-527.

Grossl, P. R., Eick, M., Sparks, D. L., Goldberg, S., & Ainsworth, C. C. (1997). Arsenate and chromate retention mechanisms on goethite. 2. Kinetic evaluation using a pressure-jump relaxation technique. *Environmental Science & Technology*, *31*(2), 321-326.

Gu, Z., Fang, J., & Deng, B. (2005). Preparation and evaluation of GAC-based iron-containing adsorbents for arsenic removal. *Environmental science & technology*, *39*(10), 3833-3843.

Gupta, A., Yunus, M., & Sankararamakrishnan, N. (2013). Chitosan-and iron–chitosan-coated sand filters: a cost-effective approach for enhanced arsenic removal. *Industrial & Engineering Chemistry Research*, *52*(5), 2066-2072.

Hammer, M. (1986). Fluoridation of Saudi Arabia's water. *Middle East Health*, *10*(5), 46D-47D.

Handa, B. K. (1979). Effect of return irrigation flows from irrigated lands on the chemical composition of groundwater from shallow unconfined aquifers. *Progress in Water Technology*.

Hao, J., Han, M. J., & Meng, X. (2009). Preparation and evaluation of thiol-functionalized activated alumina for arsenite removal from water. *Journal of Hazardous Materials*, *167*(1-3), 1215-1221.

Harley, K. L. S., Julien, M. H., & Wright, A. D. (1996). Water hyacinth: A tropical world wide problem and methods for its control.

Harman-Ware, A. E., Crocker, M., Kaur, A. P., Meier, M. S., Kato, D., & Lynn, B. (2013). Pyrolysis–GC/MS of sinapyl and coniferyl alcohol. *Journal of Analytical And Applied Pyrolysis*, *99*, 161-169.

Haul, R. (1982). SJ Gregg, KSW Sing: adsorption, surface area and porosity. 2. auflage, Academic Press, London 1982. 303 Seiten, Preis: $49.50.

Ho, Y. S., & McKay, G. (1999). Pseudo-second order model for sorption processes. *Process Biochemistry*, *34*(5), 451-465.

Howard, G. W., & Harley, K. L. S. (1997). How do floating aquatic weeds affect wetland conservation and development? How can these effects be minimised? *Wetlands Ecology and Management*, *5*(3), 215-225.

ISI (1983). Indian standard specification for drinking water. India: Indian standard institution, New Delhi.

Isosaari, P., & Sillanpää, M. (2010). Electromigration of arsenic and co-existing metals in mine tailings. *Chemosphere*, *81*(9), 1155-1158.

Jadhav, S. V., Bringas, E., Yadav, G. D., Rathod, V. K., Ortiz, I., & Marathe, K. V. (2015). Arsenic and fluoride contaminated groundwaters: a review of current technologies for contaminants removal. *Journal of Environmental Management*, *162*, 306-325.

Jafari, N. (2010). Ecological and socio-economic utilization of water hyacinth (Eichhornia crassipes Mart Solms). *Journal of Applied Sciences and Environmental Management*, *14*(2).

Jain, C. K., Ali, I., & Sharma, M. K. (1999). Fluoride contamination in ground water-Indian Scenario. *Indian Journal of Environmental Protection*, *19*, 260-267.

Jain, C. K., Bandyopadhyay, A., & Bhadra, A. (2010). Assessment of ground water quality for drinking purpose, District Nainital, Uttarakhand, India. *Environmental Monitoring and Assessment*, *166*(1), 663-676.

Jayasumana, C., Fonseka, S., Fernando, A., Jayalath, K., Amarasinghe, M., Siribaddana, S., & Paranagama, P. (2015). Phosphate fertilizer is a main source of arsenic in areas affected with chronic kidney disease of unknown etiology in Sri Lanka. *Springer Plus*, *4*(1), 1-8.

Jha, S. K., Nayak, A. K., Sharma, Y. K., Mishra, V. K., & Sharma, D. K. (2008). Fluoride accumulation in soil and vegetation in the vicinity of brick fields. *Bulletin of Environmental Contamination and Toxicology*, *80*(4), 369-373.

Jha, P. K., & Tripathi, P. (2021). Arsenic and fluoride contamination in groundwater: a review of global scenarios with special reference to India. *Groundwater for Sustainable Development*, *13*, 100576.

Joardar, M., Das, A., Chowdhury, N. R., Mridha, D., De, A., Majumdar, K. K., & Roychowdhury, T. (2021). Health effect and risk assessment of the populations exposed to different arsenic levels in drinking water and foodstuffs from four villages in arsenic endemic Gaighata block, West Bengal, India. *Environmental Geochemistry and Health*, *43*(8), 3027-3053.

Kalhorinia, S., Goli, J. K., Yadav, K. S., Naseeruddin, S., & Rao, L. V. (2014). Xylitol production from water hyacinth (Eichhornia crassipes) by Candida tropicalis Y-27405. *Biosci. Biotechnol. Res. Asia*, *11*(2), 427-434.

Kapp Jr, R. W. (2016). Book Review: Arsenic Toxicity—Prevention and Treatment. International Journal of Toxicology, 35(3), 371–372.

Kartinen Jr, E. O., & Martin, C. J. (1995). An overview of arsenic removal processes. *Desalination*, *103*(1-2), 79-88.

Khamwichit, A., Dechapanya, W., & Dechapanya, W. (2022). Adsorption kinetics and isotherms of binary metal ion aqueous solution using untreated venus shell. *Heliyon*, e09610.

Kumar, M. D., & Shah, T. (2004). Groundwater pollution and contamination in India. *Emerging challenges, Hindu Survey of Environment. Kasturi and Sons*.

Kumar, P. R., Chaudhari, S., Khilar, K. C., & Mahajan, S. P. (2004). Removal of arsenic from water by electrocoagulation. *Chemosphere*, *55*(9), 1245-1252.

Kumar, E., Bhatnagar, A., Kumar, U., & Sillanpää, M. (2011). Defluoridation from aqueous solutions by nano-alumina: characterization and sorption studies. *Journal of Hazardous Materials*, *186*(2-3), 1042-1049.

Kumar, P. S., Ramalingam, S., & Sathishkumar, K. (2011). Removal of methylene blue dye from aqueous solution by activated carbon prepared from cashew nut shell as a new low-cost adsorbent. *Korean Journal of Chemical Engineering*, *28*(1), 149-155.

Kumar, V., Talreja, N., Deva, D., Sankararamakrishnan, N., Sharma, A., & Verma, N. (2011). Development of bi-metal modified micro-and nano multi-functional polymeric adsorbents for the removal of fluoride and arsenic (V) from wastewater. *Desalination, 282*, 27-38.

Kumar, R., & Raj, H. (2013). Mitigation of groundwater depletion hazards in India. *Current Science (Bangalore)*, *104*(10), 1271.

Kundu, M. C., & Mandal, B. (2009). Assessment of potential hazards of fluoride contamination in drinking groundwater of an intensively cultivated district in West Bengal, India. *Environmental Monitoring and Assessment*, *152*(1), 97-103.

Kut, K. M. K., Sarswat, A., Srivastava, A., Pittman Jr, C. U., & Mohan, D. (2016). A review of fluoride in African groundwater and local remediation methods. *Groundwater for Sustainable Development*, *2*, 190-212.

Lal, S., Singhal, A., & Kumari, P. (2020). Exploring carbonaceous nanomaterials for arsenic and chromium removal from wastewater. *Journal of Water Process Engineering*, *36*, 101276.

Langmuir, I. (1918). The adsorption of gases on plane surfaces of glass, mica and platinum. *Journal of the American Chemical society*, *40*(9), 1361-1403.

Lata, S., & Samadder, S. R. (2016). Removal of arsenic from water using nano adsorbents and challenges: a review. *Journal of Environmental Management*, *166*, 387-406.

Lakshmanan, D., Clifford, D. A., & Samanta, G. (2010). Comparative study of arsenic removal by iron using electrocoagulation and chemical coagulation. *Water Research*, *44*(19), 5641-5652.

Lehmann, J., & Joseph, S. (Eds.). (2015). *Biochar for environmental management: science, technology and implementation*. Routledge.

Leong, Y. K., & Chang, J. S. (2020). Bioremediation of heavy metals using microalgae: Recent advances and mechanisms. *Bioresource Technology*, *303*, 122886.

Lhassani, A., Rumeau, M., Benjelloun, D., & Pontie, M. (2001). Selective demineralization of water by nanofiltration application to the defluorination of brackish water. *Water Research*, *35*(13), 3260-3264.

Li, H. R., Liu, Q. B., Wang, W. Y., Yang, L. S., Li, Y. H., Feng, F. J., & Wang, G. (2009). Fluoride in drinking water, brick tea infusion and human urine in two counties in Inner Mongolia, China. *Journal of Hazardous Materials*, *167*(1-3), 892-895.

Li, L., Li, J., Shao, C., Zhang, K., Yu, S., Gao, N., & Yin, D. (2014). Arsenic removal in synthetic ground water using iron electrolysis. *Separation and Purification Technology*, *122*, 225-230.

Liao, C., Wu, C., & Yan, Y. (2007). The characteristics of inorganic elements in ashes from a 1 MW CFB biomass gasification power generation plant. *Fuel processing technology*, *88*(2), 149-156.

Lin, Y., & Liu, F. (2020). Indoor air quality and health: empirical evidence from fluoride pollution in China. *China Economic Review*, *63*, 101282.

Liu, S., Huang, B., Chai, L., Liu, Y., Zeng, G., Wang, X., & Zhou, Z. (2017). Enhancement of As (V) adsorption from aqueous solution by a magnetic chitosan/biochar composite. *RSC advances*, *7*(18), 10891-10900.

Liu, Z., Goodwin, M., Ellwood, R. P., Pretty, I. A., & McGrady, M. (2018). Automatic detection and classification of dental fluorosis in vivo using white light and fluorescence imaging. *Journal of Dentistry*, *74*, S34-S41.

Liu, C., Ye, J., Lin, Y., Wu, J., Price, G. W., Burton, D., & Wang, Y. (2020). Removal of Cadmium (II) using water hyacinth (Eichhornia crassipes) biochar alginate beads in aqueous solutions. *Environmental Pollution*, *264*, 114785.

López-Gasco, P., Iglesias, I., Benedí, J., Lozano, R., & Blanco, M. D. (2012). Characterization and in-vitro bioactivity evaluation of paclitaxel-loaded polyester nanoparticles. *Anti-Cancer Drugs*, *23*(9), 947-958.

Maguire, A., & Zohoori, F. V. (2013). Fluoride balance in infants and young children in the UK and its clinical relevance for the dental team. *British Dental Journal*, *214*(11), 587-593.

Mahapatra S.S., Dutta A., Datta J., (2010) Temperature effect on the electrode kinetics of ethanol oxidation on Pd modified Pt electrodes and the estimation of intermediates formed in alkali medium, *Electrochimica Acta*, Volume 55, Issue 28, 2010, Pages 9097-9104, ISSN 0013-4686.

Mailu, A. M. (2001). Preliminary assessment of the cocial, economic and environmental impacts of Water Hyacinth in Lake Victoria basin and status of control. Canberra: ACIAR.

Malakootian, M., Mansoorian, H. J., & Moosazadeh, M. (2010). Performance evaluation of electrocoagulation process using iron-rod electrodes for removing hardness from drinking water. *Desalination*, *255*(1-3), 67-71.

Malik, A. (2007). Environmental challenge vis a vis opportunity: the case of water hyacinth. *Environment International*, *33*(1), 122-138.

Maliyekkal, S. M., Sharma, A. K., & Philip, L. (2006). Manganese-oxide-coated alumina: a promising sorbent for defluoridation of water. *Water Research*, *40*(19), 3497-3506.

Manyà, J. J. (2012). Pyrolysis for biochar purposes: a review to establish current knowledge gaps and research needs. *Environmental Science & Technology*, *46*(15), 7939-7954.

Masto, R. E., Kumar, S., Rout, T. K., Sarkar, P., George, J., & Ram, L. C. (2013). Biochar from water hyacinth (Eichornia crassipes) and its impact on soil biological activity. *Catena*, *111*, 64-71.

Mawia, A. M., Hui, S., Zhou, L., Li, H., Tabassum, J., Lai, C., & Hu, P. (2021). Inorganic arsenic toxicity and alleviation strategies in rice. *Journal of Hazardous Materials*, *408*, 124751.

McHenry, M. P. (2009). Agricultural bio-char production, renewable energy generation and farm carbon sequestration in Western Australia: Certainty, uncertainty and risk. *Agriculture, Ecosystems & Environment*, *129*(1-3), 1-7.

Meenakshi, S., & Viswanathan, N. (2007). Identification of selective ion-exchange resin for fluoride sorption. *Journal of Colloid and Interface Science*, *308*(2), 438-450.

Mehta, M. (2006). Status of groundwater and policy issues for its sustainable development in India. *Groundwater Research and Management: Integrating Science into Management Decisions*, (pp. 62-74). Colombo: International water management institute.

Meiers, P. (2008). 'Fluoride history', The history of fluorine, Fluoride and Fluoridation, [Online]. Available at: http://www.fluoride-history.de/index.htm

Mendoza, R. M. O., Kan, C. C., Chuang, S. S., Pingul-Ong, S. M. B., Dalida, M. L. P., & Wan, M. W. (2014). Feasibility studies on arsenic removal from aqueous solutions by electrodialysis. *Journal of Environmental Science and Health, Part A*, *49*(5), 545-554.

Mironga, J. M., Mathooko, J. M., & Onywere, S. M. (2014). Effects of spreading patterns of water hyacinth (Eichhornia crassipes) on zooplankton population in Lake Naivasha, Kenya. *International Journal of Development and Sustainability*, *3*(10), 1971-1987.

Mondal, N. C., Singh, V. S., Puranik, S. C., & Singh, V. P. (2010). Trace element concentration in groundwater of Pesarlanka Island, Krishna Delta, India. *Environmental Monitoring and Assessment*, *163*(1), 215-227.

Moosavi, S., Lai, C. W., Gan, S., Zamiri, G., Akbarzadeh Pivehzhani, O., & Johan, M. R. (2020). Application of efficient magnetic particles and activated carbon for dye removal from wastewater. *ACS Omega*, *5*(33), 20684-20697.

Mridha, D., Priyadarshni, P., Bhaskar, K., Gaurav, A., De, A., Das, A., & Roychowdhury, T. (2021). Fluoride exposure and its potential health risk assessment in drinking water and staple food in the population from fluoride endemic regions of Bihar, India. *Groundwater for Sustainable Development*, *13*, 100558.

Mukherjee, A. B., & Bhattacharya, P. (2001). Arsenic in groundwater in the Bengal Delta Plain: slow poisoning in Bangladesh. *Environmental Reviews*, *9*(3), 189-220.

Mukherjee, A., Sengupta, M. K., Hossain, M. A., Ahamed, S., Das, B., Nayak, B., & Chakraborti, D. (2006). Arsenic contamination in groundwater: a global perspective with emphasis on the Asian scenario. *Journal of Health, Population and Nutrition*, 142-163.

Mukherjee, S. C., Pati, S., Dutta, R. N., & Saha, K. C. (2009). Groundwater arsenic contamination situation in West-Bengal, India: A nineteen year study. *Bhujal News Quarterly Journal*, *24*, 1-40.

Mukherjee, A., Verma, S., Gupta, S., Henke, K. R., & Bhattacharya, P. (2014). Influence of tectonics, sedimentation and aqueous flow cycles on the origin of global groundwater arsenic: paradigms from three continents. *Journal of Hydrology*, *518*, 284-299.

Mukherjee, I., & Singh, U. K. (2018). Groundwater fluoride contamination, probable release, and containment mechanisms: a review on Indian context. *Environmental geochemistry and health*, *40*(6), 2259-2301.

Murray, J. J., & World Health Organization. (1986). *Appropriate use of fluorides for human health*. World Health Organization.

Naik, R. G., Dodamani, A. S., Vishwakarma, P., Jadhav, H. C., Khairnar, M. R., Deshmukh, M. A., & Wadgave, U. (2017). Level of fluoride in soil, grain and water in Jalgaon district, Maharashtra, India. *Journal of Clinical and Diagnostic Research: JCDR*, *11*(2), ZC05.

Naje, A. S., Chelliapan, S., Zakaria, Z., & Abbas, S. A. (2015). Enhancement of an electrocoagulation process for the treatment of textile wastewater under combined electrical connections using titanium plates. *Int. J. Electrochem. Sci*, *10*(6), 4495-4512.

Ndiaye, P. I., Moulin, P., Dominguez, L., Millet, J. C., & Charbit, F. (2005). Removal of fluoride from electronic industrial effluentby RO membrane separation. *Desalination*, *173*(1), 25-32.

Nguyen, B. T., Lehmann, J., Kinyangi, J., Smernik, R., Riha, S. J., & Engelhard, M. H. (2009). Long-term black carbon dynamics in cultivated soil. *Biogeochemistry*, *92*(1), 163-176.

Nicolli, H. B., García, J. W., Falcón, C. M., & Smedley, P. L. (2012). Mobilization of arsenic and other trace elements of health concern in groundwater from the Salí River Basin, Tucumán Province, Argentina. *Environmental Geochemistry and Health*, *34*(2), 251-262.

Nicholas, D. R., Ramamoorthy, S., Palace, V., Spring, S., Moore, J. N., & Rosenzweig, R. F. (2003). Biogeochemical transformations of arsenic in circumneutral freshwater sediments. *Biodegradation*, *14*(2), 123-137.

Nickson, R. T., McArthur, J. M., Ravenscroft, P., Burgess, W. G., & Ahmed, K. M. (2000). Mechanism of arsenic release to groundwater, Bangladesh and West Bengal. *Applied Geochemistry*, *15*(4), 403-413.

Nidheesh, P. V., & Singh, T. A. (2017). Arsenic removal by electrocoagulation process: Recent trends and removal mechanism. *Chemosphere*, *181*, 418-432.

Ning, R. Y. (2002). Arsenic removal by reverse osmosis. *Desalination*, *143*(3), 237-241.

Nowakowski, D. J., & Jones, J. M. (2005). Catalysis by potassium in the pyrolysis processes of biomass and basic biomass components. In *World Renewable Energy Congress (WREC 2005). Elsevier Ltd* (pp. 590-595).

Nriagu, J. O., Bhattacharya, P., Mukherjee, A. B., Bundschuh, J., Zevenhoven, R., & Loeppert, R. H. (2007). Arsenic in soil and groundwater: an introduction. *Arsenic in soil and groundwater environment: biogeochemical interactions, health effects and remediation, trace metals and other contaminants in the environment*, *9*, 3-60.

NWP. (1987). National Water Policy. Central Water Commission. New Delhi, India.

Ozsvath, D. L. (2009). Fluoride and environmental health: a review. *Reviews in Environmental Science and Biotechnology*, *8*(1), 59-79.

Padungthon, S., Li, J., German, M., & SenGupta, A. K. (2014). Hybrid anion exchanger with dispersed zirconium oxide nanoparticles: a durable and reusable fluoride-selective sorbent. *Environmental Engineering Science, 31*(7), 360-372.

Paikaray, S. (2015). Arsenic geochemistry of acid mine drainage. *Mine Water and the Environment*, *34*(2), 181-196.

Pepper, R. A., Couperthwaite, S. J., & Millar, G. J. (2017). Value adding red mud waste: High performance iron oxide adsorbent for removal of fluoride. *Journal of Environmental Chemical Engineering, 5*(3), 2200-2206.

Petrusevski, B., Sharma, S., Schippers, J. C., & Shordt, K. (2007). Arsenic in drinking water. *Delft: IRC International Water and Sanitation Centre*, *17*(1), 36-44.

Piekos, R., & Paslawska, S. (1998). Leaching characteristics of fluoride from coal fly ash. *Fluoride, 31*. 188-192

Plaza, M. G., Pevida, C., Martín, C. F., Fermoso, J., Pis, J. J., & Rubiera, F. (2010). Developing almond shell-derived activated carbons as CO2 adsorbents. *Separation and Purification Technology*, *71*(1), 102-106.

Plummer, M. L. (2005). Impact of invasive water hyacinth (Eichhornia crassipes) on snail hosts of schistosomiasis in Lake Victoria, East Africa. *EcoHealth*, *2*(1), 81-86.

Pontius, F. W. (1991). Fluoride regulation and water fluoridation. *Journal-American Water Works Association*, *83*(11), 20-96.

Poonia, T., Singh, N., & Garg, M. C. (2021). Contamination of Arsenic, Chromium and Fluoride in the Indian groundwater: a review, meta-analysis and cancer risk assessment. *International Journal of Environmental Science and Technology*, *18*(9), 2891-2902.

Potgeiter, J. H. (1990). An experimental assessment of the efficiency of different defluoridation methods. *Chem SA*, *16*(2), 317-327.

Rahman, M. M., Naidu, R., & Bhattacharya, P. (2009). Arsenic contamination in groundwater in the Southeast Asia region. *Environmental Geochemistry and Health*, *31*(1), 9-21.

Rahman, M. A. (2018). Pyrolysis of water hyacinth in a fixed bed reactor: Parametric effects on product distribution, characterization and syngas evolutionary behavior. *Waste Management*, *80*, 310-318.

Rajaram, T., & Das, A. (2008). Water pollution by industrial effluents in India: Discharge scenarios and case for participatory ecosystem specific local regulation. *Futures*, *40*(1), 56-69.

Ram, S., & Moolani, M. K. (2000). Herbicidal weed control of water hyacinth under semi-arid conditions. *Pestol*, *24*, 69-71.

Ramakrishna, V., & Babu, B. V. (1999). Fresh water depletion–a crisis: Causes & remedies. *Environment & People*, *6*(1), 33-39.

Rasool, A., Farooqi, A., Xiao, T., Ali, W., Noor, S., Abiola, O., & Nasim, W. (2018). A review of global outlook on fluoride contamination in groundwater with prominence on the Pakistan current situation. *Environmental Geochemistry and Health*, *40*(4), 1265-1281.

Ratnaike, R. N. (2003). Acute and chronic arsenic toxicity. *Postgraduate Medical Journal*, *79*(933), 391-396

Revelo-Mejía, I. A., Hardisson, A., Rubio, C., Gutiérrez, Á. J., & Paz, S. (2021). Dental fluorosis: the risk of misdiagnosis—a Review. *Biological Trace Element Research*, *199*(5), 1762-1770.

Robinson, C., Connell, S., Kirkham, J., Brookes, S. J., Shore, R. C., & Smith, A. M. (2004). The effect of fluoride on the developing tooth. *Caries research*, *38*(3), 268-276.

Rodríguez-Romero, J. A., Mendoza-Castillo, D. I., Reynel-Ávila, H. E., de Haro-Del Rio, D. A., González-Rodríguez, L. M., Bonilla-Petriciolet, A., ... & Camacho-Aguilar, K. I. (2020). Preparation of a new adsorbent for the removal of arsenic and its simulation with artificial neural network-based adsorption models. *Journal of Environmental Chemical Engineering*, *8*(4), 103928.

Roychowdhury, T., Uchino, T., Tokunaga, H., & Ando, M. (2002). Arsenic and other heavy metals in soils from an arsenic-affected area of West Bengal, India. *Chemosphere*, *49*(6), 605-618.

Roychowdhury, T. (2010). Groundwater arsenic contamination in one of the 107 arsenic-affected blocks in West Bengal, India: Status, distribution, health effects and factors responsible for arsenic poisoning. *International Journal of Hygiene and Environmental Health*, *213*(6), 414-427.

Ruan, T., Zeng, R., Yin, X. Y., Zhang, S. X., & Yang, Z. H. (2016). Water hyacinth (Eichhornia crassipes) biomass as a biofuel feedstock by enzymatic hydrolysis. *Bio Resources*, *11*(1), 2372-2380.

Ruthven, D. M. (1984). Principles of Adsorption and Adsorption Processes. Egypt: Wiley.

Sakhare, N., Lunge, S., Rayalu, S., Bakardjiva, S., Subrt, J., Devotta, S., & Labhsetwar, N. (2012). Defluoridation of water using calcium aluminate material. *Chemical Engineering Journal*, *203,* 406-414.

Samal, U. N., & Naik, B. N. (1988). Dental fluorosis in school children in the vicinity of an aluminum factory in India. *Fluoride*, *21*(3), 142-148.

Sandoval, M. A., Fuentes, R., Thiam, A., & Salazar, R. (2021). Arsenic and fluoride removal by electrocoagulation process: A general review. *Science of The Total Environment*, *753*, 142108.

Saxena, V., & Ahmed, S. (2001). Dissolution of fluoride in groundwater: a water-rock interaction study. *Environmental Geology*, *40*(9), 1084-1087.

Saxena, V., & Ahmed, S. (2003). Inferring the chemical parameters for the dissolution of fluoride in groundwater. *Environmental Geology*, *43*(6), 731-736.

Schneiter, R. W., & Middlebrooks, E. J. (1983). Arsenic and fluoride removal from groundwater by reverse osmosis. *Environment International*, *9*(4), 289-291.

Shabana, Y. M., & Mohamed, Z. A. (2005). Integrated control of water hyacinth with a mycoherbicide and a phenylpropanoid pathway inhibitor. *Biocontrol science and technology*, *15*(7), 659-669.

Shahmansouri, A., & Bellona, C. (2015). Nanofiltration technology in water treatment and reuse: applications and costs. *Water Science and Technology*, *71*(3), 309-319.

Shaji, E., Santosh, M., Sarath, K. V., Prakash, P., Deepchand, V., & Divya, B. V. (2021). Arsenic contamination of groundwater: A global synopsis with focus on the Indian Peninsula. *Geoscience Frontiers*, *12*(3), 101079.

Sharma, P., Goel, G., Ashekuzzaman, S. M., Saini, G., & Singh, R. (2014). Groundwater arsenic in South-East Asia: extent, effects and solutions. *Asian Journal of Water, Environment and Pollution*, *11*(2), 1-11.

Shashi, A., Kumar, M., & Bhardwaj, M. (2008). Incidence of skeletal deformities in endemic fluorosis. *Tropical Doctor*, *38*(4).

Shenvi, S. S., Isloor, A. M., & Ismail, A. F. (2015). A review on RO membrane technology: Developments and challenges. *Desalination*, *368*, 10-26.

Sher, S., & Rehman, A. (2019). Use of heavy metals resistant bacteria—a strategy for arsenic bioremediation. *Applied Microbiology and Biotechnology*, *103*(15), 6007-6021.

Singh, R. B. (2000). Environmental consequences of agricultural development: a case study from the Green Revolution state of Haryana, India. *Agriculture, Ecosystems & Environment*, *82*(1-3), 97-103.

Singh, N., Kumar, D., & Sahu, A. P. (2007). Arsenic in the environment: effects on human health and possible prevention. *Journal of Environmental Biology*, *28*(2), 359.

Smedley, P. L., Nicolli, H. B., Macdonald, D. M. J., Barros, A. J., & Tullio, J. O. (2002). Hydrogeochemistry of arsenic and other inorganic constituents in groundwaters from La Pampa, Argentina. *Applied Geochemistry*, *17*(3), 259-284.

Sohi, S., Lopez-Capel, E., Krull, E., & Bol, R. (2009). Biochar, climate change and soil: A review to guide future research. *CSIRO Land and Water Science Report*, *5*(09), 17-31.

Srivastava, S., & Flora, S. J. S. (2020). Fluoride in drinking water and skeletal fluorosis: a review of the global impact. *Current Environmental Health Reports*, *7*(2), 140-146.

Suárez-Garcıa, F., Martınez-Alonso, A., Llorente, M. F., & Tascón, J. M. D. (2002). Inorganic matter characterization in vegetable biomass feedstocks. *Fuel*, *81*(9), 1161-1169.

Subba Rao, N. (2003). Groundwater quality: focus on fluoride concentration in rural parts of Guntur district, Andhra Pradesh, India. *Hydrological Sciences Journal*, *48*(5), 835-847.

Sun, P., Li, Y., Meng, T., Zhang, R., Song, M., & Ren, J. (2018). Removal of sulfonamide antibiotics and human metabolite by biochar and biochar/H2O2 in synthetic urine. *Water Research*, *147*, 91-100.

Susheela, A. K., Mudgal, A., & Keast, G. (1999). Fluoride in water: An overview. *Water Front*, *1*(13), 11-13.

Susheela, A. K., Mondal, N. K., & Singh, A. (2013). Exposure to fluoride in smelter workers in a primary aluminum industry in India. *The International Journal of Occupational and Environmental Medicine*, *4*(2), 61-72.

Susheela, A. K., & Toteja, G. S. (2018). Prevention & control of fluorosis & linked disorders: Developments in the 21st Century-Reaching out to patients in the community & hospital settings for recovery. *The Indian Journal of Medical Research*, *148*(5), 539.

Téllez, T. R., López, E. M. D. R., Granado, G. L., Pérez, E. A., López, R. M., & Guzmán, J. M. S. (2008). The water hyacinth, Eichhornia crassipes: an invasive plant in the Guadiana River Basin (Spain). *Aquatic Invasions*, *3*(1), 42-53.

Thylstrup, A., & Fejerskov, O. (1978). Clinical appearance of dental fluorosis in permanent teeth in relation to histologic changes. *Community Dentistry and Oral Epidemiology*, *6*(6), 315-328.

TOI (2010). The Times of India: Archives | Year 2010; timesofindia.indiatimes.com. https://timesofindia.indiatimes.com/archive/year-2010.cms

Tripathi, M., Sahu, J. N., & Ganesan, P. (2016). Effect of process parameters on production of biochar from biomass waste through pyrolysis: A review. *Renewable and Sustainable Energy Reviews*, *55*, 467-481.

Tu, S., Ma, L. Q., Fayiga, A. O., & Zillioux, E. J. (2004). Phytoremediation of arsenic-contaminated groundwater by the arsenic hyperaccumulating fern Pteris vittata L. *International Journal of Phytoremediation*, *6*(1), 35-47.

Umar, R., & Sami Ahmad, M. (2000). Groundwater quality in parts of central Ganga Basin, India. *Environmental Geology*, *39*(6), 673-678.

Vasudevan, S., Lakshmi, J., Jayaraj, J., & Sozhan, G. (2009). Remediation of phosphate-contaminated water by electrocoagulation with aluminium, aluminium alloy and mild steel anodes. *Journal of Hazardous Materials*, *164*(2-3), 1480-1486.

Villamagna, A. M., & Murphy, B. R. (2010). Ecological and socio-economic impacts of invasive water hyacinth (Eichhornia crassipes): a review. *Freshwater Biology*, *55*(2), 282-298.

Viswanathan, N., Sundaram, C. S., & Meenakshi, S. (2009). Removal of fluoride from aqueous solution using protonated chitosan beads. *Journal of Hazardous Materials*, *161*(1), 423-430.

Vithanage, M., Herath, I., Joseph, S., Bundschuh, J., Bolan, N., Ok, Y. S., & Rinklebe, J. (2017). Interaction of arsenic with biochar in soil and water: a critical review. *Carbon*, *113*, 219-230.

Waghmare, S. S., & Arfin, T. (2015). Fluoride removal from water by various techniques. *Int. J. Innov. Sci. Eng. Technology*, *2*(3), 560-571.

Wan, K., Huang, L., Yan, J., Ma, B., Huang, X., Luo, Z., & Xiao, T. (2021). Removal of fluoride from industrial wastewater by using different adsorbents: A review. *Science of the Total Environment*, *773*, 145535.

Weber, W. J. (1974). Adsorption processes. *Pure and Applied Chemistry*, *37*(3), 375-392.

WHO. (2008). World Health Organization. Guidelines for drinking water quality, 3rd edition. Vol.1. WHO, Geneva

WHO. (2017). *Sugars and dental caries* (No. WHO/NMH/NHD/17.12). World Health Organization.

WHO. (2018, February 15). World Health Organization. Arsenic. https://www.who.int/news-room/fact-sheets/detail/arsenic

World Bank. (2012). India Groundwater: a Valuable but Diminishing Resource. (2012, March 6). World Bank: www.worldbank.org. https://www.worldbank.org/en/news/feature/2012/03/06/india-groundwater-critical-diminishing

Wu, J., Huang, D., Liu, X., Meng, J., Tang, C., & Xu, J. (2018). Remediation of As (III) and Cd (II) co-contamination and its mechanism in aqueous systems by a novel calcium-based magnetic biochar. *Journal of Hazardous Materials*, *348*, 10-19.

Xia, D., Tan, F., Zhang, C., Jiang, X., Chen, Z., Li, H., & Wang, Y. (2016). ZnCl2-activated biochar from biogas residue facilitates aqueous As (III) removal. *Applied Surface Science*, *377*, 361-369.

Xu, Y., Liu, Y., Liu, S., Tan, X., Zeng, G., Zeng, W., & Zheng, B. (2016). Enhanced adsorption of methylene blue by citric acid modification of biochar derived from water hyacinth (Eichornia crassipes). *Environmental Science and Pollution Research*, *23*(23), 23606-23618.

Yadav, J. P., & Lata, S. (2003). Fluoride toxicity in drinking water sources of Beri block, distt. Jhajjar, Haryana. *International Journal of Medical Toxicology & Legal Medicine*, *6*(1), 26-31.

Yu, J., Jiang, C., Guan, Q., Ning, P., Gu, J., Chen, Q., & Miao, R. (2018). Enhanced removal of Cr (VI) from aqueous solution by supported ZnO nanoparticles on biochar derived from waste water hyacinth. *Chemosphere*, *195*, 632-640.

Zektser, I. S., & Everett, L. G. (2004). Groundwater resources of the world and their use. UNESCO.

Zhang, M., Gao, B., Varnoosfaderani, S., Hebard, A., Yao, Y., & Inyang, M. (2013). Preparation and characterization of a novel magnetic biochar for arsenic removal. *Bioresource Technology*, *130*, 457-462.

Zhang, F., Wang, X., Yin, D., Peng, B., Tan, C., Liu, Y., & Wu, S. (2015). Efficiency and mechanisms of Cd removal from aqueous solution by biochar derived from water hyacinth (Eichornia crassipes). *Journal of Environmental Management*, *153*, 68-73.

Zhang, F., Wang, X., Xionghui, J., & Ma, L. (2016). Efficient arsenate removal by magnetite-modified water hyacinth biochar. *Environmental Pollution*, *216*, 575-583.

Zhang, C., Li, Y., Wang, T. J., Jiang, Y., & Fok, J. (2017). Synthesis and properties of a high-capacity iron oxide adsorbent for fluoride removal from drinking water. *Applied Surface Science*, *425*, 272-281.

Zhao, Y., Zhao, J., Wang, J., & Wang, J. (2017). Fluoride exposure changed the structure and the expressions of HSP related genes in testes of pubertal rats. *Chemosphere*, *184*, 1080-1088.

Zhu, N., Yan, T., Qiao, J., & Cao, H. (2016). Adsorption of arsenic, phosphorus and chromium by bismuth impregnated biochar: Adsorption mechanism and depleted adsorbent utilization. *Chemosphere*, *164*, 32-40.

Zhou, W., Zhu, D., Langdon, A., Li, L., Liao, S., & Tan, L. (2009). The structure characterization of cellulose xanthogenate derived from the straw of Eichhornia crassipes. *Bioresource Technology*, *100*(21), 5366-5369.

Zhou, R., Zhang, M., Zhou, J., & Wang, J. (2019). Optimization of biochar preparation from the stem of Eichhornia crassipes using response surface methodology on adsorption of Cd2+. *Scientific Reports*, *9*(1), 1-17.

Zhou, R., Zhang, M., Li, J., & Zhao, W. (2020). Optimization of preparation conditions for biochar derived from water hyacinth by using response surface methodology (RSM) and its application in Pb2+ removal. *Journal of Environmental Chemical Engineering*, *8*(5), 104198.